



LUND UNIVERSITY

Fire Safety Design Based on Calculations. Uncertainty Analysis and Safety Verification

Magnusson, Sven Erik; Frantzich, Håkan; Harada, Kazunori

1995

[Link to publication](#)

Citation for published version (APA):

Magnusson, S. E., Frantzich, H., & Harada, K. (1995). *Fire Safety Design Based on Calculations. Uncertainty Analysis and Safety Verification*. (LUTVDG/TVBB--3078--SE; Vol. 3078). Department of Fire Safety Engineering and Systems Safety, Lund University.

Total number of authors:

3

General rights

Unless other specific re-use rights are stated the following general rights apply:

Copyright and moral rights for the publications made accessible in the public portal are retained by the authors and/or other copyright owners and it is a condition of accessing publications that users recognise and abide by the legal requirements associated with these rights.

- Users may download and print one copy of any publication from the public portal for the purpose of private study or research.
- You may not further distribute the material or use it for any profit-making activity or commercial gain
- You may freely distribute the URL identifying the publication in the public portal

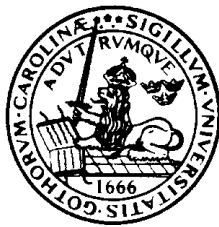
Read more about Creative commons licenses: <https://creativecommons.org/licenses/>

Take down policy

If you believe that this document breaches copyright please contact us providing details, and we will remove access to the work immediately and investigate your claim.

LUND UNIVERSITY

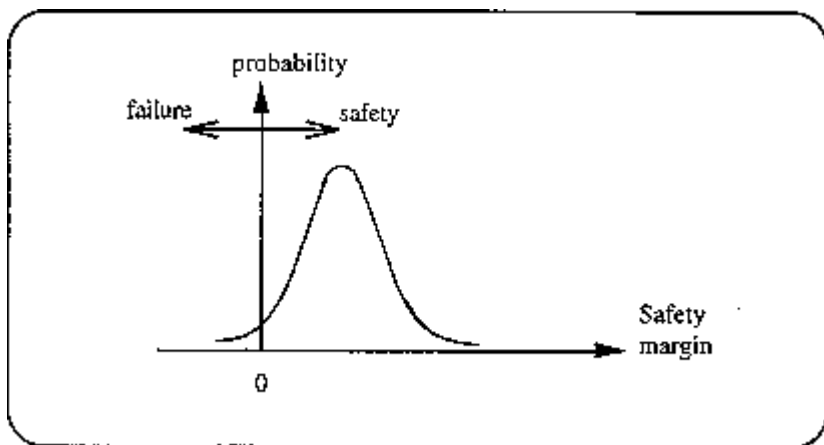
PO Box 117
221 00 Lund
+46 46-222 00 00



Report 3078

Fire Safety Design Based on Calculations

Uncertainty Analysis and Safety Verification



Sven Erik Magnusson
Håkan Frantzich
Kazunori Harada

Lund 1995

Fire Safety Design Based on Calculations

Uncertainty Analysis and Safety Verification

Sven Erik Magnusson *

Håkan Frantzich *

Kazunori Harada **

*** Dept of Fire Safety Engineering, Lund University, Sweden**

**** Dept of Architecture, Kyoto University, Japan**

ISSN 1102-8246
ISRN LUTVDG/TVBB--3078--SE

Keywords: Uncertainty analysis, fire safety, evacuation, risk assessment, Monte Carlo, FOSM, safety index, partial coefficients, design values

© Copyright Institutionen för brandteknik
Lunds tekniska högskola, Lunds universitet, Lund 1995

Omslag:

Layout: Maria Andersen

Illustrationer/Diagram: Håkan Frantzich

Tryckt av Institutionen för brandteknik, Lund 1995

Department of Fire Safety Engineering · Lund Institute of Technology · Lund Univestity

Adress/Address

Box 118 /John Ericssons väg 1
S-221 00 LUND

Telefon/Telephone

046 - 222 73 60
+46 46 222 73 60

Telefax

046 - 222 46 12
+46 46 222 46 12

E-post/E-mail

hakan.frantzich@brand.lth.se

Abstract/

Summary:

Evacuation life safety in a one-room public assembly building has been analysed with regard to uncertainty and risk. Limit state equations have been defined, using response surface approximations of output from computer programmes. A number of uncertainty analysis procedures have been employed and compared: the analytical first order second moment (FOSM) method, two numerical random sampling procedures (simple random sampling and Latin hypercube sampling), standard PRA-method. Eight scenarios have been analysed in isolation as well as aggregated into an event-tree, with branches denoting functioning/failing protection system (alarm, sprinkler and emergency door). Input parameter distributions have been subjectively quantified and classified with respect to category: knowledge or stochastic uncertainty.

Risk assessment results comprise probability of failure p_f , safety index β and CCDF (complementary cumulative distribution function) for evacuation time margin deficit. Of special interest is the calculation of confidence intervals for the distribution of CCDF's obtained by the two phase Monte Carlo sampling procedure, allowing a distinction between knowledge and stochastic uncertainty. The importance analysis carried out analytically gives data of fundamental significance for an understanding of the practical design problem.

Partial coefficients have been treated only by calculating values implicit or inherent in a few existing, sample design configurations. Future studies, preferably using optimization procedures, are needed to produce generally valid values.

1. INTRODUCTION	9
1.1 General background	9
1.2 Objectives	10
2. ASSESSMENT METHODOLOGIES IN GENERAL	13
3. OUTLINE OF CALCULATION EXAMPLE	15
4. THE BUILDING FIRE SAFETY SYSTEM	17
4.1 Definition of sub systems SS1-SS6	17
5. KNOWLEDGE UNCERTAINTY AND VARIABILITY (STOCHASTIC UNCERTAINTY)	23
5.1 The differences between knowledge uncertainty and variability	23
5.2 Description of stochastic model	24
5.3 Overall treatment of uncertainties	25
6. CALCULATION AND SIMULATION METHODS FOR METHODS A-E.	27
6.1 General outline	27
6.2 Method A. The analytical safety index β -methodology	28
6.3 Method D. Standard PRA-methodology	30
6.4 Methods B and C. The use of Monte Carlo simulation studies	34
6.5 Methods A-E and needed software	37
6.6 Response surface methods	38
7. METHODS OF SAFETY CHECKING. DERIVATION OF PARTIAL SAFETY COEFFICIENTS	39
7.1 Limit state functions and checking equations	39
7.2 Methods of safety checking	39
7.3 Partial safety coefficients	41

8. PROJECT OVERVIEW. CHARACTERIZATION OF BUILDING, CALCULATION MODEL AND INPUT DATA	43
8.1 Main building types	43
8.2 Building type #1, Places of assembly	43
8.3 Awareness time	44
8.4 Blockage of emergency door	45
8.5 Characterization of calculation model and input data	48
8.5.1 Calculation model	48
8.5.2 Calculation inputs	51
8.6 Calculated scenarios	55
9. UNCERTAINTY ANALYSIS ACCORDING TO THE FOSM METHOD	57
9.1 Safety index β (Method A)	57
9.2 Partial coefficients	57
9.3 Importance study of parameters	57
9.4 Discussion of results from risk assessment study	58
9.5 Risk assessment versus design. Partial coefficients.	64
10. UNCERTAINTY ANALYSIS ACCORDING TO NUMERICAL SAMPLING PROCEDURES	67
10.1 Two phase simulation procedure (Method C)	67
10.2 Presentation and discussion of results	67
10.3 One phase SRS-simulation procedure (Method B)	72
10.4 Merging eight CCDF to one CCDF (Method E)	75
10.5 Results from method D, standard PRA	78
10.6 Summary of numerical sampling procedures	79
11. SENSITIVITY ANALYSIS	81
11.1 Introduction	81
11.2 Sensitivity studies	81
11.3 Discussion of results	85

12. CONCLUSIONS	87
ACKNOWLEDGEMENTS	93
REFERENCES	95
APPENDIX A THE FIRST ORDER SECOND MOMENT (FOSM) METHODOLOGY. THE RACKWITZ' ALGORITHM	99
APPENDIX B SAMPLING METHODS	103
APPENDIX C DESCRIPTION OF WORKSHEET MODEL	107
APPENDIX D DERIVATION OF REGRESSION EQUATIONS AND KNOWLEDGE UNCERTAINTY	121

1. Introduction

1.1 General background

General principles and/or guidelines for a fire safety design based on calculation has recently been published by a number of standardization groups, see e.g. [1] and [2]. In these guideline documents, the evaluation of the fire safety design of a building is broken down, to simplify the process, into a number of separate subsystems: fire development in room of origin, spread of smoke to neighbouring compartment, etc. The formulation of objectives and criteria are generally closely linked to a specific subsystem or design component. Usually the interdependence of the various subsystems are not explicitly recognized; each subsystem is regarded as a "stand-alone" with its own performance requirements. The draft BSI-guide is a definite step forward in that it clearly outlines the relationship and the data flow between the various design subsystems by using an analogy to a computer "information bus".

What is absent in these references, clearly limiting their practical applicability, are guidelines regarding methods to quantify and verify the safety levels generated by a specific design procedure. Both publications refer rather loosely to a safety format based on use of characteristic values and partial safety factors without quantifying these factors or describe methods to derive them. The draft BSI-code in addition to the "deterministic" partial safety format outlines the use of PRA-methods for design purposes, again without specific guidelines on the analysis and quantification of uncertainties. As we will see later, the preferred methodology for deriving values of partial coefficients is the so called first order, second moment (FOSM) method, leading to the calculation of a safety index β . In its present version, the draft code makes no reference to this method or to the link between β and the partial coefficients γ . From a practical or application point of view, the situation in the fire safety engineering area is thus deeply unsatisfactory and even chaotic.

It is important to understand that performance requirements in the fire safety area are expressed in terms of risk; either explicitly or implicitly. There seems to be a general consensus that performance-based design equals risk-based design. With this statement as a starting point, fundamental questions remain to be discussed and eventually decided upon:

- How do we evaluate risk?
- How do risk evaluation methods differ when we look at different levels of design (the whole building level, the subsystem level, the one component level)?
- What is the link between risk calculation procedures and a deterministic design format, based on safety factors/partial coefficients?
- Calculation of risk means calculations based on models and parameters characterized by uncertainty, usually described by statistical distributions. To what extent are necessary data available for well-defined classes of buildings?
- What do we do when we are not considering a well-defined class of building such as a standard 5-storey office building with a standard layout, and where statistical data may be available, but a single complex building with a unique design layout and fire safety solutions (an example might be a sports stadium or a large underground facility)?
- And many other.

Against this background, the objectives of this paper are defined as follows.

1.2 *Objectives*

This paper will make a first attempt to structure the procedures of uncertainty analysis and safety checking. A major objective will be to illustrate the various methods and approaches by showing calculations and results for an actual design problem. A fundamental starting point is to base the analysis only on mainstream risk assessment procedures developed, tested and utilized in other engineering areas. In this paper we will concentrate on risk assessment methods taken from the area of structural engineering and from the areas of large scale technological systems (chemical process installations etc) and from environmental engineering. For now, we will adopt these methods largely unchanged but we do realize that, as fire safety engineering develops and matures, area specific methods and procedures will be developed.

The objectives of the paper are to

- introduce concepts and methods for risk assessment in areas outside building fire safety. By necessity, the description will have to be incomplete and heavily condensed, as our introduction of some basic statistical and simulation concepts. The reader, unfamiliar with the subject matter, is strongly advised to seek more complete information by reading for example references 5-9
- outline the structures of the safety index β and the PRA-methodologies
- demonstrate their complementary and interlinking characteristic with respect to
 - range of application and choice of design level (whole building, sub-system, single component)
 - uncertainty analyses
 - risk presentation
 - choice of design criteria
 - method of verification and safety checking
- calculate β -values and CCDF-curves for some fire safety system allowed by today's rules (CCDF = complementary cumulative distribution function)
- describe procedures for the derivation of partial safety factors
- discuss the need for improved consistency and quality of QRA and the international standardization efforts that are necessary
- discuss some important practical problems. Standard probabilistic failure analysis takes into consideration only the stochastic variability. It is however necessary to include other sources of uncertainty such as gross errors and the quality of the fire safety management system. A short introductory discussion will be provided, mainly by producing insight into the change of failure of specific protection systems.

2. Assessment methodologies in general

There are a number of assessment approaches available to predict and evaluate the consequences of a fire in a building. Examples include

- hazard assessment or consequence analysis
- scoring systems
- risk assessment.

Here consequence analysis refers to the analysis of the expected effects of incident outcome cases independent of frequency or probability. Deterministic procedures quantify fire growth, fire spread, smoke movement and the consequences of these for the building and its occupants. A deterministic consequence analysis involves the evaluation of a set of circumstances that will provide a single outcome; i.e. the design will be either successful or not. The existing uncertainties are dealt with by taking a (presumably) conservative approach in the selection of input data. In some cases the designer carries out a limited sensitivity analysis. The safety level acquired by a specific design remains unknown and the calculation answer to a specific problem produced by different engineers exhibit a large and inconsistent scatter.

Scoring or index systems force all cases into a common scale by assigning scales of subscores to each characteristic of the hazard and the receiving environment that are thought to be relevant and then combining these subscores into a final score on a standard scale. Systems of this type have been produced for a large number of practical applications, ranging from fire risk in health care occupancies to the ecological effects from sites contaminated with chemical wastes. A common characteristic is that the development of scales and rules for combining scaled variables tend to be arbitrary and with a high potential for bias.

Risk assessment is defined as the process of assigning magnitudes and probabilities to the adverse effects resulting from a fire in a building. The stimulus for adopting risk assessment as a fundamental component of decision making for managing a specific hazard is the recognition that (a) the cost of eliminating all of the safety and environmental impacts from fires may be impossibly high and (b) regulatory decisions must be made on the basis of incomplete scientific information. Risk assessment by providing rational criteria for prioritization of remedial actions, including explicit consideration of uncertainty, is obviously the preferred base for decision making.

3. Outline of calculation example

In order to make the following chapters somewhat less abstract we already here introduce our basic calculation example. The building type is an assembly hall and the study of the analysis is the available safe egress time (ASET) margin for a fire in the assembly room itself. The scenario event tree is shown by Figure 1, outlining the various outcome cases for functioning/non-functioning fire alarms, sprinklers and emergency doors. The event tree indicates the routes by which the initial event (including evacuation) can develop. At each branch, a question is posed related to the development of the event and branch probabilities are assigned, based on statistical data. Each path through the event tree defines a scenario, and accordingly the event tree in Figure 1 defines eight scenarios 1-8.

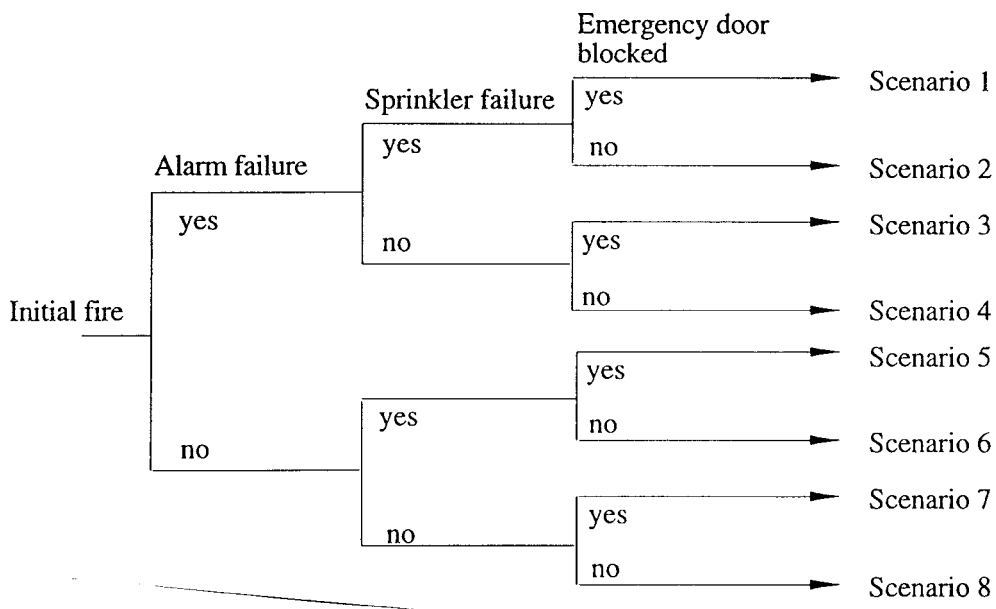


Figure 1. Event tree describing the eight scenarios

The limit state equation is formulated

$$G = S - D - R - E \geq 0 \quad (1)$$

where

S = time for smoke filling to 1.6 m above floor level

D = detection time

R = response and behaviour time prior to evacuation

E = movement

In Eq 1 all elements are considered stochastic. In the deterministic version, G would be replaced by g, etc.

Input data as well as calculated methods will be described in detail in following sections.

4. The building fire safety system

4.1 ***Definition of sub systems SS1-SS6***

The total fire safety system could be divided into a number of subsystems or design modules SS1-SS6. This system is based on the concepts described in recently developed performance-based design systems in Japan, Australia, Canada, UK [1] and the Nordic countries [2]. A more comprehensive and detailed description of the design modules and interactions between them is given in reference 1, which also contains an exhaustive bibliography. The following defines the different design modules:

- SS1 calculation of fire growth in room of fire origin
- SS2 calculation of spread of smoke to other compartments
- SS3 calculation of spread of fire (flames) to other compartments
- SS4 calculation of times to detection and activation of active systems
- SS5 fire brigade communication and response
- SS6 calculation of evacuation times.

In the integrated whole building approach, results from all these subsystems would be combined to describe primarily evacuation safety.

In addition, a characterisation module is needed, providing specific input data describing the building and its occupants.

Figure 2, taken from reference 1, outlines the total fire safety system of a building. Data flow into, out of and between the various sub systems is described via an information bus. To some extent there is a correspondence between the calculation subsystems outlined in Figure 2 and the structure of the regulatory system. Most of the national systems require that design criteria with respect to loss of load bearing capacity, smoke control, evacuation safety, internal fire spread, external fire spread can be proven to be met. One should have in mind that the information bus model in Figure 2 is primarily intended as a base for describing design strategies. The figure per se does not contain any prescription or recommendation for the choice of design strategy.

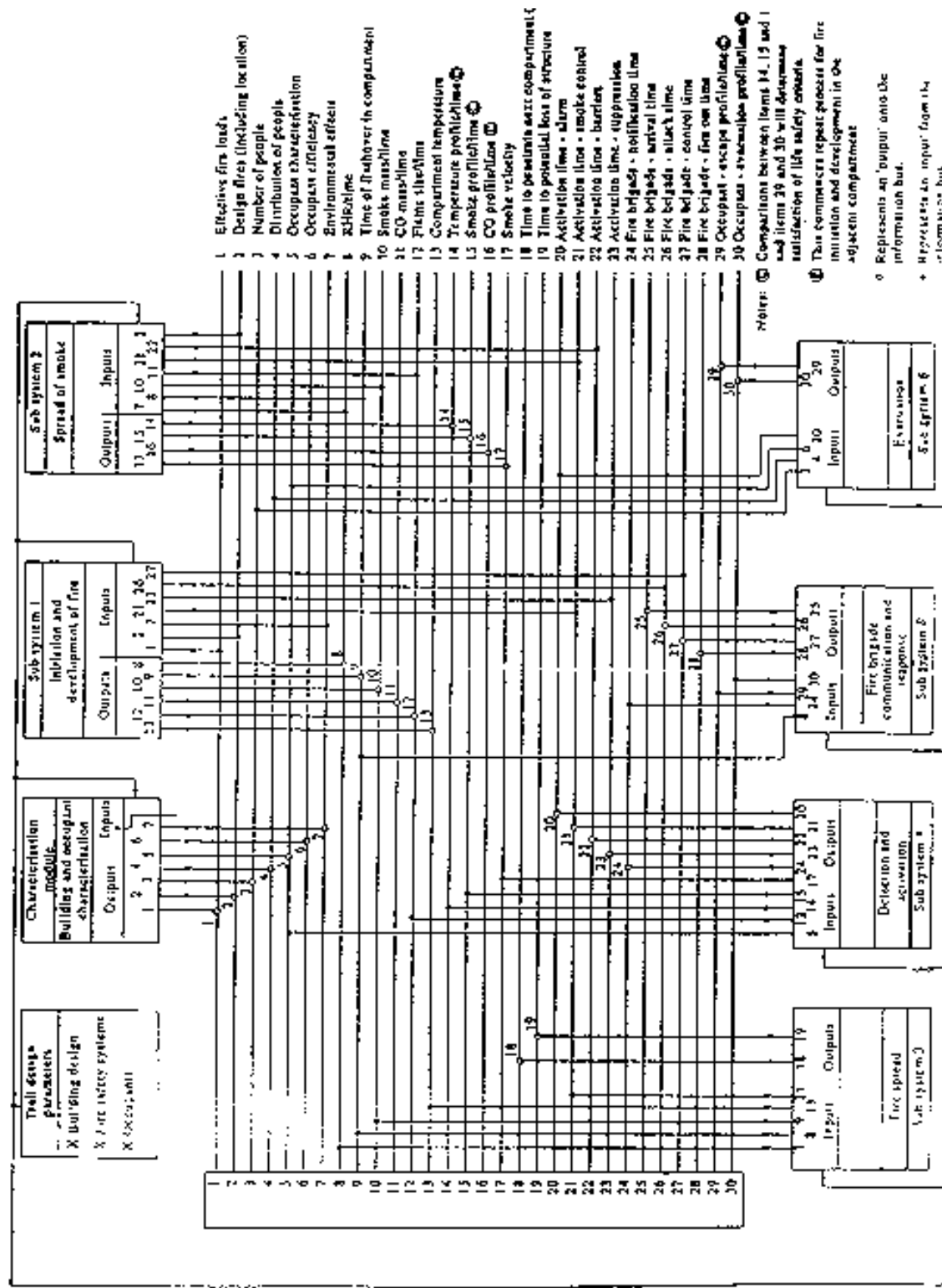


Figure 2. Building fire safety information bus, taken from reference 1

The choice of system level and system boundaries will have a fundamental influence on the choice of risk assessment approach and methodology. The optimal choice of assessment method will be dependent on factors such as

- (a) is the calculational tool a computer program or an analytical expression?
- (b) do we consider a single scenario or the whole event tree?
- (c) to what extent do we include an uncertainty analysis? (For definition, see ref 3)

If we look at Equation 1 and the event-tree depicted in Figure 1 we can outline a number of approaches for a risk and uncertainty analysis, e.g.

- (1) analyze a single scenario with a single limit state described by an analytical expression, derived by a suitable method, and with an uncertainty analysis included
- (2) analyze a single scenario with a computer program and with an uncertainty analysis included
- (3) analyze the whole event tree (8 scenarios) with each scenario described by an analytical expression and without explicit treatment of uncertainties (possibly including a sensitivity analysis of branch probabilities)
- (4) using the same analytical expressions as in (3) but including an uncertainty analysis. The main categories of uncertainty would be branch probability uncertainties, parameter and model uncertainties
- (5) using computer programs analyze the whole event-tree in Figure 1

The analytical equation mentioned in (1), (3) and (4) could basically be of two kinds:

- (a) physically derived (and preferably non-dimensional) correlation. Examples could be mass flow in plumes, smoke-filling times, radiation from flames
- (b) response surface equations describing output from a computer program (see section 6.) The use of meta-models or response surface expressions is explicitly mentioned in ASTM-standard E1355-90 "Standard Guide for Evaluating the Predictive Capability of Fire Models" [3]

NFPA 92 B "Recommended Practices for Smoke Management in Atria Malls" [4] gives numerous examples of analytical expressions of both type (a) and (b).

A number of approaches to uncertainty analysis will be employed in this paper. In order to structure the treatment and describe the use of the alternative approaches as transparently as possible, Figure 3 may be useful. The figure outlines a possible classification system for the risk assessment procedures, denoted method A - E employed in this paper.

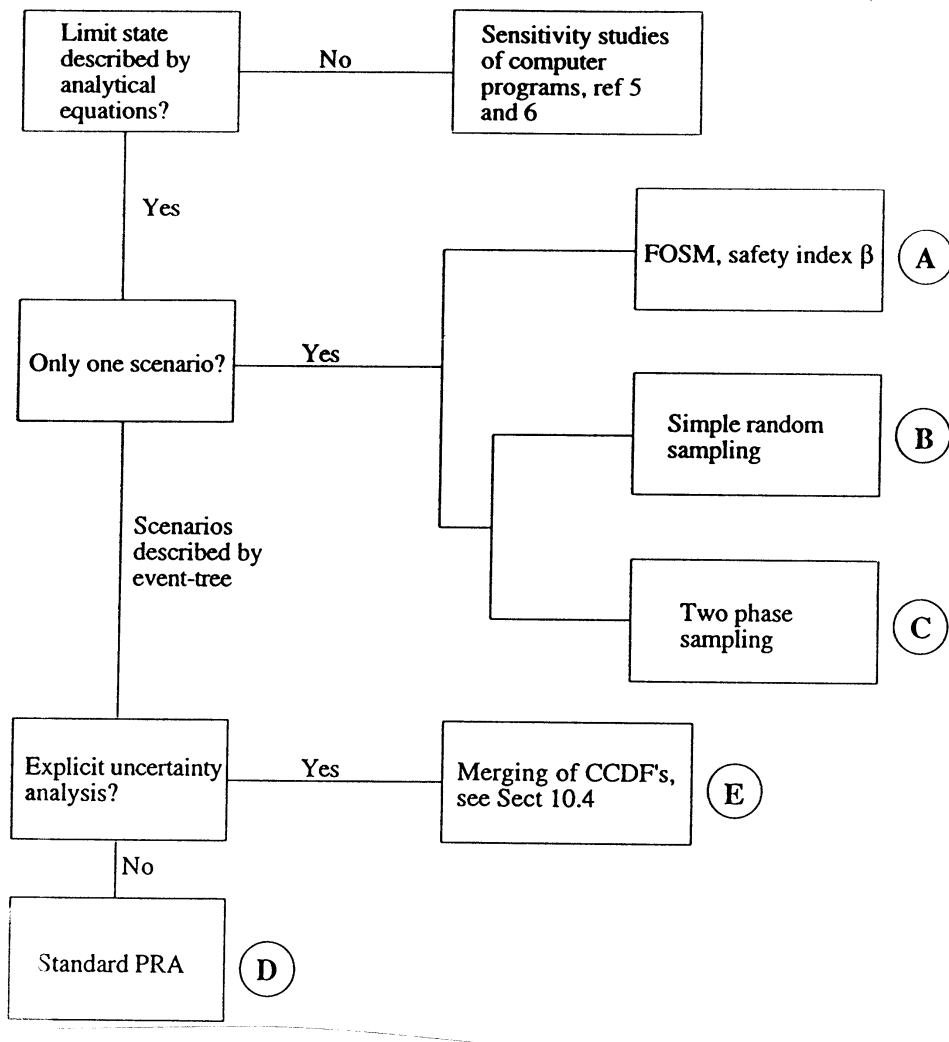


Figure 3. A taxonomy of risk assessment procedures used in this paper

The classification system starts by asking if the assessment problem is described by analytical expression(s). If the answer is no, i.e. the calculation is made numerically by a computer program, available techniques have been described e.g. in references 5 and 6. Reference 25 presents a discussion of the issues involved in conducting a sensitivity analysis of a complex fire model. To reduce the complexity and the length of the paper we will here not consider design based on direct on-line use of computer programs but limit ourselves to use computer programs in the form of response surfaces derived by statistical techniques. As we will see, this will in certain cases imply a considerable increase in model uncertainty. The direct use of computer models and methods of uncertainty analysis in this context will be treated in a future paper.

If we are restricting ourselves to the use of analytical models (i.e. response surface equations), the next question considers the number of limit state equations. If the number is one, two complementary risk prediction methods are immediately available, the analytical FOSM-approach (method A) and the Monte Carlo simulation approach.

In this paper we will distinguish between two Monte Carlo simulation procedures:

- simple random sampling without separation of variability and knowledge uncertainty (method B)
- two phase sampling procedure, involving simple random sampling and Latin hypercube sampling separating stochastic variability and knowledge uncertainty (method C)

If we are simultaneously considering more than one scenario, i.e. we are looking at an event-tree situation, the next question concerns the overall treatment of uncertainties. If these are not explicitly taken into account, we will be using what may be described as standard PRA, characterized by omitting uncertainty analyses. We will denote this method as method D. A crude and elementary uncertainty analysis of the event tree in Figure 1 will be described in section 10.4 and will be termed method E. Even if the system is described as an event tree it is possible to use the "analytical" method FOSM in deriving the relevant parameters. It is then necessary to use rather complex computer programs in solving the system. This will not be done in this paper, but it is the authors' opinion that the extension of the β -method to event tree design situations is a very interesting way forward.

We will in the following sections briefly outline methods A - E. Before doing this, it is necessary to briefly summarize the concepts of uncertainty and variability, the description of a stochastic model including output from model calculation and methods of uncertainty analysis.

5. Knowledge uncertainty and variability (stochastic uncertainty)

5.1 *The differences between knowledge uncertainty and variability*

The following definitions and background discussions are taken from reference 7.

One can distinguish between two types of uncertainties: knowledge uncertainty (fundamental, epistemic) due to lack of fundamental knowledge and variability (aleatory uncertainty, stochastic uncertainty, randomness) in a population. The former can be reduced by additional fundamental information; the latter can be reduced in principle by exhaustive study. The two types of uncertainties, however, can be measured by the same method (probability). When dealing with a single element in the population, both types of uncertainty become the same (lack of knowledge) and the risk is characterized by one probability (e.g., of failure) that represents both types of uncertainty for decision-making purposes. Knowledge uncertainty reflects a lack of knowledge that is described by a probability distribution. Variability represents heterogeneity across some dimension (population, time, space, etc.) that is represented by a frequency distribution. Conceptually, these are very different. Instead of saying that variability and knowledge uncertainty are both described by probability distributions, one should say that they are different but can both be described by probability distributions in many situations, although frequency, in theory, provides an appropriate measure of variability in some situations.

Knowledge uncertainty represents random error, systematic error, irreducible uncertainty, or lack of an empirical basis for making an estimate. It can be addressed, but not necessarily reduced, by better measurements (consider the effect of systematic error on tails of distributions - the systematic error may be revealed by better experimental designs, which could have the effect of increasing uncertainty).

Variability cannot be reduced, but it can be stratified into more nearly homogeneous sub-populations. These can be used to characterize especially sensitive sub-populations.

Variability and knowledge uncertainty have also been referred to as, respectively Type A uncertainty associated with "stochastic variability with respect to the reference unit of

the assessment question" and Type B uncertainty "due to lack of knowledge about items that are in variant with respect to the reference unit in the assessment question". Examples of parameters that are coupled to the two types of uncertainty are given below

- Variability, Type A; wind direction, temperature, fire growth rate over a class of buildings
- Knowledge uncertainty, Type B; model uncertainty, plume flow coefficient, acceptable heat dose on persons.

One should mention that several variables could be affected by both kinds of uncertainty. That could be taken into consideration in performing the calculations.

For further details, see reference 8.

5.2 Description of stochastic model

A model that uses probabilities to represent variability and/or uncertainties is called probabilistic. A probabilistic model produces prediction in distributional forms. Figure 4 illustrates the meaning of probability density functions (PDF), cumulative distribution functions (CDF) and complementary cumulative distribution functions (CCDF). Note that the CDF provides the probability $P(Y \leq y)$ while the CCDF-curve provide the probability $P(Y > y)$; that is "probability that it is worse than..." . This explains the customary use of CCDF instead of CDF in risk assessment studies. In our case the parameter Y is the evacuation time margin G in Eq 1.

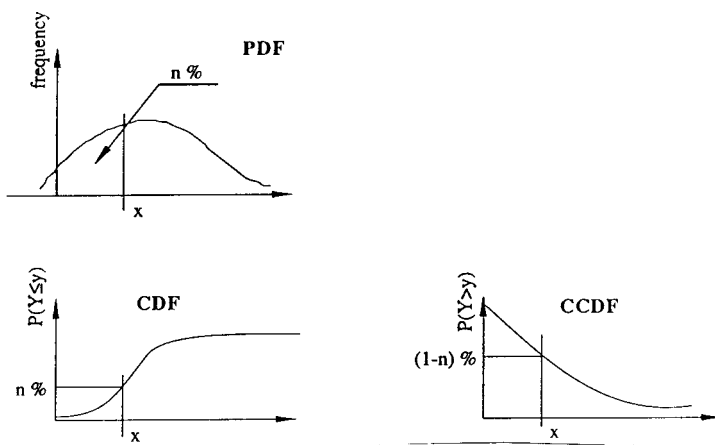


Figure 4. Description of PDF, CDF and CCDF curves

The distinction between variability (stochastic uncertainty) and uncertainty (knowledge uncertainty) will influence the way simulation results are presented. This will be explained further in section 6.4.

5.3 Overall treatment of uncertainties

The factors affecting the reliability of model predictions have been identified as belonging to five distinct categories [8]:

- (1) Uncertainty due to improper definition and conceptualization of the assessment problem or scenario
- (2) Uncertainty due to improper formulation of the conceptual model
- (3) Uncertainty involved in the formulation of the computational model
- (4) Uncertainty inherent within the estimation of parameter values, and
- (5) Calculational and documentation errors in the production of results.

The main steps involved in conducting a parameter uncertainty analysis (item 4 above) are:

- (i) List all the parameters that are potentially important contributors to uncertainty in the final model prediction.
- (ii) For each parameter listed, specify the maximum conceivable range of possibly applicable alternative values.
- (iii) Specify the degree of belief (in percentage) that the appropriate parameter value is not larger than specific values selected from the range established in Step 2 above and select a probability distribution that best fits the quoted degrees of belief.
- (iv) Account for dependences among model parameters by introducing suitable restrictions, by quoting appropriate conditional degrees of belief, or by specifying suitable measures of the degree of association.
- (v) Set up a subjective probability density function (PDF) for the combined range of parameter values. This will subsequently be referred to as a joint PDF. Propagate this joint PDF through the model to generate a subjective probability distribution of predicted values.
- (vi) Derive quantitative statements about the effect of parameter uncertainty on the model prediction.

- (vii) Rank the parameters with respect to their contribution to the uncertainty in the model prediction.
- (viii) Present and interpret the results of the analysis.

Some of the research tasks that can be identified and must be looked into include:

- Identify the important sequences of events (scenarios) and respective mathematical submodels.
- Identify type of uncertainty inherent in input parameters (type A, type B or combined). Use expert opinion or subjective judgement to derive the corresponding subjective distribution functions.
- Estimate model variability.
- Perform analysis of total uncertainty, importance analysis and sensitivity analysis by using Monte Carlo simulation techniques combined with response surface methodology.

Before moving into a treatment of the individual items enumerated above we will summarily describe some major calculation and simulation methods and give some information regarding computer software.

6. Calculation and simulation methods for methods A-E. Software requirements

6.1 General outline

Methods to propagate uncertainty and to calculate the final measure of risk, step (v) in section 5.3, differs for the methods A-E outlined by Figure 3. An important step of the uncertainty analysis involves propagation through the model of the joint distribution of the uncertain parameters to produce a distribution of model predictions, i.e. to derive the PDF or some other statistical representation of the model prediction. The general situation is outlined in Figure 5, taken from reference 8. In the calculation example we will demonstrate later, the model prediction Y in Figure 5 will describe available safe egress time (ASET) margin, the variable G in Eq 1.

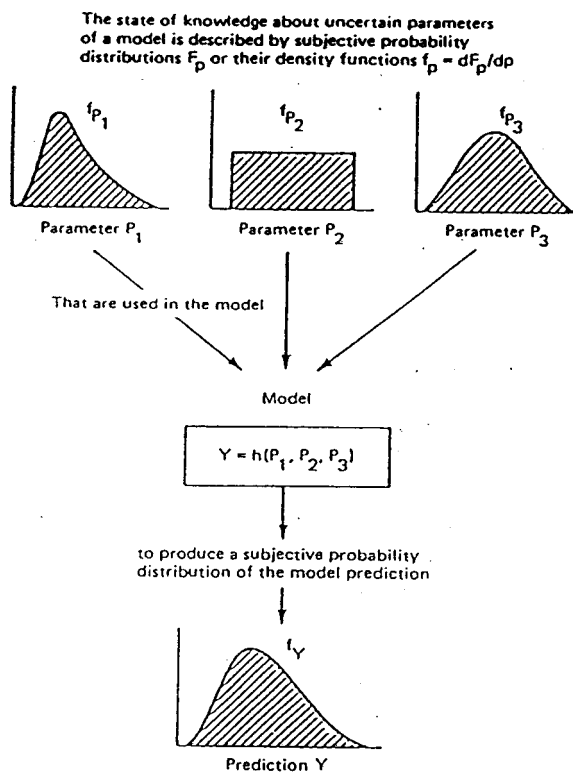


Figure 5. A diagrammatic sketch of Step v (propagation of parameter uncertainties through the model) of a parameter uncertainty analysis of a deterministic model prediction [8]

6.2 Method A. The analytical safety index β -methodology

In this section we will outline the supply-demand R-S reliability-based format and the definition of β . The term reliability is here defined as the probabilistic measure of assurance of performance. The further discussion necessitates introduction of some of the concepts used in assessment of reliability and design based on reliability. The description will be strongly condensed and incomplete and for further information the reader is referred to a standard textbook such as the one by Ang-Tang [9].

For many fire safety engineering components or subsystems the performance may be reformulated in the following way. Let the random variables R and S be defined

R = supply capacity

S = demand requirement

The objective of the reliability analysis is to ensure the event R>S expressed in terms of the probability $P(R>S)$. If the probability distributions of R and S are known and if R and S are statistically independent, probability of failure p_F may be calculated by

$$p_F = \int_0^{\infty} F_R(s) f_S(s) ds \quad (2)$$

where F and f denote the cumulative distribution and frequency functions.

If R and S are normal random variable the distributions of the safety margin M

$$M = R - S \quad (3)$$

is also normal = $N(\mu_M, \sigma_M)$

The parameter $(M - \mu_M)/\sigma_M$ is $N(0,1)$ and

$$p_F = F_M(0) = \Phi\left(-\frac{\mu_M}{\sigma_M}\right) = 1 - \Phi\left(\frac{\mu_M}{\sigma_M}\right) \quad \text{or} \quad (4a)$$

$$p_F = 1 - \Phi(\beta) \quad (4b)$$

with Φ = cumulative probability function of a standard normal variate. The quantity $\beta = \mu_M/\sigma_M$, which determines reliability $p_S = 1 - p_F$, is often called reliability or safety index β . By definition, β is the safety margin expressed in units of σ_M .

The methodology was developed in the late 1960's and has since then been systematically improved and extended in application.

Examples of application can be found in structural engineering e.g. Reference 18, civil engineering, hydraulics, environmental engineering, etc. Possibly the first systematic work on the approach in the fire engineering area is a doctoral thesis from 1974, Reference 10. Fundamental aspects on the use of the safety index β method to the evacuation safety problem have been discussed in reference 21 and 26.

Generally, if the assessment question can be redefined and condensed into a single analytical expression the safety index β method can be employed using the techniques demonstrated in Appendix A. The advantages are several

- handling and analysis of uncertainties are direct and unequivocal
- different designs are explicitly and numerically graded
- the design point, which for normally distributed parameters equals the most probable point of failure, is obtained directly. Naturally, given the design value of a specified parameter and a characteristic value (the mean value, the 80th or 95th percentile, etc) the partial safety factor is directly obtained as the ratio between these values, see section 7.2.

The last point of these three is especially important. The FOSM method has the advantage of directly producing the most probable failure point, that is the design point. The methods based on Monte Carlo simulations does not give this point. By definition, the general FOSM-method provides no information on the distribution of the limit state variable G and probability of failure p_f is obtained approximately by a complicated transformation and linearization process. Monte Carlo methods directly provide information on the probability distribution of the safety margin and thus the value of p_f . The accuracy is determined by the number of simulation runs.

6.3 Method D. Standard PRA-methodology

The standard PRA-methodology is outlined in Figure 6, taken from [11] describing the basic steps in a life risk calculation procedure. In general, the characteristic risk associated with a particular design can be written

$$RL_{TOT} = \sum_{s=1}^{S=S} \sum_{f=1}^{f=F} \sum_{t=1}^{t=T} RL(s, f, t) \quad (5)$$

where

S = number of source locations

F = number of fire scenarios

T = number of target locations

RL (s, f, t) = risk to life for a given source, scenario and target location

In Figure 1, S = 1, F = 8 and T = 1

RL is the product of two factors, the number of deaths in that target and the probability of those deaths. The term fire scenario is used to describe both the ways in which a fire may develop and the ways in each developing fire may be detected and alarm given. The term scenario is synonymous with a specific event sequence through an event tree.

An event tree is a graphical logical model that identifies and quantifies possible outcomes following an initiating event and provides a systematic coverage of the time sequence of event propagation. At each heading or node, two or more alternatives are analyzed until a final outcome is obtained for each node. Each heading corresponds to a conditional probability of some outcome if the preceding event has occurred. The frequency of each outcome may be determined by multiplying the initiating event frequency with the conditional probabilities along each path leading to that outcome. The most common procedure to represent the information obtained by a event tree analysis is by a complementary cumulative distribution function (CCDF). The CCDF provides a display of the information contained in the probabilities pE and the consequences cE (a risk profile). A simple example will illustrate the procedure. Let us go back to our event tree description of possible scenarios, Figure 1. Assume that all uncertainties are negligible

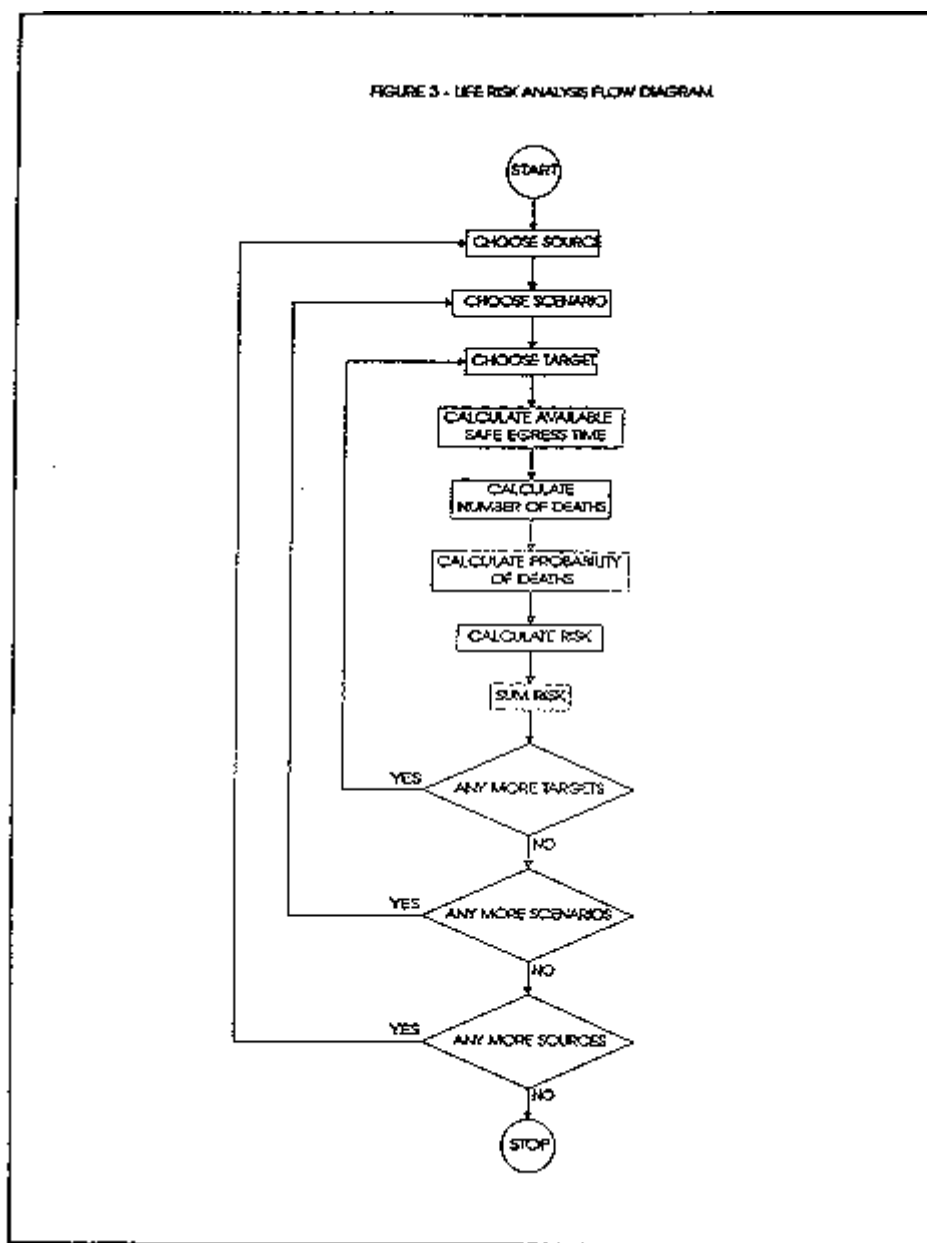


Figure 6. Life risk analysis flow diagram (reference 11)

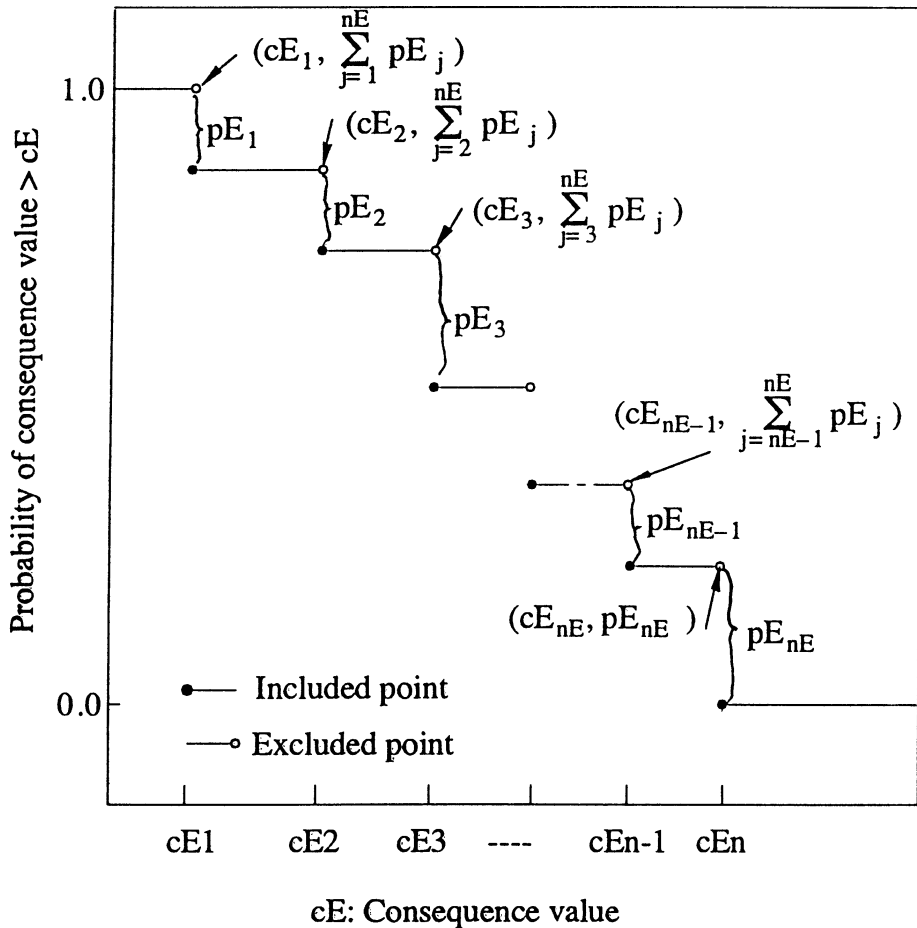


Figure 7. Construction of a CCDF [6]

and all branch probabilities are fixed. The eight consequence results cE_i , $i = 1, \dots, 8$, may be ordered so that $cE_i \leq cE_{i+1}$. The associated CCDF is shown in Figure 7. The CCDF answers the question "How likely is it to be this bad or worse", the frequency of exceedance.

The CCDF curve in Figure 7 is "deterministic" in the sense that probabilities only enter in the form of fixed branch probabilities. Consequence calculations are based on design values of input parameters. The CCDF arises from the fact that the probabilities pE_i define a stochastic variable. If we keep this stochastic variable constant but include knowledge (type B) uncertainties we will have a distribution of CCDF's described by Figure 8. If regard is taken both of stochastic and knowledge uncertainties, the distribution of CCDF's will follow Figure 9. Figures 7-9 are taken from reference 6, to which the reader is referred for further information.

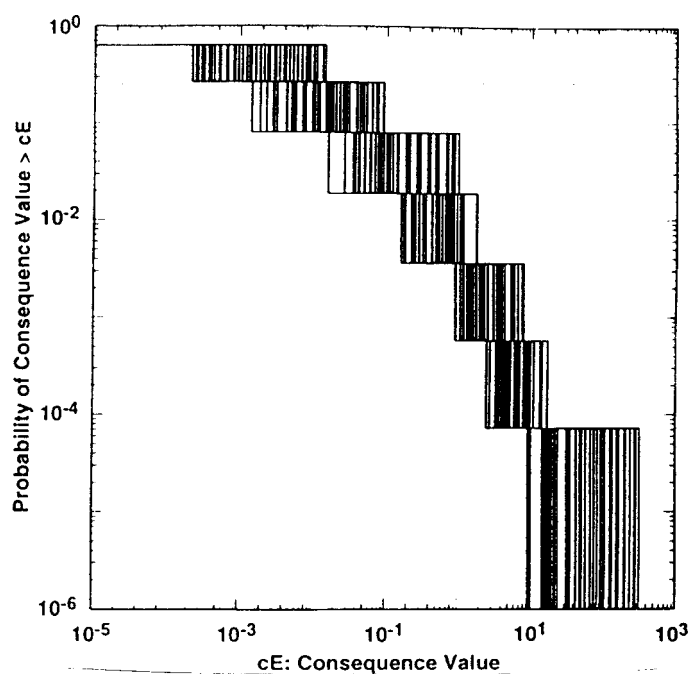


Figure 8 Distribution of CCDFs due to knowledge uncertainty with no uncertainty in the probabilities for individual scenarios [6]

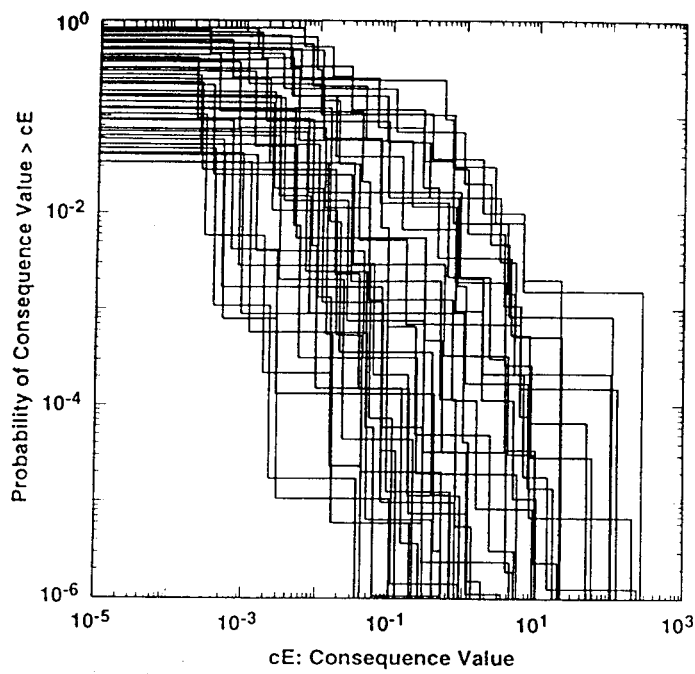


Figure 9. Distribution of CCDFs due to combined uncertainty [6]

6.4 Methods B and C. The use of Monte Carlo simulation studies

In modern quantitative risk analysis, Monte Carlo simulation studies employ a central role. Historically, Monte Carlo methods have been regarded as a last resort to be used only when analytical methods are not available or applicable, the reasons being, firstly the need to write your own software, secondly computer calculating capacity. Rapid growing processor power combined with easily obtained and easy-to-use commercial software has fundamentally changed situation, see section 6.5.

It is the opinion of the authors that the availability of modern personal computers and modern software makes possible a practical implementation of quantitative risk analysis which has not been possible previously.

Applying Monte Carlo methods to the situation outlined in Figure 5 is conceptually straight forward and implies drawing a triplet of values from the three density functions f_{p_1} , f_{p_2} and f_{p_3} and calculate a Y value. By repeating this exercise a large number of times, say 5000, an approximation of density f_Y is obtained and can be treated and analysed by all available statistical methods. The set of triplet is called a sample and here we will limit our description to two kind of sampling procedures, simple random sampling (SRS) and Latin hypercube sampling (LHS), described in Appendix B. The reason for choosing both these methods is also presented in Appendix B.

In Figure 5 the statistical representation of the prediction Y is straight forward. The input parameters p_1 , p_2 and p_3 all represent general uncertainty (either Type A or Type B uncertainty) and the subjective probability distribution of Y represents our degree of belief for Y to be situated in a specific interval. For the situation when both parameters representing variability (stochastic uncertainty) and knowledge uncertainty are present, a two-phase sampling procedure is employed [7], [8], [12], see Figure 10.

Briefly, the procedure is the following: Let \bar{X}_s denote the vector of parameters with variability and \bar{X}_k the vector of parameters characterized by knowledge uncertainty. Single stochastic elements of the vectors are called $X_{S,i}$ and $X_{K,i}$ respectively. Sample vectors are called \bar{x}_k and \bar{x}_s , respectively. First, single values are randomly sampled using SRS, from distributions $X_{K,i}$ representing knowledge uncertainty. Thus we obtain a vector \bar{x}_k . With this vector given, we take a random sample, using LHS, from each of the stochastically varying parameters $X_{S,i}$, giving a vector \bar{x}_s . Using the sample

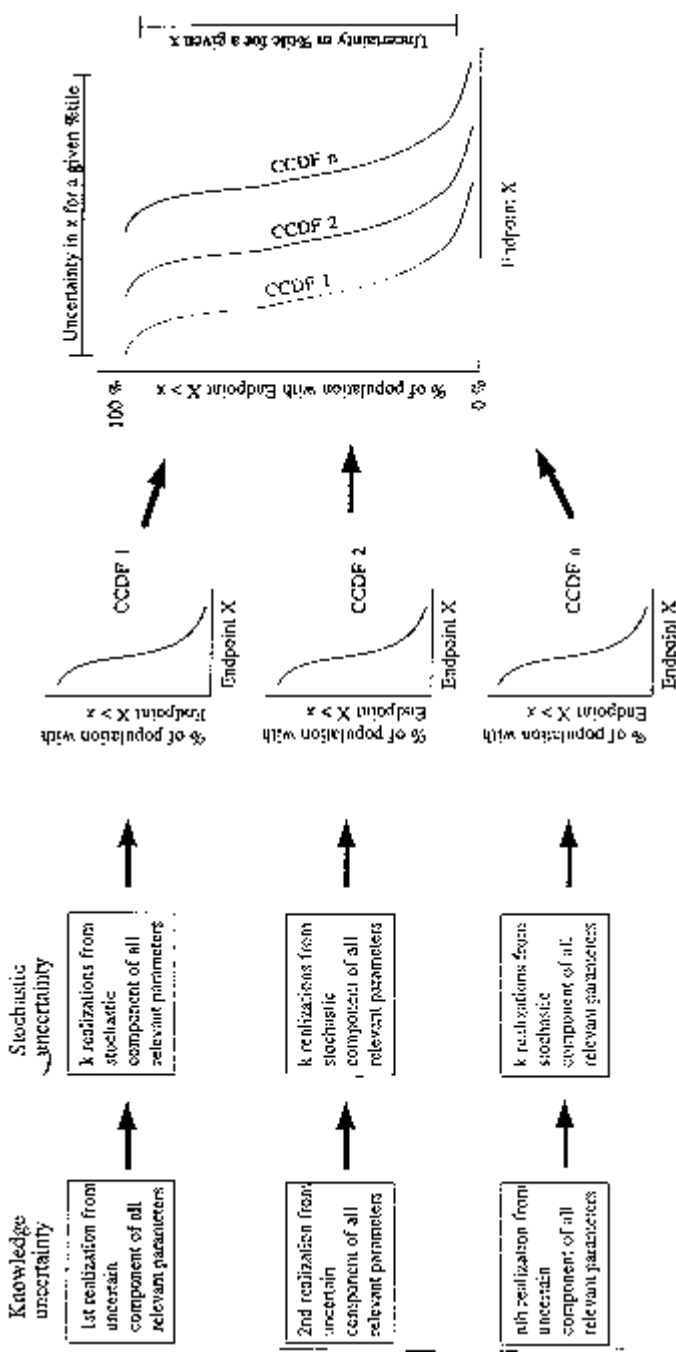


Figure 10. Schematic of the two-phase sampling structure in deriving a set of CCDF's

vectors \bar{x}_k and \bar{x}_s we obtain an endpoint value of limit state equation. Keeping the \bar{x}_k vector constant, the last step is repeated, let us say $k = 100$ times, resulting in a single CCDF-curve for the assessment endpoint variable (in our case ASET margin). Finally, new values are sampled from \bar{X}_k and the procedure repeated n times, producing n CCDF-curves for the evacuation time margin.

In the calculations presented later in this paper using this method a number of n equal to 59 is used. The number 59 was chosen for the following reason [8], describing the derivation of distribution free statistical limits from a simple random sample:

"Upper (u%, v%) statistical tolerance limits are upper v% confidence limits for the desired u% fractile. Therefore one may be v% confident that they are not underestimates of the desired u% fractile. The smallest value n that satisfies the requirement

$$1 - (\text{fractile percentage } u/100)^n \geq \text{confidence level percentage } v/100$$

is the size of a simple random sample such that the maximum prediction value in the sample is an upper (u%, v%) statistical tolerance limit. For $u = v = 95$ one obtains a sample size of $n = 59$. Thus computation of the prediction value for only 59 m-tuples of parameter values from a simple random sample suffices for the maximum prediction value in the sample to be an upper 95% confidence limit of the desired 95% fractile of the subjective probability distribution of the model prediction. It is not necessary to assume a particular type of distribution of the model prediction in the derivation of these limits. For this reason they are called 'distribution free' tolerance limits. It should be noted that the sample size required to obtain a distribution free (u%, v%) statistical tolerance limit is independent of the number m of uncertain parameters and is determined by u and v only."

Practically this means that the left and right hand extreme curves in a diagram with 59 CCDF's equals the 5th and 95th %-tile respectively with a confidence of 95%. In this way it is possible to obtain a confidence interval for the safety margin.

The CCDF's from the 59 different calculations can simply be interpreted in terms of uncertainty. The uncertainty due to variability (Type A) can be observed as differences in the slope of the CCDF's or more precise the difference between the highest and lowest value of a single CCDF. Larger difference or lower slope indicates a high

variability. The uncertainty coupled to knowledge uncertainty (type B) can be seen as the deviation between the far left and far right CCDF in the diagram. A large distance between these two curves indicates a large Type B uncertainty.

As will be demonstrated later, this two-phase parameterization and sampling strategy allows the probabilistic prediction of evacuation time margin as well as the uncertainty in this prediction resulting from knowledge (type B) uncertainty, see Section 10.1.

Mainly, the difference between method B and C is that in method C a distinction is made between variability (Type A) and knowledge uncertainty (Type B). In this way, a distinction can be made between uncertainty which, at least in theory, can be eliminated and variability which always will be present.

6.5 Methods A-E and needed software

Method A: The purpose here is the calculation of the safety index β and the corresponding design values X_i^* . For the simplest cases hand-calculation is possible [9]. For somewhat more complicated cases, appendix C describes a computer calculation procedure based on the spread-sheet program MS EXCEL. Software packages are available commercially.

Method B: Monte Carlo simulation procedures (simple random sampling, Latin hypercube sampling, etc) is offered by a number of commercial simulation packages. We have been using @RISK by Palisade Corporation [13], which is based on the MS EXCEL or Lotus 1-2-3 spread-sheet programs.

Method C: Monte Carlo simulation of a scenario where a distinction between stochastic variability and knowledge uncertainty is made. The calculations were done using the soft-ware @RISK.

Method D: Basic PRA-analysis for various engineering areas is usually carried out by tailor-made commercial software. For the chemical process industry, some packages are described in [14]. A general spread-sheet based approach is outlined in [15].

Method E: Monte Carlo simulation on a system described by an event tree. The results from each branch can be merged into one system probability distribution. The method can be used both for the cases where the uncertain parameters are divided in Type A and Type B as when no distinction between these is made.

6.6 Response surface methods

Some of the standard techniques for performing uncertainty and sensitivity analysis on computer models are described in reference 5. Here we will mention only two of the approaches

- response surface replacement for the computer model
- to use the original computer model but to minimize the required number of samples (computer runs) by replacing simple random sampling with Latin hypercube sampling (see Appendix B)

In this paper we will restrict our treatment to the first approach, derivation of appropriate response equations by use of regression analysis. The derivation of the response surface equation for the terms S and D in Eq 1 is described in Appendix D. We will return to this point later.

7. Methods of safety checking. Derivation of partial safety coefficients

7.1 Limit state functions and checking equations

It is assumed that a scenario has been defined and the appropriate variables (quantities and parameters) have been selected in the form of a random vector $\bar{X} = (X_1, \dots, X_n)$. For a given scenario each variable $x_i, i = 1 \dots n$, is considered a realization of the random variable X_i . In other words, the variable \bar{X} is a point in the n -dimensional basic variable space. Assume that the general condition for a limit state not to be exceeded can be written as

$$G(X_1; \dots, X_n) = G(\bar{X}) > 0 \quad (6)$$

where \bar{X} are the n basic random variables which influence the limit state and G is the limit state function (failure function) and

$$P(G(X_1; \dots, X_n) < 0) < P(\text{target}) \quad (7)$$

where $P(\cdot)$ denotes probability. The equivalent deterministic criterion for safety checking (i.e. checking the sufficiency of fire safety system whose design properties are given) is

$$g(x_{1;d}; x_{2;d} \dots x_{n;d}) > 0 \quad (8)$$

where

g is the same limit state function as above, involving the n quantities \bar{x}_d .

x_{id} is the deterministic design value of the random variable X_i .

7.2 Methods of safety checking

A classification system for different methods of safety checking was developed by the Joint Committee on Structural Safety during late 1970-ies, dividing the methods into three broad classes or levels. This classification is still useful. [18]

Level 1: Design methods in which the appropriate degree of safety is provided by the use of a number of partial, safety factors or partial coefficients, related to pre-defined characteristic or nominal values of the major variables

Level 2: Methods involving certain approximate iterative calculation procedures to obtain an approximate failure probability

Level 3: Methods in which calculations are made to determine the "exact" probability of failure, utilizing the full stochastic description of the random variables X_i and of their joint occurrence and taking into account the true description of the failure domain. In practice, use of Monte Carlo simulation techniques is necessary

A level 1 code is a conventional deterministic code where the appropriate, and in most practical cases unknown, degree of safety is provided by a two step procedure; determination of characteristic values and determination of partial safety factors. The characteristic value x_k of a basic random variable X is defined as the p^{th} fractile of X given by

$$x_k = F_x^{-1}(p) \quad (9)$$

where F_x^{-1} is the inverse distribution function of X .

The selection of the probability p is to a large extent arbitrary but influenced by the following considerations

- characteristic values should rarely be exceeded in practice
- the value of p should not be so large that values of x_k are not occasionally encountered
- for practical reasons it is generally necessary when applying a level 1 code to work with specified values of the design variables rather than with actual characteristic values because the statistical information is insufficient. A specified characteristic value will be denoted, $x_{i,sp}$

The components of the design value vector $\bar{x}_d = (x_{1,d}, \dots, x_{n,d})$ are then given by

$$x_{i,d} = \gamma_i x_{i,sp} \quad (10)$$

with γ_i denoting the relevant partial coefficient. Other ways of defining the partial coefficient could be found in the literature. The one presented here only gives a general description of the partial coefficient. In a level 1 code the partial coefficients are to be seen as a set of control parameters to be selected by an optimization procedure in such a way that the outcome of all designs undertaken to the code is in some sense optimal. Reference 18 describes evaluation methods of partial coefficients and also give examples of probabilistic code calibration exercises in the structural engineering area.

Design according to level 2 involves the mapping of the set of n random variables \bar{X} to a set of independent standard normal variables \bar{X}' with the limit state failure surface given by

$$f(x'_1, \dots x'_n) = 0 \quad (11)$$

The reliability index β is defined in X' -space as the shortest distance from the origin to the failure surface. The corresponding point on the failure surface is referred to as the design point \bar{x}'^* and is obtained by an approximate iterative calculation procedure. If the failure surface is linear and the basic variables $X_i, i = 1 \dots n$, are normally distributed the probability of failure P_f is related to the safety index β by the equation

$$\beta = -\Phi^{-1}(P_f) \quad (12)$$

where Φ is the standardized normal distribution function. For this special case no iteration is necessary. In the general case we obtain the set of values \bar{x}^* for the original basic variables \bar{X} corresponding to the design point \bar{x}'^* by use of inverse mapping. The safety index β according to above is equal to the one presented by Hasofer and Lind, Reference 19. Further details are found in section 6.2 and appendix A.

7.3 Partial safety coefficients

If the values \bar{x}^* are to be used as the design values in a deterministic level 1 design calculation the resulting firesafety subsystem would have a reliability index β and a corresponding value of P_f . The corresponding set of partial coefficients would be

$$\gamma_i = \frac{X_{i,d}}{X_{i,sp}} = \frac{x_i^*}{x_{i,sp}} = \frac{F_{x_i}^{-1}(\phi(x_i'^*))}{X_{i,sp}} \quad (13)$$

However, the use of this relation must be based on a level 2 probabilistic analysis and if this is undertaken there is little point in following it with a level 1 safety check. Furthermore, this leads to a partial coefficient on every basic variable, which is too many in practical design. For the process of producing guidelines and regulations, the partial coefficients are screened for their importance with the less important ones being aggregated into a single partial coefficient. The practical consequence is that design values are evaluated and used directly without the factorization implied by Eq 10.

8. Project overview. Characterization of building, calculation model and input data

8.1 Main building types

The project consists of three building types or evacuation situations on which calculation of the risk of not having enough evacuation time available will be performed. The main building types are

- #1 Places of assembly
- #2 Health care facility
- #3 Hotel incl apartments

In each case fire safety installations are installed. These installations might be operating or not. The fire installations which are investigated upon operation or not are

- Automatic fire detection alarm, with or without evacuation alarm
- Automatic sprinkler system
- Escape route availability

For each building type an event tree, Figure 1, can be set up showing all the events or scenarios that can occur in that building. In every branch a probability of failure or operation can be given.

The events or scenarios will get different probabilities according to their respective branch probabilities. This event tree is not complete in the sense that it takes care of all safety measures. Other fire safety installations or activities such as smoke ventilation or training of people could also be included. The probabilities used in this publication are the following: alarm operation 0.9, sprinkler operation 0.95 and all doors available 0.8.

In this paper we will consider only building type #1, places of assembly.

8.2 Building type #1, Places of assembly

This class of buildings contains rooms and buildings such as theatres, cinemas, shopping centres, restaurants, churches, discotheques, dancing halls, large auditoriums,

indoor sports arenas etc. The characteristics of this group of rooms are that they are large, they contain people with little or no familiarity with the building or the escape routes and the number of people is large. This building type could be divided into two subgroups. The first subgroup contains rooms where the overall visibility is good. It is possible to see what happens in the room wherever a person can stand. This does not mean that it is possible to see everything that could happen in that room but a fire is clearly visible everywhere in the room. Examples are cinemas, theatres, indoor sports arenas, churches and auditoriums. The other subgroup of assembly rooms is those rooms where it is more difficult to observe a fire due to other persons, walls, interior decorations or furniture. This group contains all the places of assembly which are a combination of more than one room, department stores etc.

This means that the times it takes to detect a fire must differ in between the two subgroups if an automatic fire alarm is missing. In Sweden however an automatic fire detection alarm is necessary in this class of building, according to the building code.

In the next sections 8.3 and 8.4 we will in somewhat more detail discuss alternatives in calculating evacuation time and possible changes of the event tree in Figure 1.

8.3 Awareness time

To be able to give an estimate of the awareness time (detection of fire) it is necessary to distinguish between the two groups of places of assembly. In type one rooms people will be able to observe the outbreak of a fire and the consequent time to make this observation will be short. In the calculation this time is assumed to be lognormal with mean=10 and standard deviation=5 seconds. The time is assumed to be given for the last person to observe the fire. Calculating the detection time with DETACT-QS [16], when a fire detection alarm is present, would probably give longer awareness times. This could however be necessary if the fire starts in an adjacent room. This case could be treated as rooms belonging to subgroup two.

In places of assembly in subgroup two, where the visibility is not very good, the awareness time is dependant whether or not an automatic fire detection alarm is installed and working. If it exists the awareness time could be calculated using the DETACT-QS model. If this alarm does not exist or is not working the time to detection

is dependant on the room configuration and fire compartmentation. Determining the detection or awareness time is very difficult for this situation and is dependant on the specific building. A first approximation could be taking the double value calculated with DETACT. This is consistent with data from a fire officers enquiry [17].

Summary

Awareness time could be calculated as follows:

Subgroup 1 rooms (with good overview): lognormal(10,5)

Subgroup 2 rooms (without good overview):

- a if fire alarm is operating: DETACT result
- b if fire alarm is not operating: 2 x DETACT result

8.4 Blockage of emergency door

One of the other branches in the event tree is whether or not one emergency door is blocked. This blockage could be caused by either the fire or by the locking of the door. If the fire occurs close to an emergency exit that exit will not be used and people tend to use other exits. Locked emergency doors are not very frequent but a door could be blocked by other reasons. Goods could be stored in front of a door preventing it from being used. An emergency exit could also be unused because of reasons not tied to a physical blockage of the door. If people are not familiar with the building layout and the fire exits, these exits will not be used to any large extent. This will result in consequences, as if the door was blocked. In places of assembly this is almost always the case i.e. people tend to use the same ways out as they entered the building through. It is however possible to some extent guide people to different exits with the use of exit signs and evacuation alarms with verbal messages. Using the latter a quicker evacuation is to be expected. In conclusion emergency doors are not used if

- a the fire is close to the door
- b the door is locked or blocked
- c the door is unfamiliar to the people.

Fire close to the door

The door will be unused because people can not come close to the door due to the heat radiation from the fire and the believed threat from the fire and its propagation. To be able to do calculations on this, a condition must be formulated telling when this

happens. The radiation condition must be determined by some distance between the door and the fire and could be area-dependant. A more simple approach is to assume that a door will not be used if the fire is closer to the door than 1/3 of the room distance, Figure 11.

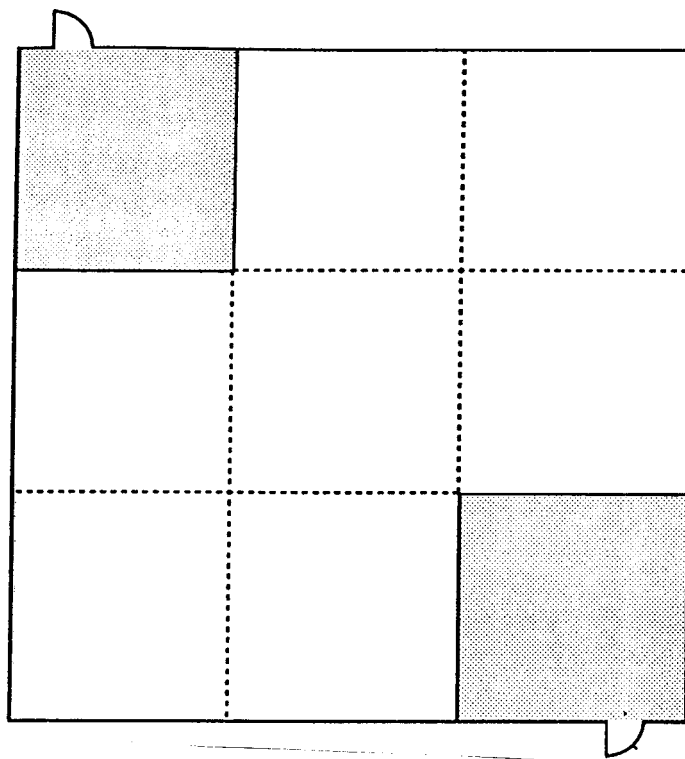


Figure 11. Exit being blocked by an adjacent fire

If the fire is in one of the grey areas then the door will be assumed blocked. In this case the probability of blocked door will be 2/9. In Sweden like in most other countries at least two exit doors are required in this class of buildings. A more refined blocking condition could be when the probability of not using a door is dependent of the room area. If we chose gray areas of $5 \times 5 \text{ m}^2$ the probability of blockage could be calculated as $p_f = 2 * 25 / \text{Area}$.

Locked or blocked doors

Normally doors from places of assembly are kept open during the time when people visit the room. In more seldom cases some doors in shopping centres are blocked by goods. It is not necessary to take locked doors into account.

Door unused due to unfamiliarity of the exit

In places of assembly people tend to use familiar exits even if closer and more secure doors are available. Exact figures indicating the tendency to move towards the familiar exits is not available. An estimate is that 80 % of the people use the normal entrance to the room as the emergency exit. This is dependant on the type of assembly room. In rooms where it is possible to see the emergency exits, like in a theatre or a cinema, it is likely that these exits will be used to a larger extent.

Modifications of the event tree

As more than one exit could be blocked it might be possible to use more than two options at the branch tied to the emergency doors as in Figure 12.

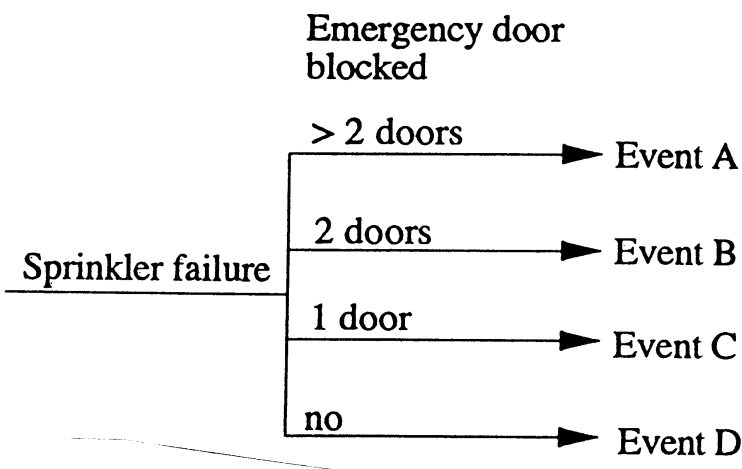


Figure 12. Event tree describing door availability options

In event D all doors from the room are available and the people can evacuate through the closest. In the previous alternatives, A - C, one or more doors are blocked. It is possible to set fixed values on the probability of every branch but this is not realistic. If more than one door is going to be blocked there must be extra doors available to let the people out. According to the building code in Sweden the room must contain more than 600 persons to have three exits stipulated. If 1000 or more persons are permitted, four is necessary. In this project these figures does not have to be taken as obligatory but it shows that it is only in very large rooms that more than one exit could be blocked. The event tree could then be modified as to Figure 13. In our calculation later the probability of one door being blocked is chosen as a fixed value equal to 0.8. This is done to simplify the calculations.

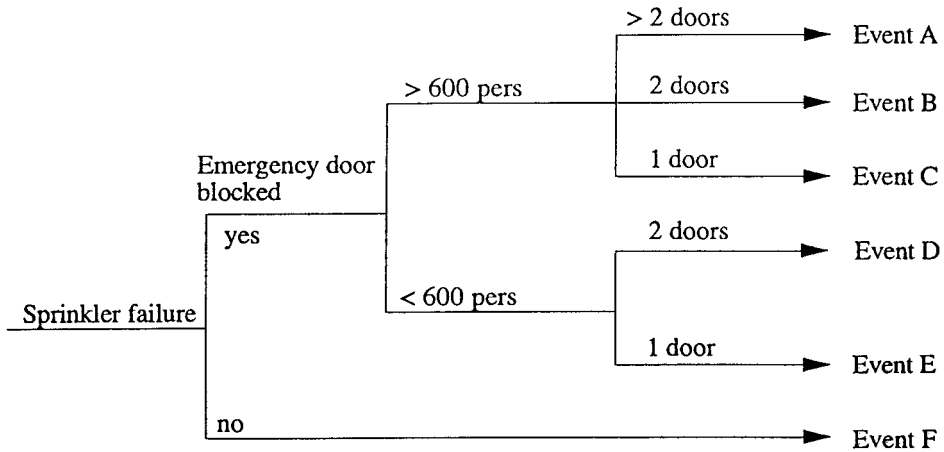


Figure 13. Event tree describing door availability options

8.5 Characterization of calculation model and input data

8.5.1 Calculation model

The basic limit state equation is formulated

$$G = S - D - R - E \geq 0 \quad (1a)$$

where

S = critical time for smoke filling to 1.6 m above floor

D = detection time

R = response and behaviour time prior to evacuation

E = movement time

In addition, modelling uncertainties M_s , M_d and M_e have been introduced into the calculation, transforming equation 1a to the following

$$G = M_S \cdot S - M_D \cdot D - R - M_E \cdot E \quad (1b)$$

The various times are described below.

Critical time S

The fire in each scenario is described as heat output $Q = \alpha t^2$. If the room is equipped with an automatic sprinkler system this will affect the heat output. At the time of activation of the sprinkler system the heat output from the fire will decrease to only a small Q . This small level is then maintained during the rest of the simulation. This is described in more detail in Appendix D. Equations describing the time to reach critical conditions in a fire compartment are derived in the same appendix for these cases when sprinkler is installed and when sprinkler is not installed or not operating. The time to critical conditions is then depending on the fire growth rate α , the room area and the room height, but is only valid for a one-room-scenario. The time to reach critical conditions could also be depending on the presence of smoke vents. If smoke vents are available and working these will open either on a signal from an automatic fire alarm (smoke or heat detectors) or through heat sensors on the specific vent (heat detectors).

The case with smoke vents will be treated in a later publication.

Detection time D

The awareness time is dependant on the type of room, the presence of fire alarm, the room height and fire growth rate. Equations describing the detection time for smoke detectors is derived in Appendix D with the varying parameters room height and fire growth rate. The basic equation describe heat detector activation. The input are chosen in such a way that smoke detection is being simulated.

Behaviour and response time R

The behaviour and response time, denoted R, is depending on the type of evacuation alarm present in the building. The information used in the calculations are obtained from a enquiry among fire officers in Sweden [17]. The data could perhaps be modified according to the type of assembly room, number of rooms, type of occupants, previous training and room area. The present information has a large coefficient of variation, approx 1.0, which indicates a wide scatter in the data.

Movement time E

The evacuation time or more precisely the movement time is simply calculated by looking at the time it takes for a crowd to pass a doorway. The movement time is composed of the time it takes to walk to the door and the time consumed having a crowd passing a door. But as the passing time usually is much larger than the walking time to reach the door the latter is omitted. The movement time is dependant on the number of

available exits, their width and the number of persons in the room. The number of persons in a room is dependant on the type of assembly room and the floor area. In some rooms the number of persons is fixed by the number of seats but in others the number could vary depending on the type of occupancy in the room. The blockage of the exits could be determined according to the information given above.

The dependance from different inputs could be summarized in the following Figure 14.

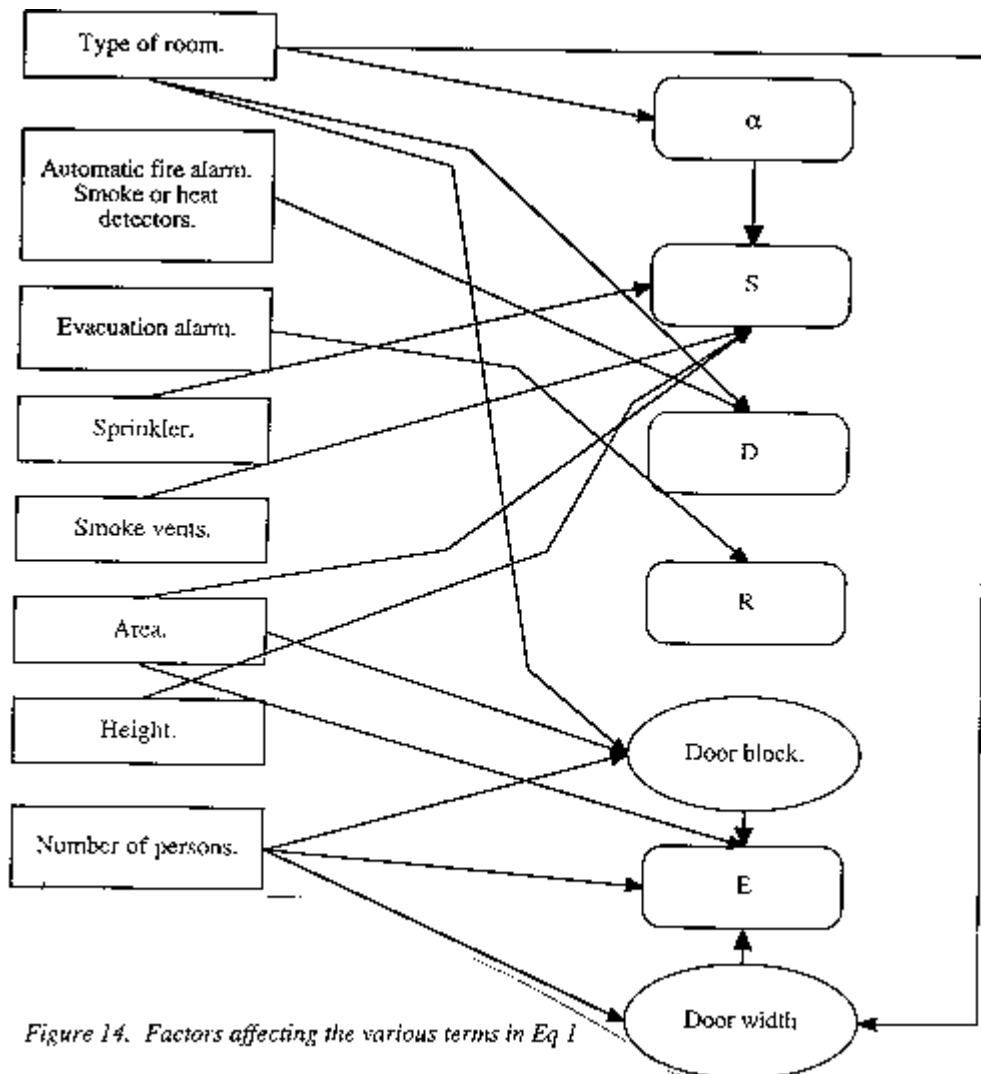


Figure 14. Factors affecting the various terms in Eq 1

8.5.2 Calculation inputs

The different scenarios are described following the event tree given in Figure 1. In this demonstration calculation it is assumed that only one door could be blocked and that it is independent of the room size and occupancy. The calculations are performed in an assembly room. The different scenarios in Figure 1 are described in the following.

Scenario 1 and standard set of distributions

This is the worst case when all the fire safety equipment are unavailable. Fire alarm and sprinkler system is either not installed in the room or not working. One door from the room is blocked during the simulation. The calculation of the time to critical condition is expressed by the response surface equation (see Appendix D)

$$S = 1.67 \cdot \alpha^{0.26} H^{0.44} \text{Area}^{0.54} \quad (14)$$

The awareness time D is determined by introducing D as a stochastic parameter

$$D = \text{lognormal} (10,5) \quad (15)$$

The people behaviour is dependant on the type of evacuation alarm. The room could be equipped with an automatic evacuation alarm with different signals available. In this case when no automatic fire alarm is installed no automatic trigger is available for the evacuation alarm. If the room has an evacuation alarm this has to be manually started. Two different scenarios 1a and 1b could be seen, with or without a manually started evacuation alarm, scenarios 1 a and 1 b. The behaviour and response time for the two cases are chosen as

$$\text{Scenario 1a } R = 30 + \text{lognormal} (130,120) \quad (16a)$$

$$\text{Scenario 1b } R = \text{lognormal} (300,300) \quad (16b)$$

The behaviour and response times are taken from an investigation where fire officers were asked about their opinion [17]. The values are valid for a shopping centre. Both mean values as well as standard deviations are quite large and really not suitable for the present calculations as shopping centre is a class 2 assembly room. It might be better to use some kind of area dependant behaviour and response time given by expert opinion.

The R-value in case 1a is supposed to describe a case with an evacuation alarm with a verbal message plus an extra starting up time. In the following calculation behaviour and response time according to 1b is chosen.

The time for movement of people out from the room is calculated using the following expression

$$E = \frac{N \cdot \text{Area}}{F \cdot W} \quad (17)$$

where F is the specific flow capacity of a doorway.

The number of doors available is set to three. The total numbers of doors in this particular case is then actually four but then one is blocked. Each available door has a minimum free width of 1,2 m which in total gives 3,6 m evacuation width. The number of doors is appropriate for a assembly room of more than 1000 persons according to the Swedish building code and is too many for smaller rooms. But in this first simple calculation the door width is fixed. It is possible to have the door width set to a distance according to the actual room depending on the number of persons present. This will not be done here.

The expressions determining for example the time to reach critical conditions have been performed using computer models and deriving response surfaces with regression analysis, see Appendix D. These computer models do have some deficiencies in predicting the correct values wanted. To be able to correct these values specific parameters have to be introduced describing calculation model uncertainties. For details, see Appendix D.

In the above equations parameters with stochastic variability comprise α ; the growth rate of the fire, D; detection time, R; behaviour and response time and N; the people density. The model uncertainty comes in as correction factors for the specific parameter. The statistical distributions for the parameters and model uncertainties are chosen as follows

α ; uniform (0.001, 0.1) kW/s^2

D; lognormal (10, 5) s

H; uniform (3, 12) m

Area; uniform (200, 1200) m²

R; lognormal (300, 300) s. See scenario 5

N; triangular (0.1, 0.8, 1.0)

M_S; normal (1.35, 0.1)

M_D; normal (1.0, 0.2)

M_E; normal (1.0, 0.3)

The total expression to be used for a Monte-Carlo-simulation is then

$$g = [1.67 \cdot \alpha^{-0.26} H^{0.44} \text{Area}^{0.54}] \cdot M_s - D - R - E \cdot M_E \quad (18)$$

The set of distributions defined above constitutes the "standard set of distributions".

Scenario 2

This scenario has many similarities to the previous one. The only thing that is different is that all emergency exits are available which gives a total free exit width of 4,8 m. All the stochastic parameters are also the same as in scenario 1.

Scenario 3

The parameters that separates this scenario from scenario 1 is that the sprinkler system is working, giving longer time to reach critical conditions. As in scenario 1 one of the evacuation exits are not available giving the total exit width equal to 3,6 m. The fact that the sprinkler system is working will change the response surface expression for the time to reach critical conditions to

$$S = 0.025 \cdot \alpha^{-0.114} \cdot H^{0.457} \cdot \text{Area}^{1.28} \quad (19)$$

Observe that for this case total model uncertainty will be substantially increased, see Appendix D. The awareness time, behaviour and response time and the movement time will be unchanged compared to scenario 1.

Scenario 4

In this scenario the detection system is not working (the same goes for scenario 1-3) but the sprinkler system is working and no emergency doors are blocked. The response surfaces could be found in the above scenarios.

Scenario 5

This is the first scenario where an automatic fire alarm is installed and operating. The people in this room will therefore be alerted either by the means of evacuation alarm or by seeing the fire as was the case in the previous scenarios. The time to critical conditions is calculated with equations for the nonsprinklered case.

$$S = 1.67 \cdot \alpha^{-0.26} \cdot H^{0.44} \cdot \text{Area}^{0.54} \quad (20)$$

The time for the people to be aware of the fire could be determined by the calculated time for detector response (smoke detectors) using the following expression.

$$D = 5.36 \cdot \alpha^{-0.478} \cdot H^{0.7} \quad (21)$$

But people could also be aware of the fire by seeing it and probably get notified earlier than by the detection system. If the detection system is working it could however start an evacuation alarm with a verbal message to the people and that will result in a shorter behaviour and response time. The total of this is that although the awareness time by detectors is longer than human detection the behaviour time is shorter when using the evacuation alarm giving a shorter total evacuation time. The behaviour and response time could be taken from the distribution

$$R = \text{lognormal}(130, 120)$$

The movement time is calculated using the total free exit width of 3,6 m, that is one door blocked.

Scenario 6

This scenario is very much like the previous one but with a movement time calculated using 4,8 m exit width. In this scenario all doors are available.

Scenario 7

In this scenario the detection alarm and the sprinkler system is operating. This will give a time to critical conditions as

$$S = 0.025 \cdot \alpha^{-0.114} \cdot H^{0.457} \cdot \text{Area}^{1.28} \quad (22)$$

The movement time is calculated using the door width of 3,6 m. One door is blocked. Other values are like in scenario 5.

Scenario 8

In this scenario all fire protection installations are working as intended. This means that all exit doors are operational as both the fire detection system as the sprinkler system. The movement time is calculated using the door width of 4,8 m and all other expressions as in scenario 7.

8.6 Calculated scenarios

In the following two chapters 9 and 10, calculations will be presented using some or all of the scenarios described in this chapter. The scenarios will be calculated using the different methods described in previous chapters. The methods are according to Figure 3 FOSM (A), simple random sampling (B) and two phase sampling (C). For the results obtained in the simple random sampling and the two phase sampling calculation, a merging procedure is performed (E) to look at an entire event tree system analysis. The standard set of distribution is defined as in the previous section. Door widths are also specified in this section.

Results from method A are presented in chapter 9, method B in section 10.3, method C in section 10.1 - 10.2 and method E in section 10.4. A simple calculation using method D ("standard PRA") will be shown in section 10.5.

9. Uncertainty analysis according to the FOSM method

9.1 Safety index β (Method A)

Using the methodology described in Chapter 6, the safety index β and corresponding probability of failure were calculated for the scenarios. A worksheet model was developed to carry out the calculation. A brief description of this model is available in Appendix C.

The distributions are the same as in section 8.5.2.

In this methodology it is not possible to distinguish between stochastic variability and knowledge uncertainty. The scenarios calculated are the same as in section 8.5.2.

9.2 Partial coefficients

The safety index β and its corresponding probability of failure $p_f = \Phi(-\beta)$ are calculated for each door width. In the course of calculations, most probable failure points (MPFP) are directly obtained. From which, partial safety factors are calculated by taking the ratio MFFP/mean value

$$\gamma_{x_i}^* = \frac{x_i^*}{\mu_{x_i}} \quad (13)$$

where x may be any of the variables, α , R , N ,

Observe that here the characteristic value is defined as the mean value. Some other possibilities of choosing the characteristic value are mentioned in References 1 and 18 and are also discussed in Section 7.3.

9.3 Importance study of parameters

It is possible to study the sensitivity of each variables, and to decompose the total variance (variance in limit state function) into components. The total variance in limit state function, g , is approximated by first order method as

$$\sigma^2(g) = \sigma^2\left(\sum_i \frac{\partial g}{\partial x_i} x_i\right) = \sum_i \left(\frac{\partial g}{\partial x_i}\right)_{x_i=x_i^*} \sigma^2(x_i) = \sum_i \left(\frac{\partial g}{\partial x_i}\right)_{x_i=x_i^*} \sigma_{x_i}^2 \quad (23)$$

which allows the decomposition of the total variance into components. The fraction of variance caused by the i -th variable, x_i , is,

$$\frac{\left(\frac{\partial g}{\partial x_i}\right)_{x_i=x_i^*} \sigma_{x_i}^2}{\sum_i \left(\frac{\partial g}{\partial x_i}\right)_{x_i=x_i^*} \sigma_{x_i}^2} \quad (24)$$

9.4 Discussion of results from risk assessment study

The calculation of the safety index β and its corresponding probability of failure using the FOSM method is performed according to the procedure in appendix C. The results are presented in Figures 15 and 16. Included in these diagrams are results from a merging procedure (method E), in detail described in section 10.4, for comparison.

As the β -values are quite low we investigated how the door width affected the outcome of the β -value. This calculation was performed on scenario 6.

The results are shown in Figure 17 for β values and probability of failure. As the door width is increased from 1 to 20m, the β value is increased from a negative value ($W=1$) to 1.18 ($W = 20$ m). At the extreme when $W \rightarrow \infty$, β will reach the value of 1.26. At the same time, the probability of failure is decreased to 10.3% as $W \rightarrow \infty$.

Figures 18 a - h describes the composition of the total variance or uncertainty into component variances, for scenarios 1 - 8. A quantification of component variances is necessary from at least two objectives:

- to define the uncertainty (the knowledge uncertainty) which at least from a theoretical point of view may be reduced as distinct from the variability,
- to identify the most cost-effective way of reducing the knowledge uncertainty (and increase the safety index β)

Figures 18 a - h indicates that the major contributors to the overall uncertainty comes from parameter R (variability or stochastic uncertainty) and Area (variability or stochastic uncertainty). For non-sprinklered fires (scenarios 1,2 5 and 6), the variance in R is dominating while for fires with a sprinkler operating (scenarios 3,4 7 and 8), the variance derived from Area becomes increasingly more important. The reason is given by comparing the two equations 14 and 19.

The decomposition of the total uncertainty into component uncertainties for scenario 6 is plotted in Figure 19 over a range of evacuation door widths. When the door width is relatively small, the largest component uncertainties are linked to variables N and R. For larger door widths, the variable Area is becoming increasingly important with R still providing the largest uncertainty. Fire growth factor α is of very small significance. The variances caused by M_E , M_D and M_S are insignificant, implying that knowledge uncertainty is very much smaller than the stochastic uncertainty, i.e. the variability. This in turn implies that for practical design purposes, the major part of the uncertainty is irreducible and has to be accepted.

Some conclusions from Figures 15-19:

1. Human behaviour is clearly the controlling process. The consequences are at least two
 - a) much more data will be needed in this area
 - b) quantified criteria in a regulation must be based on standardized distribution, at least in R
2. The underlying uncertainties are so large that a commonly used design criteria with safety index $\beta = 2$ cannot be met
3. This is a pilot investigation and the distributions characterizing the stochastic elements have been chosen subjectively by a small group of persons. It is clearly possible that we have chosen the distributions conservatively, i.e. by exaggerating the actual or real uncertainty. This could explain a basic result: calculated safety levels seem rather low. (Naturally, all figures are calculated supposing a fire has actually started)
4. For larger evacuation widths W, the personal risk is nearly independent on W

5. Figure 19 shows that stochastic uncertainty is by far more important than knowledge uncertainties
6. We are considering a whole class of buildings with a large range of values for the height and the floor area design parameters. Figure 19 implies that a subdivision into several classes with a lesser variation in H and A might substantially decrease the final uncertainty. Observe that the relative importance of uncertainty sources varies strongly with chosen evacuation door width.
7. For a fixed door width, the relative importance of a specific stochastic variable can change drastically from one scenario to another.

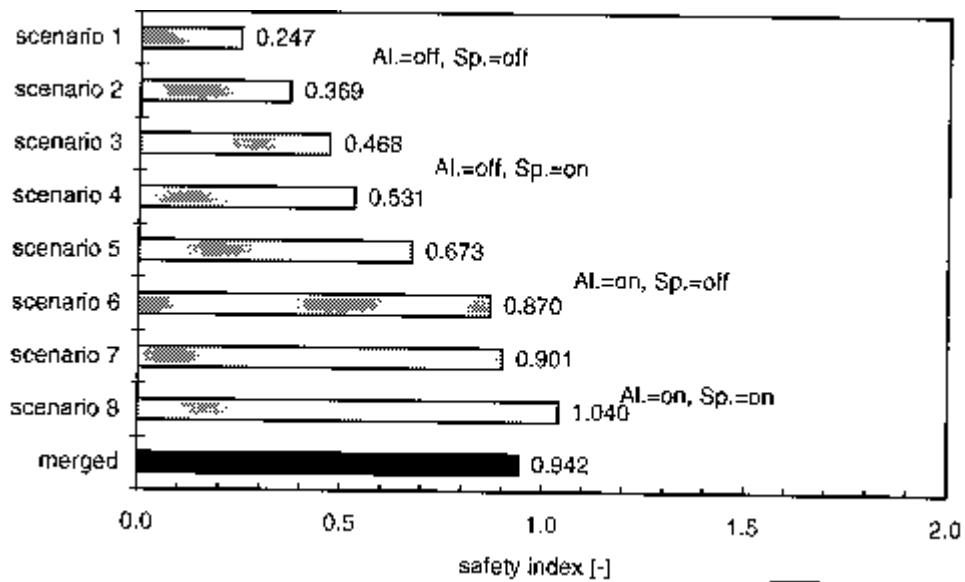


Figure 15. Safety index β for scenarios 1-8 using method B

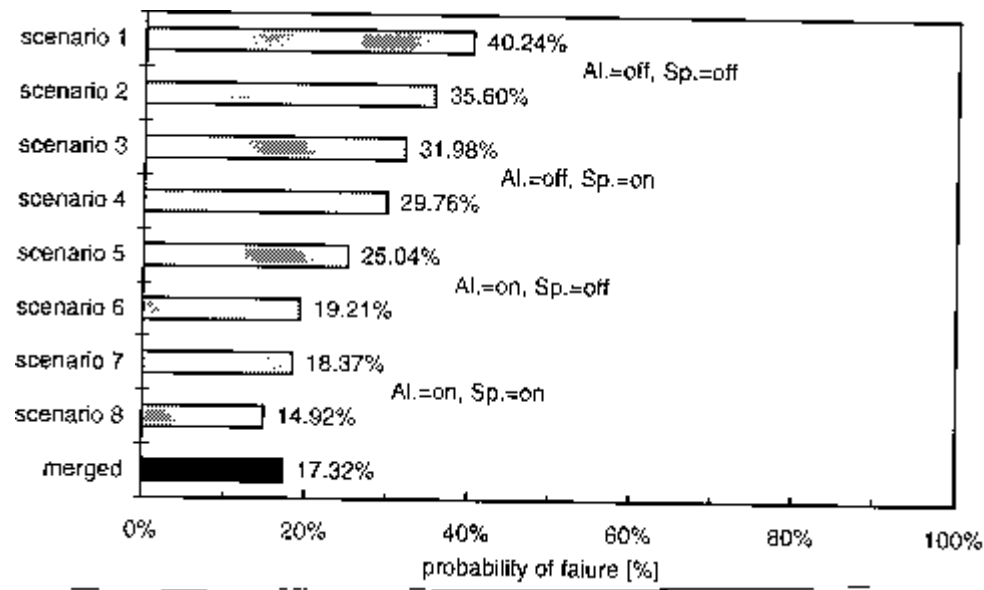


Figure 16. Probability of failure for scenarios 1-8 using method B

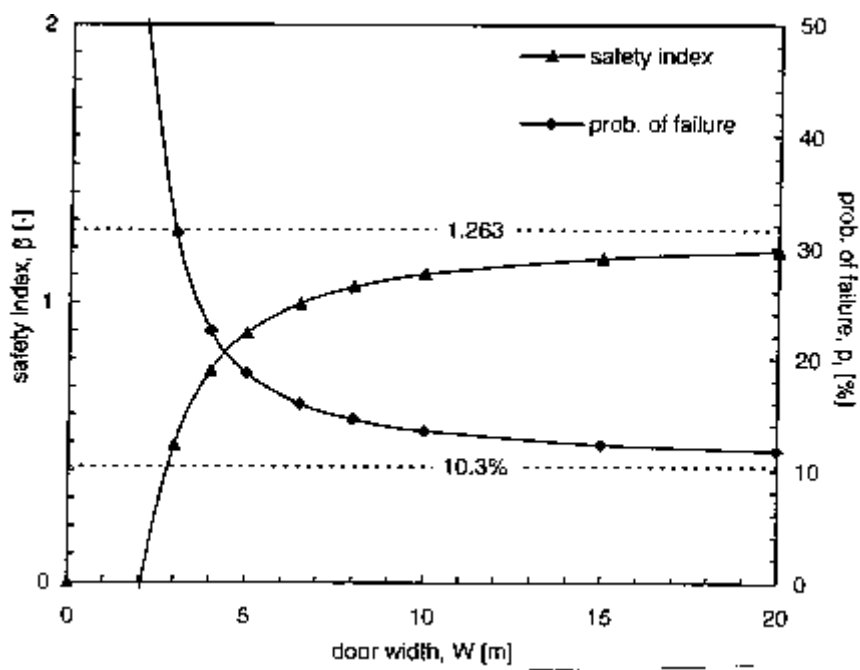


Figure 17. Safety index β and probability of failure with FOSM method for scenario 6

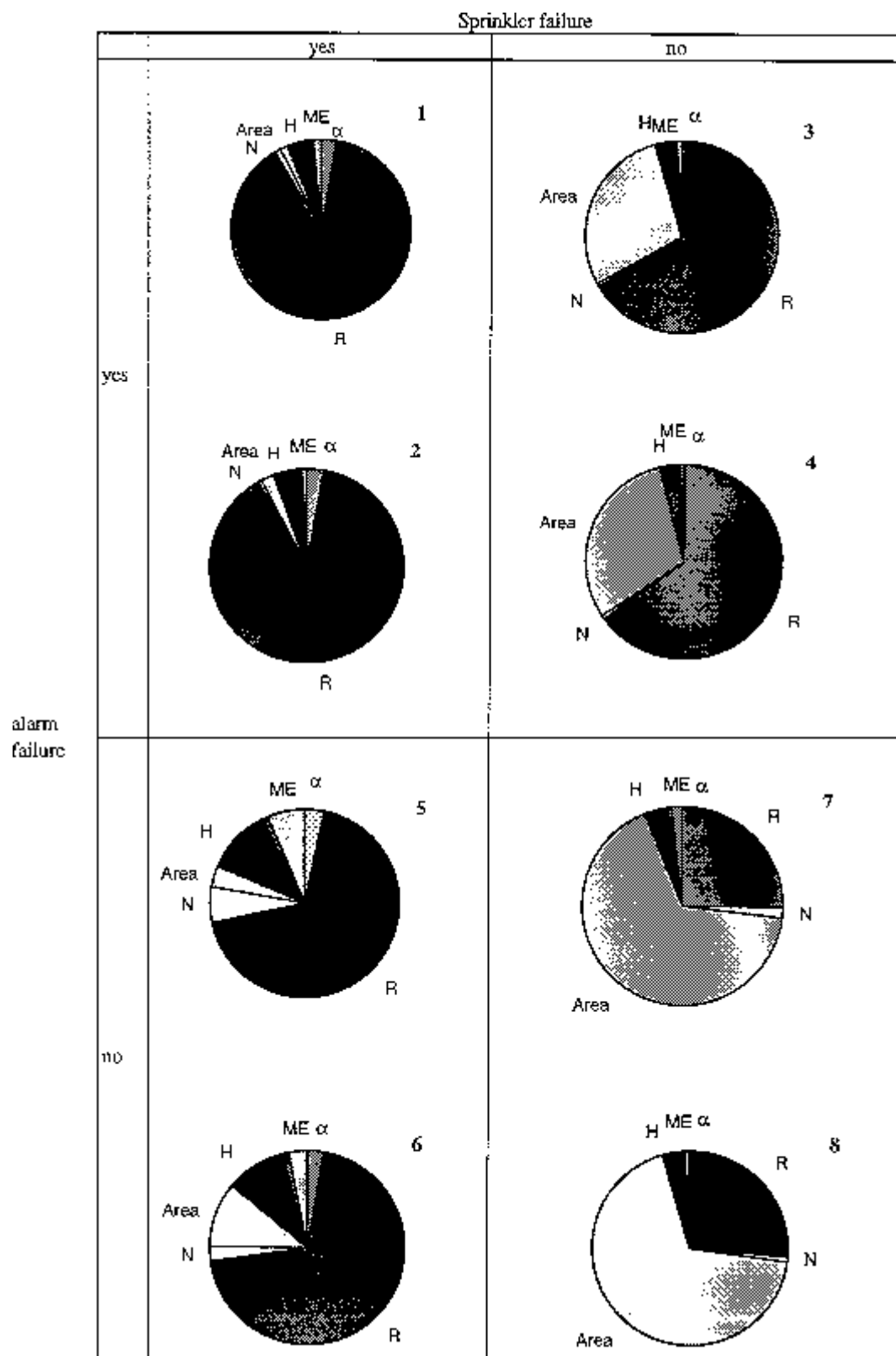


Figure 18. Division of total uncertainty into component variances for scenarios 1 - 8.

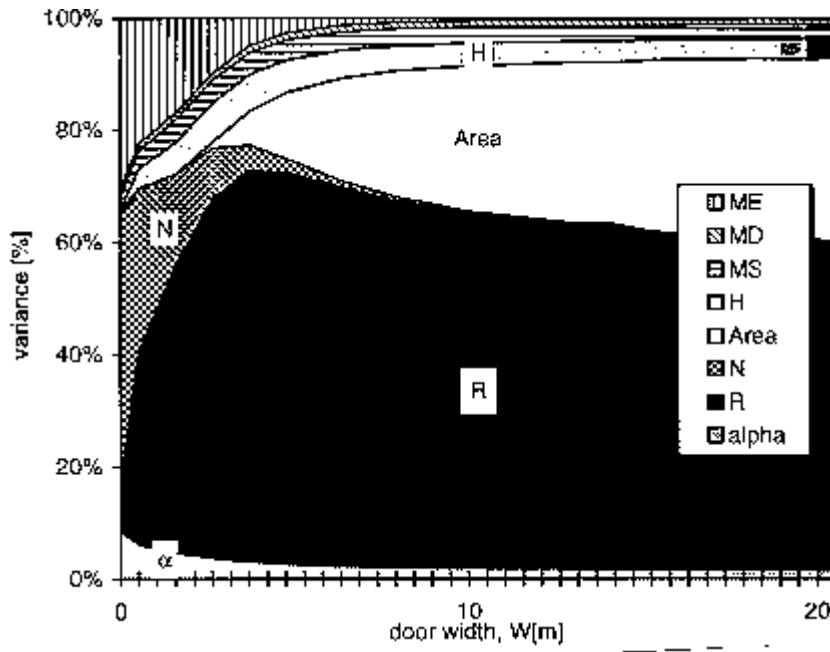


Figure 19. Decomposition of total variance of variables using FOSM method (method A). The results are from calculations on scenario 6

9.5 Risk assessment versus design. Partial coefficients.

The uncertainty analysis carried out in this chapter so far assume that we are studying the evacuation safety level for a whole class or population of buildings on, let us say, the national level. In other words, we have carried out a risk assessment of existing buildings. When we are looking at the practical design situation, some parameters like the building area and height will be deterministic and the problem will be to derive values for the exit width W such that a particular safety level (expressed as β or p_f) will be obtained. In a level 1 design method, partial coefficients will have to be provided for the major stochastic variables in Equation 1, see Equation 13. From a building regulation point of view, the problem is to prescribe a set of partial coefficients γ_i such that, taken over the practical range of H and Area, the deviations from the selected safety level is minimized. The procedure is described more in detail in section 11.4.3 of reference 18. We will return to this problem in a future publication. Here we will just indicate some of the problems that will have to be dealt with. Table 9.1 shows values of β and p_f and design values of α and N for different combinations of building area and height. All calculations are made for scenario 6 and an exit width of 4.8 m. The β -value

varies between -0.48 and 1.38 while design values for α and N exhibit a low variation. The high variability of β implies that in a code calibration procedure it may prove difficult to derive a unique and universally valid set of partial coefficients.

Table 9.1 Scenario 6. Derivation of p_f , β and design point values for a variation of area (200 - 1600 m²) and height (3 - 8 m).

Height, Area	p_f	β	α^*	N^*
3, 200	68.6	-0.48	0.047	0.64
5, 200	59.8	-0.25	0.049	0.65
8, 200	52.5	-0.06	0.05	0.66
3, 1000	33.7	0.42	0.056	0.69
5, 1000	19.8	0.85	0.06	0.71
8, 1000	11.2	1.22	0.062	0.72
3, 1600	33.7	0.42	0.057	0.7
5, 1600	17.7	0.93	0.063	0.74
8, 1600	8.5	1.38	0.066	0.75
m, m ²	%		kW/s ²	Pers/m ²

10. Uncertainty analysis according to numerical sampling procedures

10.1 Two phase simulation procedure (Method C)

The effect of knowledge uncertainty was analyzed for the scenarios 1. The two phase Monte Carlo simulations were carried out as described in chapter 7. In the first phase, 59 values were sampled for knowledge uncertain parameters, M_s , M_d and M_e by simple random sampling. In the next phase, Latin hypercube sampling was applied to stochastic variables. As a result, we got 59 CCDF curves for each scenario. According to the statistical theory, the upper and lower bound of the 59 CCDF's are the good estimate of 5 and 95 percentile values of confidence interval.

The distribution functions for knowledge uncertainty parameters are, (as previously):

$$M_s = \begin{cases} N(1.35;0.11) & \text{(non - sprinklered fires)} \\ N(1.35;0.23) & \text{(sprinklered fires)} \end{cases},$$
$$M_d = N(1.0;0.2),$$
$$M_e = N(1.0;0.3).$$

Observe that the process of approximating computer output with a response surface equation considerably influences the uncertainty in the factor M_s .

10.2 Presentation and discussion of results

The results for scenario 1 are shown in Figure 20. Y is a stochastic parameter describing evacuation time deficit (= - g in Eq 18) and p = probability $P(Y > y)$ for any given value of y. The assessment question may be formulated: Given a fire in an assembly type of building (room) what is the distribution of the evacuation time deficit as a consequence of that fire? The prediction is a single probability distribution but the correct distribution is unknown because of type B uncertainties. This implies that quantitative uncertainty statements are given in the form of subjective confidence limits (fractiles) at a high ($\geq 95\%$) confidence level. The sample size was = 59 in order to obtain a distribution free statistical 95% confidence limit for the 95% fractile. Studying Figure 20 it is possible to make statements such as: At a subjective confidence limit of 95% the conditional probability for the evacuation time deficit to exceed y is below the ordinate value of y of

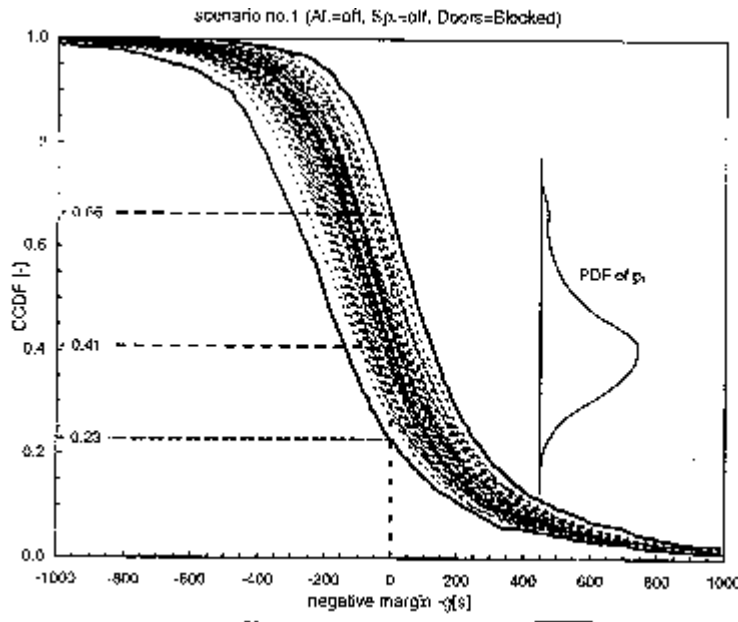


Figure 20. Evacuation time deficit (negative time margin) for scenario 1 using method C

the extreme righthand curve. Selecting $y = 0$ gives $p = 0.66$. Selecting the confidence limit $v = 50\%$ gives $p = 0.41$. Expressed differently: we can be 95% confident that probability of failure will be lower than 0.66 and 50% confident that it will be lower than 0.41.

The CCDF's are cut at the line of $g = 0$. The distribution of the intersect of CCDF's on this line is the PDF of the probability of failure. The PDF of these 59 p_f is shown in the right side in the figures. Note that the distribution is not symmetric at the median value ($p_f = 41\%$). Rather the distribution looks like lognormal distribution. (This will be still more pronounced in the scenario 8) .

The corresponding results for scenarios 6 and 8 are shown in Figures 21 and 22. In scenario 8, the scatter is much increased mainly due to the large standard deviation in M_s . The 90% confidence interval for the probability of failure is (5%-64%) i.e. an order of magnitude difference. The median value is in good agreement with what will be shown in the next sections. The PDF of probability of failure looks like a lognormal distribution.

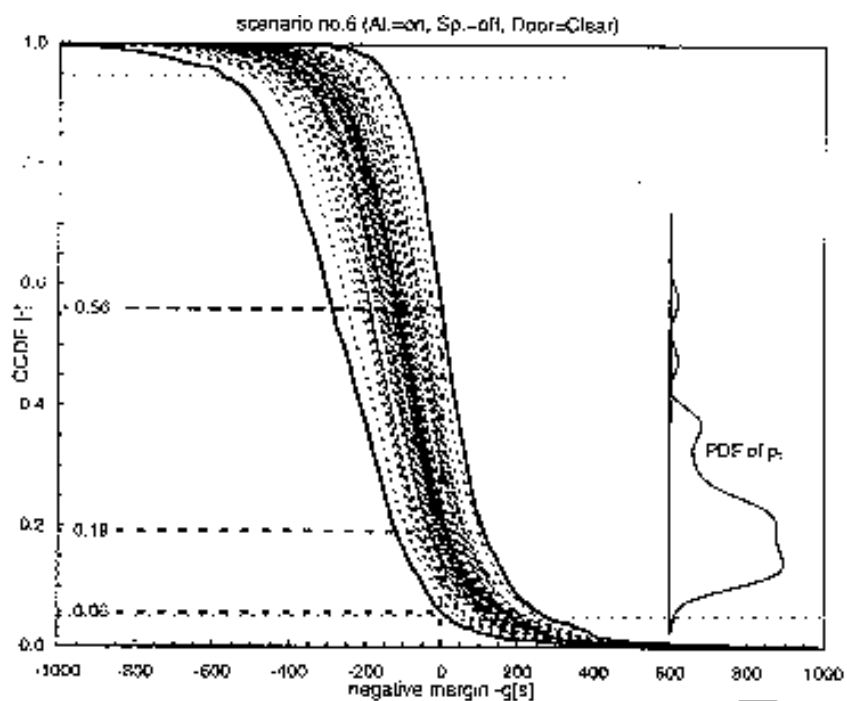


Figure 21. Evacuation time deficit (negative time margin) for scenario 6 using method C

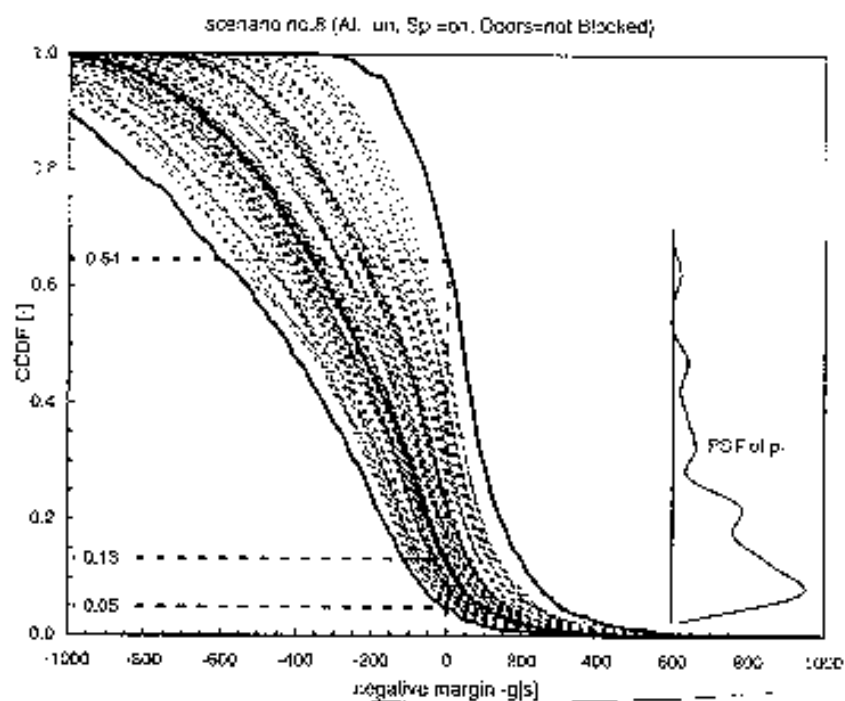


Figure 22. Evacuation time deficit (negative time margin) for scenario 8 using method C

For the other scenarios we only present the values of the probability of failure at different confidence levels. In Figure 23 the probability of failure is presented at the 5th, median and 95th percentile for knowledge uncertainty. The merged values according to method E presented in section 10.4 is also displayed for clarity.

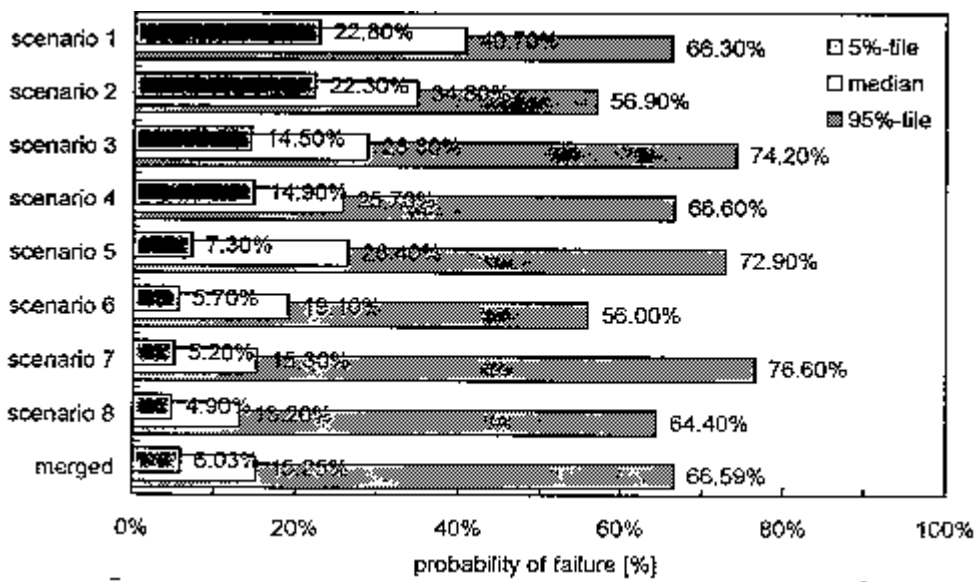


Figure 23. Probability of failure for the different scenarios at different confidence levels

The principles behind the two-phase simulation procedure and the interpretation of results are described in Figures 24 and 25. The solid line in Figure 24 represents expected value of Y corresponding to the confidence on the vertical axis. The solid line represents a reference curve with knowledge uncertainty parameters chosen as e.g. the mean or median values of the corresponding distribution. Stochastic variability may be described by the range of Y values lying in the range $0.05 < p < 0.95$. In this way we obtain a 90% confidence interval for the variability in Y. The dashed lines represent upper (95%) and lower (5%) confidence intervals on the location of the true CCDF for a specified p. As a result the confidence interval is increased in the way indicated by the figure. As an illustration, we look at scenario 6 and Figure 25. The 90% confidence interval in Y considering variability only is $-325 \text{ s} < Y < 170 \text{ s}$. Considering the combined influence of variability and knowledge uncertainty, this range is enlarged to $-580 \text{ s} < Y < 290 \text{ s}$.

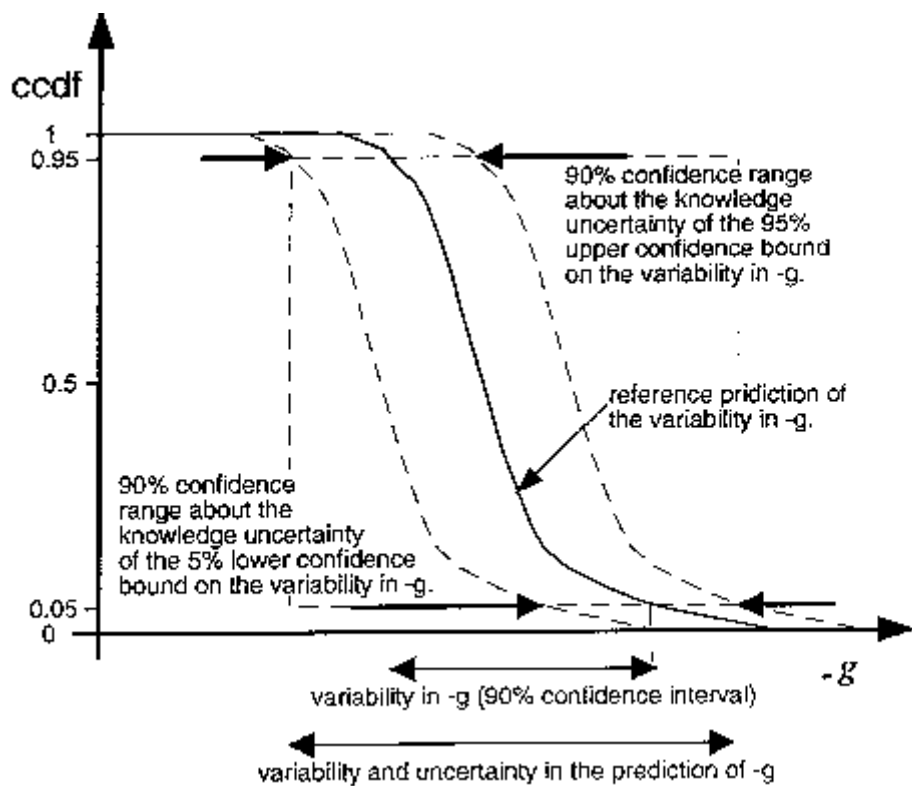


Figure 24. Two phase Monte Carlo simulation procedure and the interpretation of results

Summing up, the two phase simulation procedures enables a separation and a measurement of the two kinds of uncertainties. This in turn makes possible a rational discussion of various methods to decrease uncertainty in design and the amount of uncertainty which never can be eliminated and which we will have to accept in all circumstance.

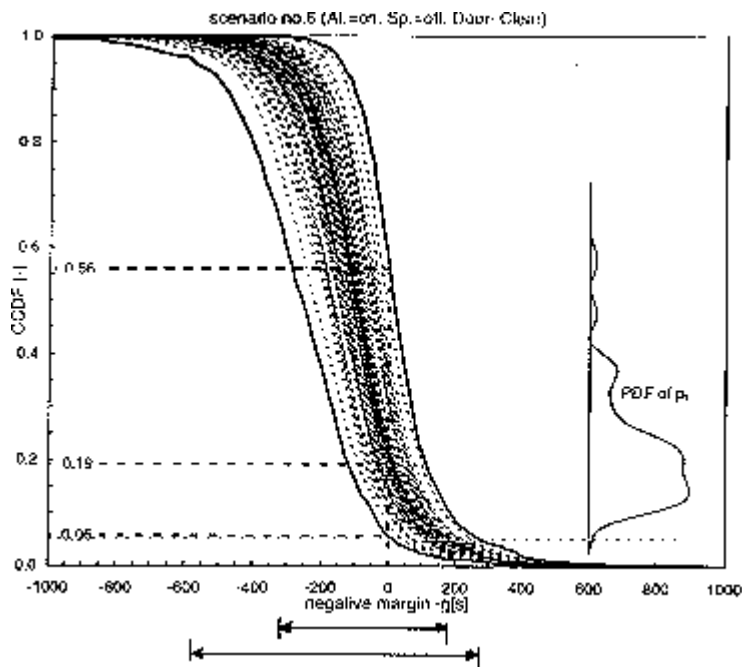


Figure 25. The 90% confidence intervals for variability only and for variability and knowledge uncertainty combined

In Figure 23, the p_f -value for the reference CCDF (the median curve) can be compared to the total confidence interval. Again, it is clear that a two-phase simulation procedure enables a much more detailed discussion of results than would have been possible by a one-phase simulation procedure, where only a point estimate of p_f would have been available.

10.3 One phase SRS-simulation procedure (Method B)

The eight CCDF's, one for each scenario, are calculated using Latin hypercube sampling with 1,000 samples in each simulation. In these simulations, we did not distinguish between stochastic variability and knowledge uncertainty. Each simulation procedures a single CCDF-curve and a specific value of P_f and β . Comparing Figures 23 and 27 we can see a close correspondence between the reference values of P_f (the median values) from the two phase sampling and the SRS-results.

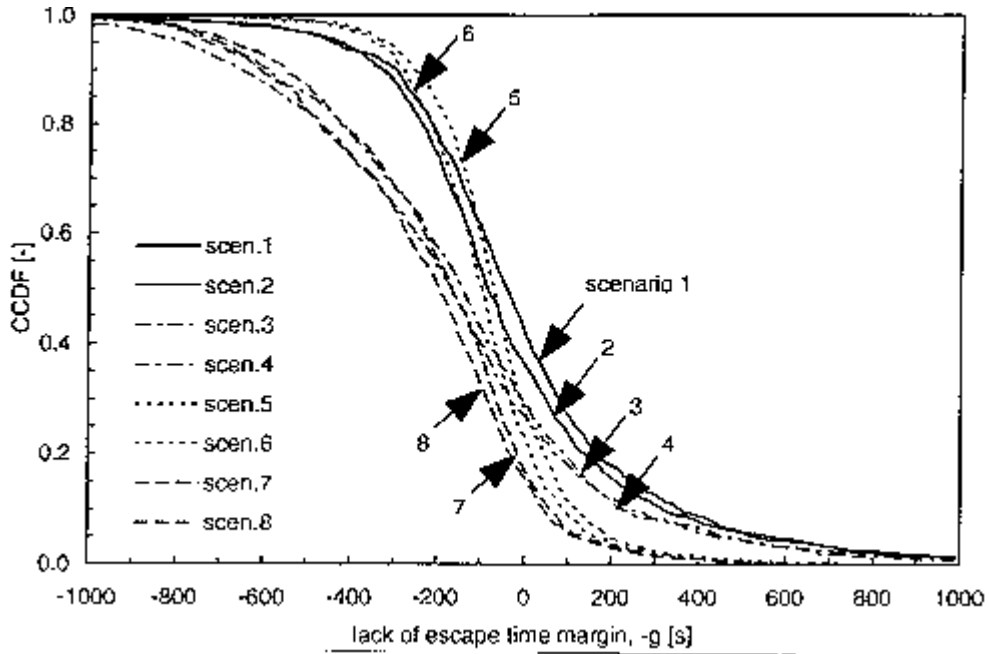


Figure 26. CCDF's for the eight scenarios using method B (simple random sample)

The resultant CCDF's are shown in Figure 26. In the scenario 1, when all the fire safety strategies fail, the CCDF curve is far above the rest of seven other CCDF's. It results in low safety level. Conversely in the scenario 8, when all the strategies are successful, the CCDF curve locates at lower position, which shows the high safety levels.

In Figures 27 and 28, the probability of failure and safety index for each scenario are shown. Comparing the results for scenario (1 and 2 or, (3 and 4) or (5 and 6) or (7 and 8), we can see the effect of door blockage. The effect is most significant in scenarios 7 and 8, when both alarm and sprinkler fails. In other combinations of comparison, the effects are less significant. The effect of alarm system can be seen in the differences in scenario (1 and 5) or (2 and 6) or (3 and 7) or (4 and 8). Similarly the effect of sprinkler can be seen in (1 and 3) or (2 and 4) or (5 and 7) or (6 and 8).

From a practical point of view, one important conclusion from Figure 26 is that an eye inspection only would be unreliable for a proper risk ranking of the 8 scenarios. There are cross-overs among the 8 CCDF's or risk profiles. Some risk profiles exhibit a clear stochastical dominance over an alternative scenario risk profile, but others do not

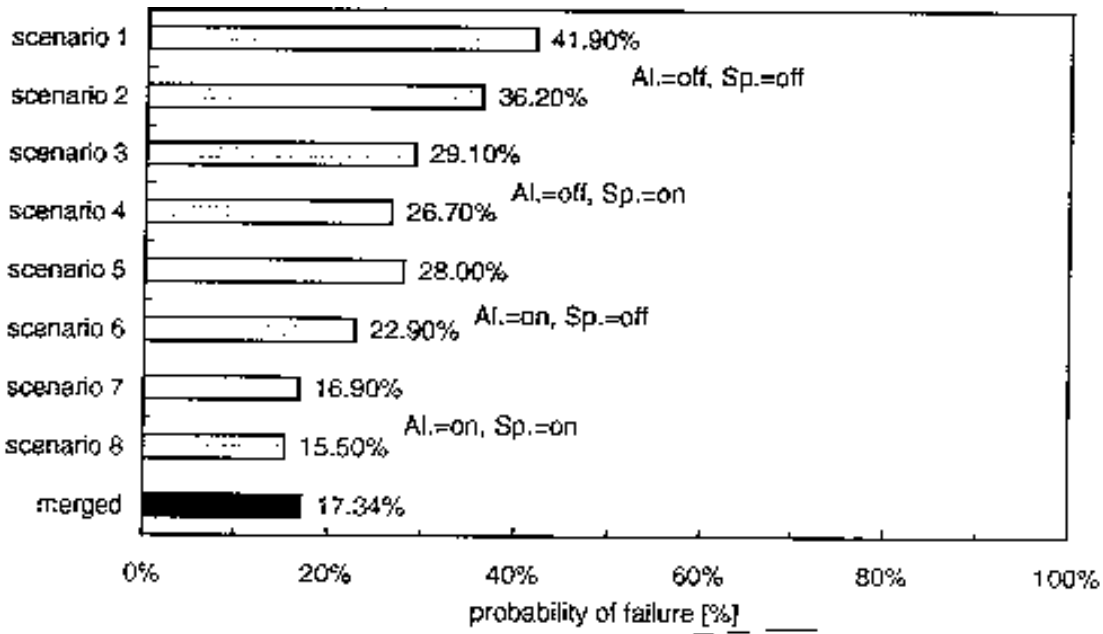


Figure 27. Probability of failure for the eight scenarios using method B. The merged results using method E is also displayed

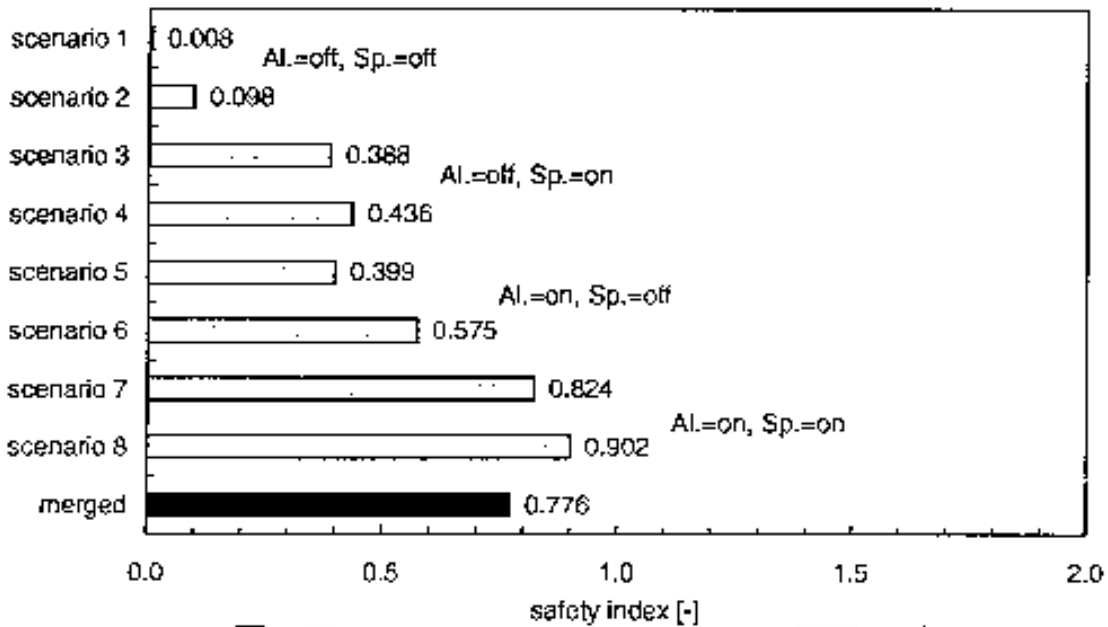


Figure 28. Safety index β for the eight scenarios using method B. The merged result using method E is also displayed

(stochastical dominance for one scenario over a second scenario occurs when the CCDF for the first scenario lies entirely to the left of the risk profile for the second scenario). Clearly, risk quantification requires the simultaneous consideration of Figures 26-28.

10.4 Merging eight CCDF to one CCDF (Method E)

The eight PDF's are merged to one PDF with the weight depending on the probability of each scenario.

$$PDF_{merged} = \sum_{i=1}^8 p_i PDF_i \quad (25)$$

where p_i is the probability of scenario i, PDF_i is the PDF curve for scenario i. The mean value and variance for the merged PDF are calculated by

$$\mu_{merged} = \sum_{i=1}^8 p_i \sum_{j=1}^n \frac{g_{i,j}}{n} = \sum_{i=1}^8 p_i \mu_i \quad (26)$$

$$\begin{aligned} \sigma_{merged}^2 &= \sum_{i=1}^8 p_i \sum_{j=1}^n \frac{(g_{i,j} - \mu_{merged})^2}{n} \\ &= \sum_{i=1}^8 p_i \sum_{j=1}^n \frac{\{(g_{i,j} - \mu_i) + (\mu_i - \mu_{merged})\}^2}{n} \\ &= \sum_{i=1}^8 p_i \{\sigma_i^2 + (\mu_i - \mu_{merged})^2\} \end{aligned} \quad (27)$$

where μ_i , σ_i are the mean and standard deviation in scenario i while, μ_{merged} , σ_{merged} are those for the merged PDF and the corresponding CCDF.

$g_{i,j}$ is the j:th result in scenario i, and n is the number of samplings in each scenario.

The branch probabilities have been derived using published data or subjective estimates and are shown in Figure 29.

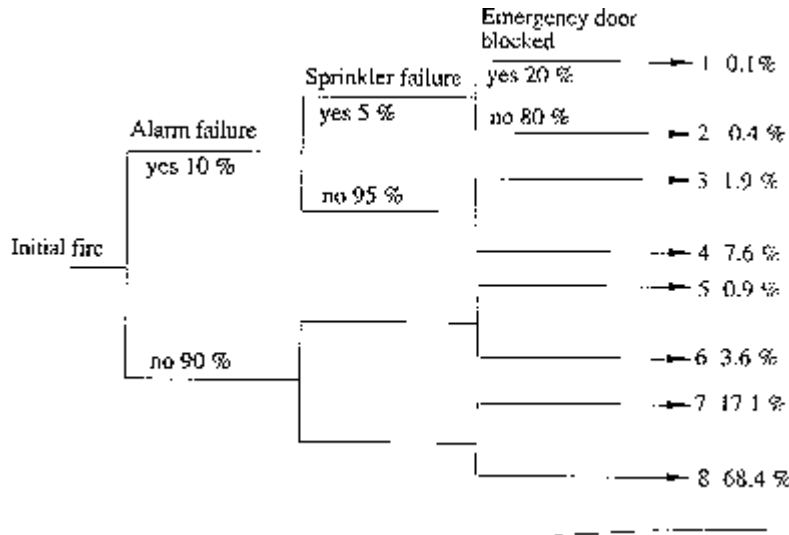


Figure 29. Branch and scenario probabilities

The results are shown in Figure 30. The merged CCDF is close to that for scenario 8. From this CCDF, probability of failure and safety index are calculated as

$$p_f = 16.0\% \quad (28a)$$

$$\beta = \frac{\mu_{merged}}{\sigma_{merged}} = \frac{223}{277} = 0.804 \quad (28b)$$

In the results above no distinction was made between uncertainties of Type A and Type B. In other words, CCDF's from calculations with method B is used in the event tree giving a merged CCDF for the whole system. The same could be done using CCDF's where we have distinguished between variability and knowledge uncertainty. Information from calculations using method C could be merged into a new set of 59 CCDF's but weighted by their respective branch probabilities. Performing this action we end up with a CCDF for the whole system and with information about the uncertainty related to variability and knowledge uncertainty separated. In Figure 31 the event tree CCDF is displayed with the 5th and 95th confidence limits. To the right in the figure is the PDF of p_f displayed for $g(\cdot) = 0$.

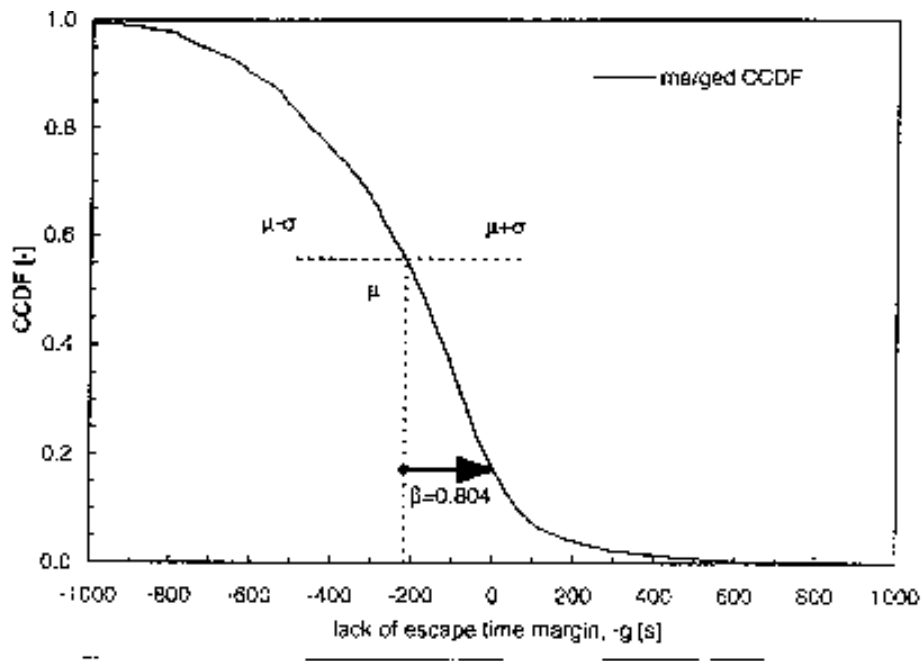


Figure 30. Merged CCDF from the eight scenarios considered their respective branch probabilities (method E)

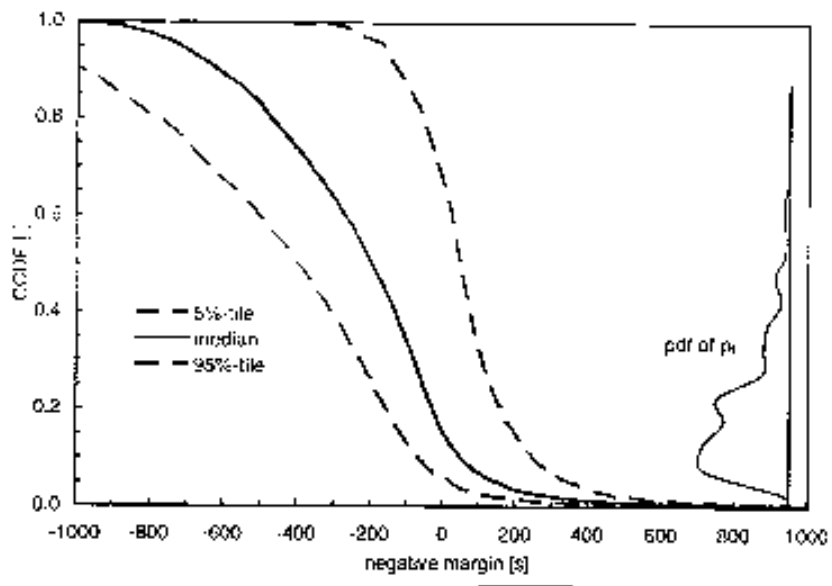


Figure 31. Confidence limits of knowledge uncertainty for the event tree analysis of evacuation safety

10.5 Results from method D, standard PRA

As explained by Figure 7, the results from a deterministic event tree evaluation can be combined into an event tree CCDF. Four such curves are shown in Figure 32. Branch probabilities are the same as in Figure 29. The four curves represent input data chosen as mean, median, 80% and 95% values of the corresponding distribution. The values of the design parameter W (evacuation door width) follows data in section 8.5.2. Each curve is determined by eight point values corresponding to the eight scenarios. In some assessments input parameters (including branch point probabilities) are deterministic, c.f. the remarks to Figures 7 - 9.

Remembering that positive values on the horizontal axis imply an evacuation time deficit, the figure leads to at least three conclusions:

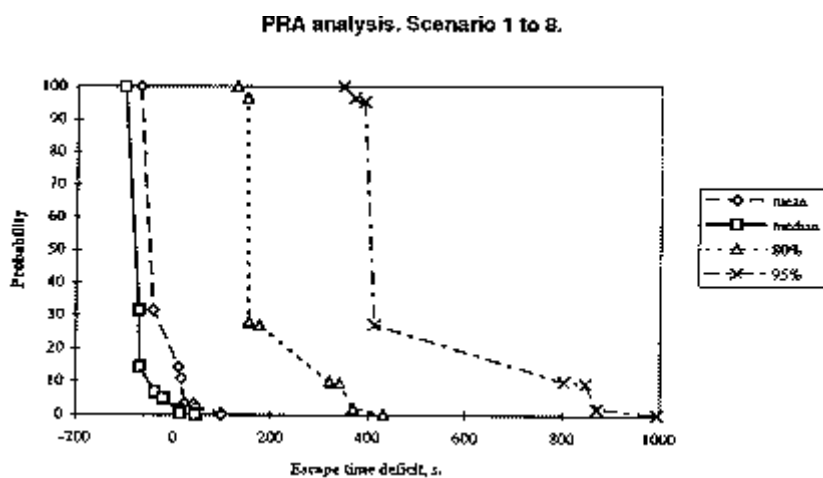


Figure 32. Standard PRA-study without uncertainty analysis

- choice of characteristic value or design value will heavily influence the acceptance of a particular design. Choosing the mean or median values as design values will provide risk profiles that superficially looks acceptable. Choosing the 95 percentiles produces a risk profile that is clearly unacceptable
- unwise and unsubstantiated choice of design values can very easily lead to unrealistic results or safety levels

- the specification of design values (or characteristic values and partial coefficients) requires a careful scientific investigation

10.6 Summary of numerical sampling procedures

Confidence intervals of CCDF's

From Figures 20, 21 and 22, it can be seen that the knowledge uncertainty is relatively small compared with stochastic variability. However we still have significant width in the confidence interval. This can be true especially in scenario 8 (Figure 22), where we have large standard deviation in knowledge uncertainty in smoke filling time (M_s). In order to be more confident with the results, we must develop more accurate prediction models as well as regression equations with a smaller modelling variability. The alternative is to directly use the computer model and avoid use of response surface equations.

CCDF's associated with event tree

From the results in Figures 26 to 28, it can be said that the fire safety strategies are effective in reducing probability of failure and increasing level of fire safety. The presentations in these figures are useful to investigate the effect of each fire safety strategy.

For example if we look into Figure 28, the following can be said;

- (1) When all the fire safety strategies (alarm, sprinkler and emergency doors) fail, the probability of failure is increased substantially. If at least one of the strategies is successful, the probability of failure will be considerably reduced.
- (2) When the sprinkler fails, the role of emergency door is very important. There is a large difference in the probability of failure in the scenario 5 and 6, and in the scenario 1 and 2.
- (3) When the sprinkler is activated, the emergency doors will be less important. This means that the sprinkler helps the occupant to escape easily.

(4) The alarm system is important. When it fails, the probability of failure is increased considerably.

Merged CCDF

The merged CCDF gives an information on the over all safety level both in a single scenario as for a whole event tree system. It is useful as a tool to check for the safety level of a specific problems. However some criteria should be established to evaluate the results given by the CCDF. This is already done in other safety problems such as nuclear engineering, environmental impacts and so on. Individual as well as societal risk criteria will have to be considered. Further guidance is given in reference 1.

11. Sensitivity analysis

11.1 Introduction

A brief sensitivity analysis was performed on the event tree in Figure 1. The study was performed on the scenario 6 which in the origin is a nonsprinklered case. In this study the varying parameter distributions was altered compared to the original. Apart from being nonsprinklered the fire alarm and all doors are available in this scenario. This means that the total free exit width is 4.8 m. The standard set of distributions and other input data are given in section 8.5. The result in the original scenario 6 gives a β -value of 0.57 and the corresponding probability of failure of 22.1 %. These results are also presented in the following figures and denoted ‘scen 6’.

11.2 Sensitivity studies

Study A

In the sensitivity analysis the standard set of distributions are changed and the result of the β -value and probability of failure is determined. In study A changes are made for one parameter at a time according to the following list

- A1; N is triangular (0.1, 0.5, 1.0) pers/m²
- A2; N is triangular (0, 1, 2) pers/m²
- A3; α is triangular (0.001, 0.05, 0.1) kW/s²
- A4; α is triangular (0.001, 0.07, 0.15) kW/s²
- A5; Area is 300 m²
- A6; Area is 500 m²
- A7; Area is 1000 m²
- A8; Area is 1500 m²
- A9; H is triangular (3, 6, 10) m

When a new parameter is changed all other parameters resume the original distribution. The results are shown in Figure 33.

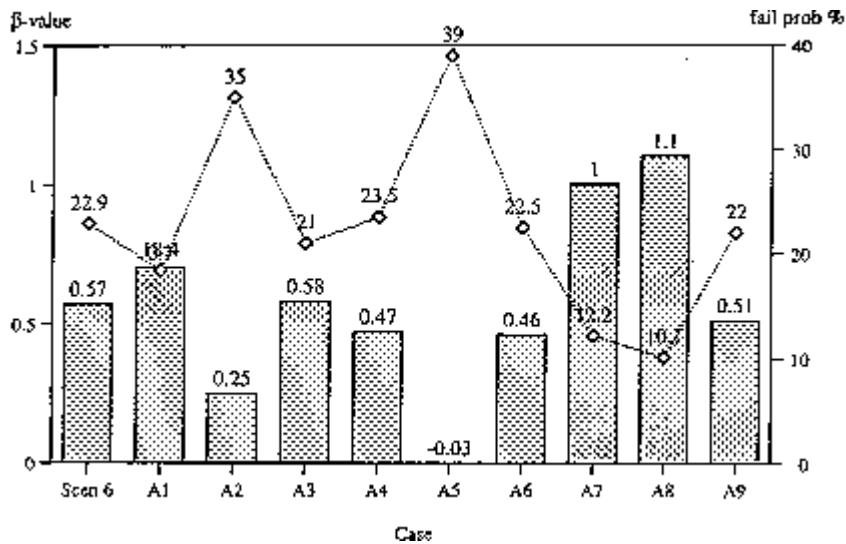


Figure 33. Results from study A. β -value and probability of failure for the different cases

Study B

In study B all the parameters have been changed to either normal or lognormal distributions. This is because it is then possible to easily compare the calculations from the numerical simulation with analytical results. The parameters have the following distributions;

- α is lognormal (0.025, 0.015) kW/s^2
- H is normal (8, 1.5) m
- Area is normal (800, 150) m^2
- N is normal (0.8, 0.2) pers/ m^2
- R is lognormal (130, 120) seconds
- Ms is normal (1.35, 0.1)

The parameter that is changed in this study is the total free exit width. The width is changed from 2.4 m to infinity giving increasing β -values and decreasing probabilities of failure. The results are presented in Figure 34. The original scenario 6 has a free exit width of 4.8 m.

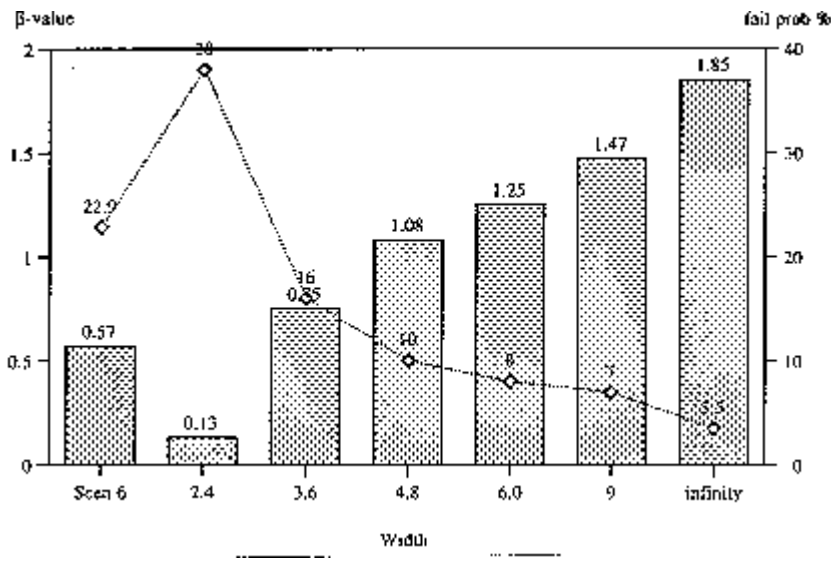


Figure 34. Results from study B. β -value and probability of failure for different exit door widths

Study C

Study C is very much like study B but the behaviour and response time R has a different distribution, R is lognormal (130, 60) seconds. All the other parameters are unaffected. The β -values and probabilities of failure are calculated for different exit widths. The results are shown in Figure 35.

Study D

In the last study of sensitivity, study D, the varying parameter is the building area. The other parameters are as in the previous study with a smaller standard deviation for the behaviour and response time. The different area distributions used are;

- Area is normal (1000, 150) m^2
- Area is normal (1000, 200) m^2
- Area is normal (1200, 150) m^2
- Area is normal (1200, 200) m^2 .

The results in form of β -values and probabilities of failure are found in Figure 36.

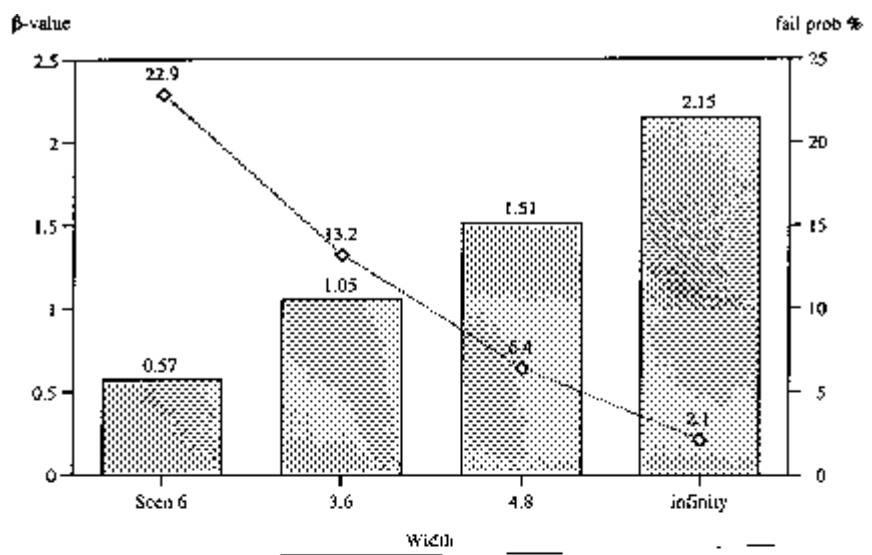


Figure 35. Results from study C. β -value and probability of failure for different exit door widths. The standard deviation for the behaviour and response time is reduced

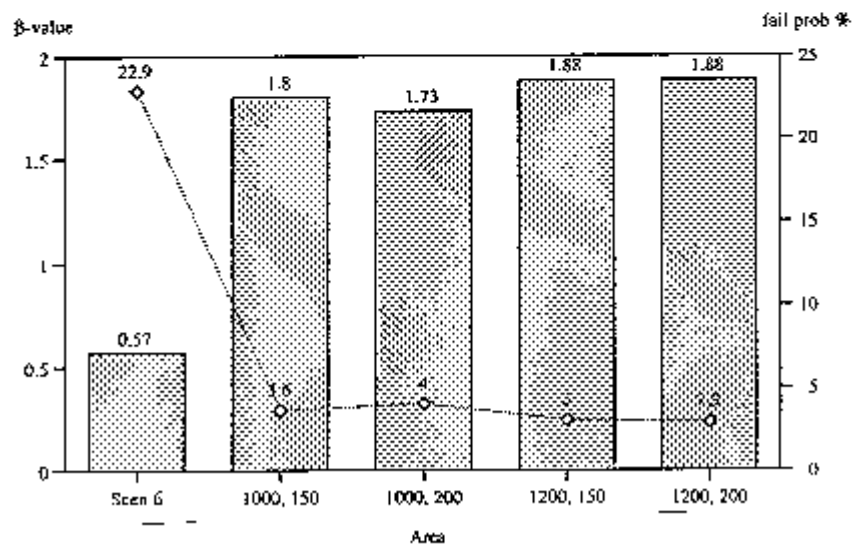


Figure 36. Results from study D. β -value and probability of failure for different area descriptions

11.3 Discussion of results

This sensitivity study was made primarily with the purpose of getting to know the distributions rather than doing a complete sensitivity study. A complete sensitivity study could be very large and practically without limits. Some conclusions can however be made from this four different studies. From study A it seems that different distributions for α does not affect the safety level so much as increasing area and the distribution in N. The results is also quite insensitive to differences in height-descriptions.

In study B the β -value is increasing when the door width is increasing which is to be expected. The maximum value of $\beta = 1.26$ could be compared to the maximum value for another scenario in Figure 17.

The study C gives also an expected result. If the deviation in the behaviour and response time is decreasing the β -value is increasing indicating higher safety.

In study D small changes in the area representation is performed. The results are small changes in β -values.

12. CONCLUSIONS

(1) Objectives

In this pilot report an investigation has been carried out on the evacuation safety from a fire in an assembly room. Some of the main objectives have been

- to assess a number of uncertainty and reliability methods used in other engineering areas
- to describe major uncertainty parameters by subjective probability distribution
- to derive safety indices β and probability of failure P_f corresponding to these distributions. Both point estimates and confidence intervals of β and P_f have been calculated (depending on calculation methodology)
- to make an importance study of major parameters
- to study sensitivity of β and P_f to choice of probability distributions
- to make an initial study into the derivation of partial coefficients

(2) Calculation methods

The following calculation or simulation methods have been looked into:

Method A, an analytical procedure (FOSM) to derive β and P_f

Method B, a simple random sampling Monte Carlo procedure

Method C, a two phase Monte Carlo procedure, separating stochastic variability and knowledge uncertainty

Method D, event tree evaluation by standard PRA

Method E, event tree evaluation by Monte Carlo simulation

Methods A-C are relevant for the one-scenario situation, D and E for multiple scenario problem.

(3) Quantity and quality of information obtained from various risk calculation procedures

Method A produces a safety index β and an approximate value of P_f . The perhaps most important factor is that design points are given directly. In addition, the method gives directly the relation importance of component variances in the total uncertainty. This type of importance analysis is important for determining the most cost-effective way of increasing the safety level.

Method B produces a statistical distribution curve of the limit state variable which can be treated by available statistical methods to produce P_f , safety index β , etc. The design point is normally not obtained. Confidence intervals describe total uncertainty.

In method C, uncertainty is separated into two components, variability and knowledge uncertainty; allowing the total uncertainty to be separated into corresponding parts for further study. The method produces a distribution of CCDF's and a distribution of P_f . The PDF of P_f can of course be translated into a β -value for the stochastic variable P_f .

For the event-tree situation, merging procedures can be devised, producing output corresponding to the methods B and C above. This is done in what we have defined as method E.

Finally, and for the sake of completeness, the event-tree has been evaluated using standard, deterministic PRA-methodology (method D). The numbers of scenarios is to small to make this method illustrative and effective.

(4) Point estimates versus description by use of confidence intervals

Compared to simple random sampling, the two phase sampling procedure produces more information and information that is clearly valid and of importance for the decisionmaking.

(5) Range and level of β

One relevant result from our study is that using our selected probability distributions, we arrive at surprisingly high values of P_f and low values of β . Another important result is that the range of β over a number of scenarios (absence/presence of various protection systems) is smaller than one perhaps intuitively thinks.

(6) Sensitivity of β and P_f to choice of distribution

Our limited sensitivity study has revealed that the calculated values of β and P_f are sensitive to choice of distribution function and that the influence may be of the same order as the influence of changing scenarios.

(7) Need for derivation of standard distributions and international cooperation

The facts that are mentioned under items (5) and (6) underline the need for internationally agreed and accepted standard distributions for major uncertainty parameters. It is important that the activity initiated by the CIB/W14 subgroup "Engineering Evaluation of Building Fire Safety" [24] is starting up and being effective as soon as possible.

(8) Risk assessment and importance studies of parameters

The results shown in sections 9.3 and 9.4 indicate that

- the relative importance of uncertainty in parameters varies considerably from one scenario to another. For non-sprinklered fires, the variance linked to reaction time R is dominating absolutely. For sprinklered fires, the uncertainty linked to the parameter Area becomes significant and even dominating for one scenario.
- in general, variability or stochastic uncertainty dominates over knowledge uncertainty, implying that the potential for safer design by increased knowledge may be limited.

(9) Partial coefficients

Most likely, and as indicated in section 9.5 partial coefficients for design on level 1 will have to be derived by an optimization procedure outlined in reference 18. Table 9.1 gives resulting safety levels and design values over the whole class of buildings and indicates that, for a fixed evacuation width and scenario, probability of failure and safety index β vary strongly with building height and floor area.

(10) Variability versus knowledge uncertainty

Figure 19 implies that for the risk assessment study or determination of the level of risk inherent in the use of existing buildings, variability is dominating over knowledge uncertainty. For a design situation with area and height being deterministic, the situation may look different. Again, future studies will examine this problem.

(11) Computer models versus response surface representations

This paper is based on the use of response surface models derived by regression analysis. As seen, for some scenarios the increased model uncertainty will have an influence. Basically, the question is to choose between making an exact analysis of an approximate model (the response surface equation) or an approximate analysis of a more exact model (the computer model). Much more work is needed in this area.

(12) Choice of design methodology and criteria

This is an area where we obviously first now can start an introductory rational discussion on the quantitative aspects. Some rather obvious suggestions include:

On the whole building level

To use the standard PRA-approach (method D) calculation would have to be based on automated computer program package or toolkit. Transparency and quality assurance are key problems and issues when developing a quantified risk assessment, QRA-model. It is interesting to note that a recent paper outlines the following specification for an off-shore industry QRA-toolkit (Reference 15).

- linkage of QRA models should be visible and easy to document
- transfer of data should be safe and easy to document
- consequence models should be built-in, compiled, incorruptible and reliable
- it should be possible to add alternative models
- quality assurance should be much easier
- results should be believable by clients and regulatory authorities.

An effort similar to the one described in Reference 15 should be started by the prestandardization and standardization bodies working in the fire safety engineering area.

On the subsystem or component level

For those situations where an analytical treatment is possible, the safety index β approach should be preferred. For the design situation where numerical simulation is used, design can be based on a CCDF curve and with the curve chosen on an appropriate confidence level; e.g. the 50, 80 and 95% confidence level. For the selected CCDF-curve, requirements could be expressed in terms of a safety index β , by quantifying criteria for specified fractiles or by comparison with a specified limit curve.

(13) Need for international pre-standardization work

Calculation methods, choice of statistical distributions, model validation procedures and choice of limit criteria must be discussed in an international cooperation. This work is now being started up [24].

(14) Equivalency

The problem of demonstrating equivalency is automatically solved by using the safety verification methods employed in this publication.

(15) Future studies

Our plans are to continue this study by looking into the following problems, among others

- reliability based design directly based on computer models

- methods for deriving partial safety factors (design values) and methods of code calibration
- the use of societal risk criteria (F/N-curves)
- methods to rank individual parameters with respect to their contribution to the uncertainty in the final model prediction by the use of statistical methods such as calculation of correlation coefficients, partial correlation coefficients, standardized partial regression coefficients or rank correlation coefficients
- the extension of the safety index β -methodology to the analysis of event-tree design situation.

Acknowledgements

The authors wish to thank the Development Fund of the Swedish Construction Industry, Svenska Byggbranschens Utvecklings Fond (SBUF), for providing funding for this project.

References

1. Draft British Standard Code of Practice for The Application of Fire Safety Engineering Principles to Fire Safety in Building, BSI 1994
2. Nordic Committee for Building Regulation Working Report 1994:07 Performance Based Firesafety Requirements and Technical Guidelines for the Calculation Process (In Danish)
3. Standard Guide for Evaluating the Predictive Capability of Fire Models, ASTM E 1355-90, ASTM Philadelphia 1990
4. NFPA 92 B. Recommended Practices for Smoke Management in Atria Malls NFPA Quincy, MA 1991
5. Iman, R.L. and Helton, J., An Investigation of Uncertainty and Sensitivity Analysis Techniques for Computer Models, Risk Analysis, vol 8 No 1, 1988
6. Helton, J., Treatment of Uncertainty in Performance Assessments for Complex Systems, Risk Analysis, Vol 14, No 4, 1994
7. EPA Workshop April 18-20 1993: When and How Can You Specify a Probability Distribution When You Don't Know Much? Editors: Haimes, Y.Y., Barry, T. and Lambert, J.H., Risk Analysis, Vol 4, No 5 1994
8. IAEA Safety Series No 100 Evaluating the Reliability of Predictions Mode Using Environmental Transfer Models IAEA, Vienna 1989
ISBN 92-0-124089-9
9. Ang, A. H-S., Tang, W.H., Probability concepts in Engineering Planning and Design, Volume II, John Wiley & Sons, 1984
10. Magnusson, S.E., Probabilistic Analysis of Fire Exposed Steel Structures, Bulletin 27, Div. of Structural Mechanics and Concrete Construction, Lund Institute of Technology, 1974

11. Hay, A., Quantitative Risk Assessment in Fire Safety, in Integrated Risk Assessment, Ed. Klein and Pallister, ECIRAS-94, Cambridge 21-22 March 1995, CFRS Consultancy Service
12. MacIntosh, D.L., Suter II, G.W. and Hoffmann, F.O.: Uses of Probabilistic Exposure Models in Ecological Risk Assessment of Contaminated Sites, Risk Analysis, vol 14, No 4, 1994
13. @RISK, Palisade Corporation, 31 Decker Rd, Newfield NY 14867, USA
14. Pitblado, R.M. and Nalpanis, P., Quantitative Assessment of Major Hazard Installations: 2, Computer Programs. In Safety Cases, ed. F.P. Lees and M.L. Ang, Butterworth, 1989
15. Ramsay, C.G. et al., Quantitative Risk Assessment Applied to Offshore Process Installations. J. Loss Prev. Process Ind., Vol 7 No 4, 1994
16. DETACT-QS. Evans, D.D., Stroup, D.W., NBSIR 85-3167 National Bureau of Standards, Gaithersburg 1985
17. Frantzich, H., Reaction times prior to evacuation for shops, restaurants and public dance-halls. Estimates done by fire officers, LUTVDG/TVBB 3071 SE, Department of Fire Safety Engineering, Lund University, Lund 1993
18. Thoft-Christensen, P., Baker, M.J., Structural Reliability Theory and Its Applications. Springer-Verlag, Berlin 1982
19. Hasofer, A.M., Lind, N.C., An Exact and Invariant First Order Reliability Format. Proc. ASCE, J. Eng. Mech. Div., 1974, pp 111-121
20. Cornell, C.A., First Order Analysis of Model and Parameter Uncertainty. Proc Int Symp on Uncertainties in Hydrol. Water Resour. Syst., University of Arizona, vol 2, pp 1245-1275, 1972

21. Magnusson, S.E., Frantzich, H., Karlsson, B. and Särdqvist, S.; Determination of Safety Factors in Design Based on Performance. *Fire Safety Science - Proceedings of the 4th Intern'l Symp IAFSS*, pp 937-948, Gaithersburg 1994
22. Peacock, R.D., Jones, W.W., Forney, G.P., Portier, R.W., Reneke, P.A., Bukowski, R.W., Klote, J.H., An Update Guide for HAZARD I Version 1.2, NISTIR 5410, US Department of Commerce, National Institute of Standards and Technology, 1994
23. Bragason, F., Determination of modeling uncertainty for two fire models, Department of Fire Safety Engineering, Lund University, 1994
24. Bukowski, R.W., Report to the CIB W14 Plenary Meeting, Espoo, Finland, Jan 12-13 1995
25. Peacock, R.D. and al., Understanding Sensitivity Analysis for Complex Fire Models. Building and Fire Research Laboratory, National Institute of Standards and Technology, Gaithersburg, Maryland 20899-0001
26. Ramachandran, G., Probabilistic Evaluation of Design Evacuation Times, CIB W14 International Symposium and Workshops Engineering Fire Safety in the Process of Design: Demonstrating Equivalency, 13-16 September 1993, University of Ulster at Jordanstown, Northern Ireland

APPENDIX A The first order second moment (FOSM) methodology. The Rackwitz' algorithm

In a reduced variate system β can be interpreted as the distance from the origin to a failure line (limit state). Redefine the safety margin $M = X - Y$ and introduce the reduced variates

$$X' = \frac{X - \mu_X}{\sigma_X} \quad Y' = \frac{Y - \mu_Y}{\sigma_Y}$$

The limit state equation $M = 0$ then becomes

$$\sigma_X X' - \sigma_Y Y' + \mu_X - \mu_Y = 0$$

and it follows from linear algebra that

$$\beta = d = \frac{\mu_X - \mu_Y}{\sqrt{\sigma_X^2 + \sigma_Y^2}}$$

If X and Y are normal random variables then $p_s = 1 - p_f = \Phi(d)$ as before.

For other statistical distribution of X and Y the probability of failure has to be calculated by integration, which in most cases requires use of Monte Carlo simulation techniques. It is obviously a very attractive idea to base design on the concept of the safety index β , that is on mean values and variances, and disregard the actual statistical distribution of X and Y [20]. In reference 20 the following arguments can be found:

An approach based on means and variances may be all that is justified when one appreciates: (1) That data and physical arguments are often insufficient to establish the full probability law of variable; (2) that most engineering analyses include an important component of real, but difficult to measure, professional uncertainty; and (3) that the final output, namely the decision or design parameters, is often not sensitive to moments higher than the mean and variance.

In practice \mathbf{X} and \mathbf{Y} may be functions of several basic random variables or design parameters. A performance or state function g may be formulated

$$g(\mathbf{X}) = g(X_1, X_2, \dots, X_n)$$

where $\mathbf{X} = (X_1, X_2, \dots, X_n)$ is a vector of basic state or design variables. $g(\mathbf{X}) = 0$ defines a limit state of the system and a n -dimensional failure surface. Based on a first order approximation (Taylor expansion) of the function $g(\mathbf{X})$, procedures are available to find the most probable point of failure $\mathbf{x}^* = (x_1^*, x_2^*, \dots, x_n^*)$ and the corresponding safety index β .

The point $\mathbf{x}'^* = (x_1'^*, x_2'^*, \dots, x_n'^*)$ denotes the point on the failure surface with minimum distance β to the origin of a reduced variate system. It can show that the reliability index $\beta = \mu_g/\sigma_g$ as before. In a first order approximation

$$\mu_g \approx - \sum_{i=1}^n x_i^* \left(\frac{\partial g}{\partial X_i} \right)_* \quad \sigma_g^2 \approx \sum_{i=1}^n \left(\frac{\partial g}{\partial X_i} \right)_*^2$$

Accordingly, β is given by

$$\beta = \frac{- \sum_i x_i^* \left(\frac{\partial g}{\partial X_i} \right)_*}{\sqrt{\sum_i \left(\frac{\partial g}{\partial X_i} \right)_*^2}}$$

with \mathbf{X}' denoting a reduced variate and the derivative evaluated at $\mathbf{x} = \mathbf{x}^*$, which is unknown and has to be determined in the calculation procedure.

For a linear performance equation

$$g(\mathbf{X}) = a_0 + \sum a_i X_i$$

the value of β is given explicitly by

$$\beta = \frac{a_o + \sum_i a_i \mu_{xi}}{\sqrt{\sum_i (a_i \sigma_{xi})^2}}$$

and the value of β may be computed directly. For the general non-linear performance equation $g(\mathbf{X}) = 0$ the point of failure \mathbf{X}^* will have to be determined by iteration (the Rackwitz procedure) or by constrained non-linear optimization.

In this case it is necessary to make an integration of the joint probability density functions to obtain the probability of safety. As this is a nonattractive solution an iteration process using the same technics as for the linear case is often used in determining the safety factor. The distance to the tangent plane pertinent to the failure surface at the point $(x_1^*, x_2^* \dots x_n^*)$ is used as an approximation, making it possible to evaluate the safety index as in the linear case.

This approximation will either be on the safe or unsafe side depending on how the actual failure surface looks. The term first-order, second moment is implied from the use of a linearized, first order expansion and the first two statistical moments.

The problem is that the point x_i^* is not known which makes the iteration process necessary.

The most probable failure point in the reduced variable space is

$$x_i^* = -\alpha_i^* \cdot \beta$$

where α_i^* is the direction cosines in the x_i^* direction

$$\alpha_i^* = \frac{\left(\frac{\partial g}{\partial X_i} \right)_*}{\sqrt{\sum_i \left(\frac{\partial g}{\partial X_i} \right)_*^2}}$$

The derivates are evaluated at $(x_1^*, x_2^* \dots x_n^*)$ which gives

$$x_i^* = \sigma_{x_i} x_i^* + \mu_{x_i} = \mu_{x_i} - \alpha_i^* \sigma_{x_i} \beta$$

If this expression is put into the limit equation and solved for $g(\mathbf{X}) = 0$ then the β value has been obtained.

Rackwitz has suggested the following simple numerical algorithm which is outlined in reference 11.

1. Assume initial values of x_i^* for $i = 1, 2, 3 \dots n$.
2. Calculate $x_i^* = \frac{x_i^* - \mu_{x_i}}{\sigma_{x_i}}$
3. Evaluate $\left(\frac{\partial g}{\partial X_i} \right)_*$ and α_i^* at x_i^*
4. Calculate $x_i^* = \mu_{x_i} - \alpha_i^* \sigma_{x_i} \beta$
5. Substitute x_i^* in $g(x_1^*, x_2^* \dots x_n^*) = 0$ and solve for β
6. Use β to improve the values of $x_i^* = -\alpha_i \beta$
7. Repeat steps 3 to 6 until convergence of β is obtained.

In the case where the distributions of X_i are nonnormal, it is necessary to transform X_i into equivalent normal distributions. Techniques for this process is available.

An example using this methodology is presented in Reference 21.

APPENDIX B Sampling methods

In this appendix the two sampling procedures used in the report are described. The two methods of sampling the parameters according to their distributions are simple random sampling (SRS) and Latin hypercube sampling (LHS). The text is mainly from reference 13.

Simple random sampling (SRS)

Simple random sampling techniques are entirely random - that is, any given sample may fall anywhere within the range of the input distribution. The random number generated are sampled from a uniform distribution (0,1). Samples, of course, are more likely to be drawn in areas of the distribution which have higher probabilities of occurrence. With enough iterations, simple random sampling will "recreate" the input distributions through sampling. A problem of clustering, however, arises when a small number of iterations are performed.

In the illustration shown here (Figure 37), each of the 5 samples drawn falls in the middle of the distribution. The values in the outer ranges of the distribution are not represented in the samples and thus their impact on the results is not included in the simulation output.

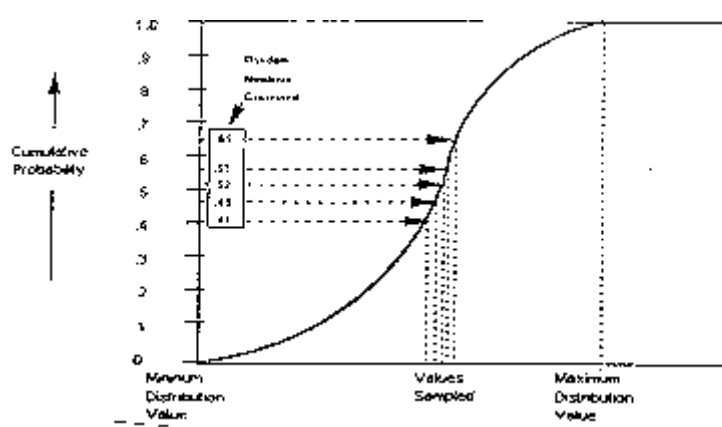


Figure 37. Five iterations of simple random sampling

Clustering becomes pronounced when a distribution includes low probability outcomes which could have a major impact on the results. It is important to include the effects of

these low probability outcomes and, to do this, these outcomes must be sampled. But if their probability is low enough, a small number of simple random sampling may not sample sufficient quantities of these outcomes to accurately represent their probability. This problem has led to the development of stratified sampling techniques such as the Latin hypercube sampling.

Latin hypercube sampling (LHS)

Latin hypercube sampling is a recent development in sampling technology designed to accurately recreate the input distribution through sampling in fewer iterations when compared with the Monte Carlo method. The key to Latin hypercube sampling is stratification of the input probability distributions. Stratification divides the cumulative curve into equal intervals on the cumulative probability scale (0 to 1.0). A sample is then randomly taken from each interval or "stratification" of the input distribution. Sampling is forced to represent values in each interval, and thus, is forced to recreate the input probability distribution.

In the illustration in Figure 38, the cumulative curve has been divided into 5 intervals. During sampling, a sample is drawn from each interval. Compare this to the 5 clustered samples drawn using SRS method. With Latin hypercube, the samples more accurately reflect the distribution of values in the input probability distribution.

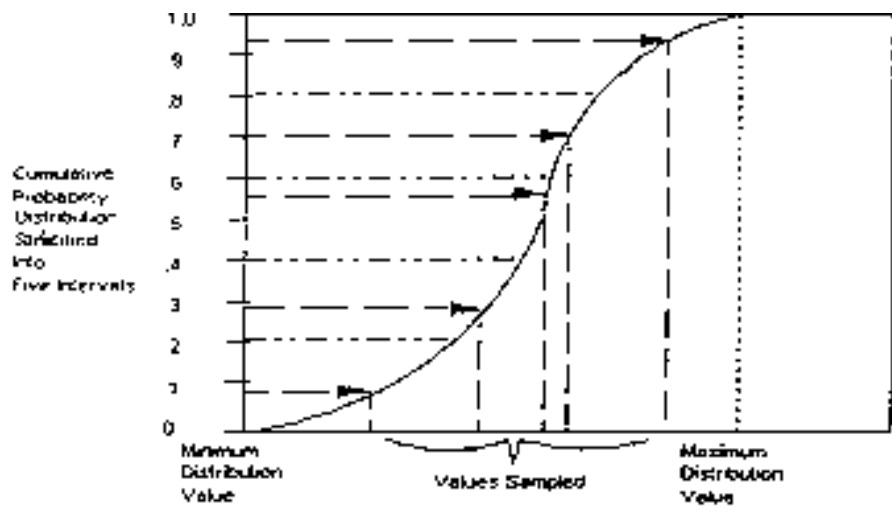


Figure 38. Five iterations of Latin hypercube sampling

The technique being used during Latin hypercube sampling is "sampling without replacement". The number of stratifications of the cumulative distribution is equal to the number of iterations performed. In the example above there were 5 iterations and thus 5 stratifications were made to the cumulative distribution. A sample is taken from each stratification. However, once a sample is taken from a stratification, this stratification is not sampled from again - its values are already represented in the sampled set.

When using the Latin hypercube technique to sample from multiple variables, it is important to maintain independence between variables. The values sampled for one variable need to be independent of those sampled for another (unless, of course, you explicitly want them correlated). This independence is maintained by randomly selecting - for each variable - which interval to draw a sample from. In a given iteration, Variable #1 may be sampled from stratification #4, Variable #2 may be sampled from stratification #22, and so on. This preserves randomness and independence and avoids unwanted correlation between variables.

As a more efficient sampling method, Latin hypercube offers great benefits in terms of increased sampling efficiency and faster runtimes. These gains are especially noticeable in a PC based simulation environment. Latin hypercube, however, also helps the analysis of situations where low probability outcomes are represented in input probability distributions. By forcing the sampling of the simulation to include these outlying events, Latin hypercube sampling assures they are accurately represented in your simulation outputs.

When low probability outcomes are very important it often helps to run an analysis which just simulates the contribution to the output distribution from the low probability events. In this case the model simulates only the occurrence of low probability outcomes - they are set to 100% probability. Through this you will isolate those outcomes and directly study the results they generate.

The drawback with LHS is that it at the moment is not possible to derive confidence limits from such a sample. That is why the less effective SRS method has to be used for those occasions.

APPENDIX C Description of Worksheet Model

1. Problem to be solved
2. Implementation of the Problem
 - 2.1 Closed Form of Limit State Function
 - 2.2 Algorithm
 - 2.3 Treatment of Non Normal Distributions
3. Using the Worksheet
 - 3.1 Structure of the worksheet
 - 3.2 'main' sheet
 - 3.3 'lsf' sheet
 - 3.4 Graphic Output

An Excel 5.0 worksheet has been developed to perform a FOSM (First Order Second Moment) analysis for our scenario No. 6. This appendix is to describe the structure and implementation of the worksheet.

1. Problem to be solved

In the scenario No. 6, alarm is working. Sprinkler is not activated. Emergency doors are not blocked. In this case we have the following limit state function

$$g = M_S S - M_D D - R - M_E E \quad (1)$$

where S is the smoke filling time [s], D is the detection time [s], R is the reaction time [s], E is the evacuation time. The coefficients M_S , M_D and M_E are added to account for the correction of model predictions.

The terms in the limit state function are,

$$\text{Smoke Filling Time} \quad S = 1.67 \alpha^{-0.26} H^{0.44} A^{0.54} \quad (2)$$

$$\text{Detection Time} \quad D = 5.36 \alpha^{-0.478} H^{0.7} \quad (3)$$

$$\text{Reaction Time} \quad R = (\text{stochastic}) \quad (4)$$

$$\text{Evacuation Time} \quad E = \frac{NA}{fW}, \quad (5)$$

where N is the population density [Persons/m²], f is the specific flow [Persons/m.s], W is the door width [m].

2. Implementation of the Problem

2.1 Closed Form of Limit State Function

Combining all the equation, we get a closed form of limit state function as

$$g(\mathbf{x}) = 1.67 M_s \alpha^{-0.26} H^{0.44} A^{0.54} - 5.36 M_d \alpha^{-0.478} H^{0.7} - R - \frac{M_e N A}{f W} \quad (6)$$

where $\mathbf{x} = \{\alpha, R, N, A, H, W; M_s, M_d, M_e\}^T$ is the vector of variables, f is a deterministic constant.

2.2 Algorithm

The Rackwitz's algorithm described in Chapter 6 was applied as follows.

Step 1 Assume initial values for most probable failure point x_i^* .

$$x_i^* = \alpha^*, R^*, N^*, A^*, H^*, W^*, f; M_s^*, M_d^*, M_e^*.$$

Step 2. Calculate reduced (non dimensional) variables

$$x_i^{*'} = \frac{x_i^* - \mu_{x_i}}{\sigma_{x_i}}$$

Step 3a. Calculate partial derivatives with respect to all the variables.

Differentiating the limit state function (6) with respect to all the variables, we get ,

$$\frac{\partial g}{\partial \alpha} = -0.43 M_s \alpha^{-1.26} H^{0.44} A^{0.54} + 2.56 M_d \alpha^{-1.478} H^{0.7}, \quad (7)$$

$$\frac{\partial g}{\partial R} = -M_R, \quad (8)$$

$$\frac{\partial g}{\partial N} = -\frac{M_E A}{fW}, \quad (9)$$

$$\frac{\partial g}{\partial M_S} = 1.67 \alpha^{-0.26} H^{0.44} A^{0.54}, \quad (10)$$

$$\frac{\partial g}{\partial M_D} = -5.36 \alpha^{-0.478} H^{0.7}, \quad (11)$$

$$\frac{\partial g}{\partial M_E} = -\frac{NA}{fW}, \quad (12)$$

Step 3b. Calculate partial derivatives with respect to reduced variables.

$$\frac{\partial g}{\partial x_i^*} = \frac{\partial g}{\partial x_i} \frac{\partial x_i^*}{\partial x_i} = \sigma_{x_i} \frac{\partial g}{\partial x_i}, \quad (13)$$

Step 3c. Calculate direction cosines of all the reduced variables.

$$\cos(\beta, x_i^*) = \frac{(\frac{\partial g}{\partial x_i})_*}{\sqrt{\sum_i (\frac{\partial g}{\partial x_i})_*^2}}, \quad (14)$$

Step 4. Calculate new variables as functions of β .

$$x_i^* = \mu_{x_i} - \cos(\beta, x_i) \sigma_{x_i} \beta = a_{x_i} - b_{x_i} \beta, \quad (15)$$

where $a_{x_i} = \mu_{x_i}$, $b_{x_i} = \cos(\beta, x_i) \sigma_{x_i}$

Step 5. Substitute into $g(\mathbf{x}) = 0$ and solve for β .

In this special case, we get

$$\begin{aligned} g(\beta) = & 1.67(a_{M_S} - b_{M_S} \beta)(a_\alpha - b_\alpha \beta)^{-0.26} H^{0.44} A^{0.54} \\ & -5.36(a_{M_D} - b_{M_D} \beta)(a_\alpha - b_\alpha \beta)^{-0.478} H^{0.7} \\ & -(a_R - b_R \beta) \\ & -\frac{A}{fW}(a_{M_E} - b_{M_E} \beta)(a_N - b_N \beta) \end{aligned} \quad (16)$$

Newton's method was applied to solve this equation. Namely, we start with some appropriate value of β ($= \beta^{old}$). An improved estimate of β ($= \beta^{new}$) is obtained by

$$\beta^{new} = \beta^{old} - \frac{g(\beta^{old})}{\left(\frac{\partial g}{\partial \beta}\right)^{old}}. \quad (17)$$

This procedure was iterated until convergence is archived as shown in Figure C1.

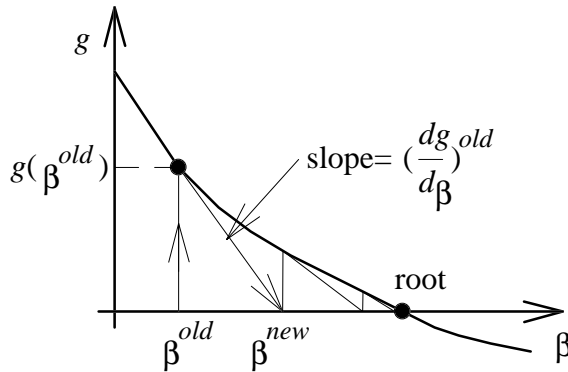


Figure C1 Newton's iterative method to solve $g(\beta) = 0$.

A closed form of the derivative is given by,

$$\begin{aligned} \frac{dg}{d\beta} = & -1.67 H^{0.44} A^{0.54} \left[b_{M_S} (a_\alpha - b_\alpha \beta)^{-0.26} + b_\alpha (a_{M_S} - b_{M_S} \beta) (a_\alpha - b_\alpha \beta)^{-1.26} \right] \\ & + 5.36 H^{0.7} \left[b_{M_D} (a_\alpha - b_\alpha \beta)^{-0.478} + b_\alpha (a_{M_D} - b_{M_D} \beta) (a_\alpha - b_\alpha \beta)^{-1.478} \right] \\ & + b_R (a_{M_R} - b_{M_R} \beta) \\ & + \frac{A}{fW} \left[(a_N - b_N \beta) b_{M_E} + b_N (a_{M_E} - b_{M_E} \beta) \right] \end{aligned} \quad (18)$$

Step 6. Use β to improve the values of x_i^* .

$$x_i^{*,new} = -\beta \cos(\beta, x_i^*) \quad (19)$$

Step 7. Calculate new estimate of MPFP.

$$x_i^{*,new} = \mu_{x_i} + x_i^{*,new} \sigma_{x_i} \quad (20)$$

Using new estimate of the MPFP, the whole procedure (Step 1 to 6) is repeated until the convergence is archived.

2.3 Treatment of non Normal distributions

FOSM accepts only normally distributed variables. However, the other type of distribution function can be approximated by an equivalent normal distribution function. The equivalent normal distribution is defined so that the probability density function and cumulative distribution function coincide with original functions, $f(x)$ and $F(x)$, at a given failure point x^* . Namely

$$f(x) = \frac{1}{\sigma_{eq}} \varphi\left(\frac{x^* - \mu_{eq}}{\sigma_{eq}}\right), \quad (21)$$

$$F(x) = \Phi\left(\frac{x^* - \mu_{eq}}{\sigma_{eq}}\right), \quad (22)$$

must be satisfied where $\varphi(x)$ is the standardized probability density function for a normally distributed variable,

$$\varphi(z) = \frac{1}{\sqrt{2\pi}} \exp\left(-\frac{z^2}{2}\right), \quad (23)$$

and $\Phi(x)$ is its cumulative function,

$$\Phi(x) = \int_{-\infty}^x \frac{1}{\sqrt{2\pi}} \exp\left(-\frac{(t - \mu_{eq})^2}{2\sigma_{eq}^2}\right) dt. \quad (24)$$

There are two methods of transformation. Analytical method can be applied to log normal distribution, while the numerical method are applied to the other distributions such as uniform and triangular distributions.

(1) analytical transformation for log normal distribution

Assume that a variable x is log normally distributed with mean $=\mu$ and standard deviation $=\sigma$. The probability density function is

$$f(x) = \frac{1}{x\zeta\sqrt{2\pi}} \exp\left(-\frac{-(\ln x - \lambda)^2}{2\zeta^2}\right), \quad (25)$$

where λ and ζ are the log normal parameters,

$$\lambda = \ln \frac{\mu^2}{\sqrt{\mu^2 + \sigma^2}} \quad (26)$$

$$\zeta = \sqrt{\ln \frac{\sigma^2 + \mu^2}{\mu^2}} \quad (27)$$

In this case, analytical expressions can be derived for the mean and standard deviation. We get ;

$$\sigma_{eq} = x^* \zeta \quad (28)$$

$$\mu_{eq} = x^* - (\ln x^* - \lambda) \frac{\sigma_{eq}}{\zeta} = x^* (1 - \ln x^* + \lambda) \quad (29)$$

An example is given in Figure C2 where ($\mu = 100$, $\sigma = 100$, $x^* = 150$) and ($\mu_{eq} = 37$, $\sigma_{eq} = 125$).

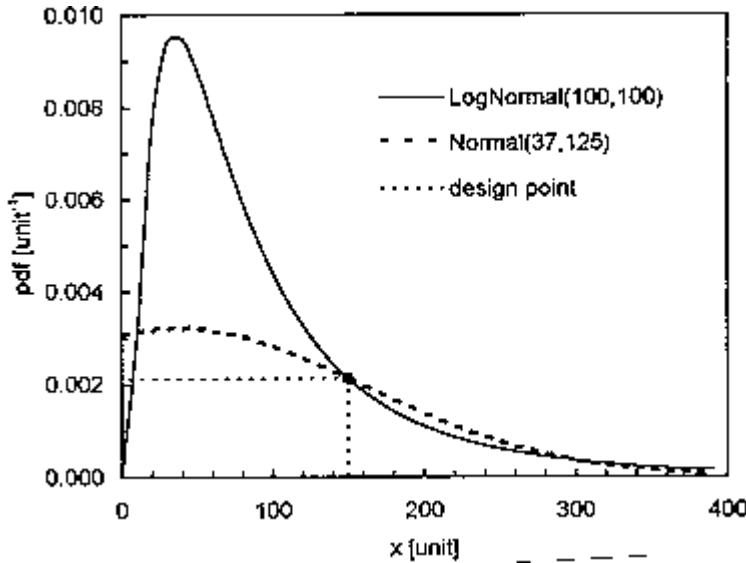


Figure C2 Transformation of log normal distribution to an equivalent normal distribution ($\mu = 100$, $\sigma = 100$, $x^* = 150$)

(2) numerical transformations for general distribution functions

In case of more general types of distribution, such as uniform, triangular, it is not possible to derive a closed form of expressions for equivalent normal distribution. Thus the transformations must be done numerically. Solving equations (21) and (22) for the equivalent mean and standard deviation, we get

$$\sigma_{eq} = \frac{\varphi\{\Phi^{-1}[F(x^*)]\}}{f(x^*)} \quad (30)$$

$$\mu_{eq} = x^* - \Phi^{-1}[F(x^*)]\sigma_{eq} \quad (31)$$

The inversion function of the cumulative normal distribution, $\Phi^{-1}(x)$, is evaluated numerically¹⁾. An example is shown in Figure C3 for uniform distribution

¹⁾ Commonly used spreadsheet packages have an intrinsic function for this purpose.

$$f(x) = \begin{cases} 0 & (x < x_{min}) \\ \frac{1}{x_{max} - x_{min}} & (x_{min} < x < x_{max}), \\ 0 & (x_{max} < x) \end{cases} \quad (32)$$

$$F(x) = \begin{cases} 0 & (x < x_{min}) \\ \frac{x - x_{min}}{x_{max} - x_{min}} & (x_{min} < x < x_{max}), \\ 1 & (x_{max} < x) \end{cases} \quad (33)$$

with $x_{min} = 50$, $x_{max} = 60$ and $x^* = 58$, which results in $\sigma_{eq} = \varphi\{\Phi^{-1}(0.8)\} \times 10 = 2.8$, $\mu_{eq} = 58 - \Phi^{-1}(0.8) \times 2.8 = 55.6$. Another example is shown in Figure C4 for triangular distribution,

$$f(x) = \begin{cases} 0 & (x < x_{min}) \\ \frac{2(x - x_{min})}{(x_{likely} - x_{min})(x_{max} - x_{min})} & (x_{min} < x < x_{likely}) \\ \frac{2(x_{max} - x)}{(x_{max} - x_{min})(x_{max} - x_{likely})} & (x_{likely} < x < x_{max}) \\ 0 & (x_{max} < x) \end{cases} \quad (34)$$

$$F(x) = \begin{cases} 0 & (x < x_{min}) \\ \frac{(x - x_{min})^2}{(x_{likely} - x_{min})(x_{max} - x_{min})} & (x_{min} < x < x_{likely}) \\ 1 - \frac{(x_{max} - x)^2}{(x_{max} - x_{min})(x_{max} - x_{likely})} & (x_{likely} < x < x_{max}) \\ 1 & (x_{max} < x) \end{cases} \quad (35)$$

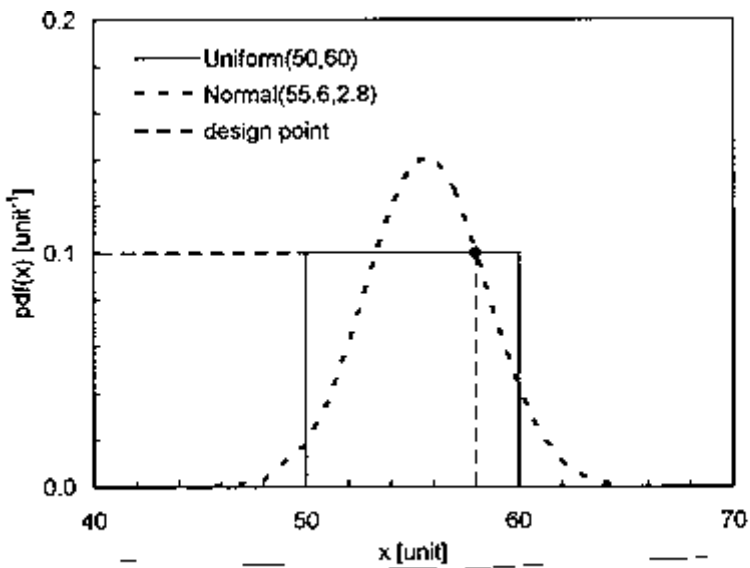


Figure C3 Uniform distribution and corresponding equivalent normal distribution

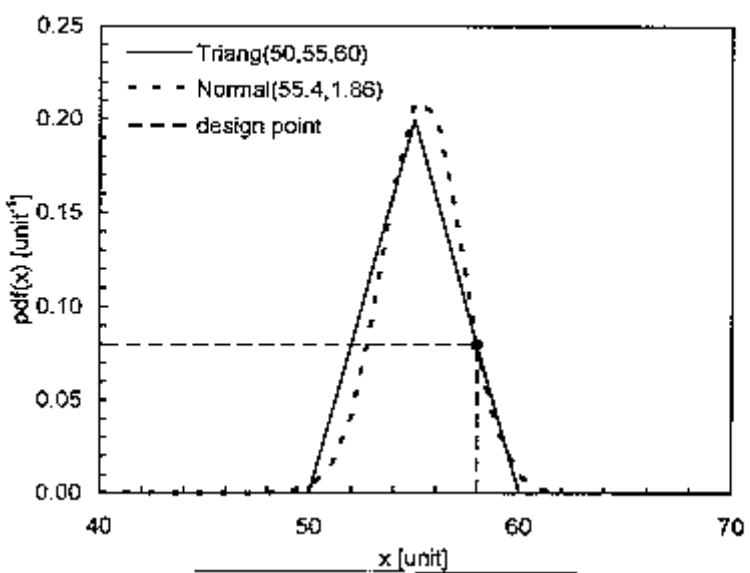


Figure C4 Triangular distribution and corresponding equivalent normal distribution

3. Using the Worksheet

3.1 Structure of the worksheet

To open the worksheet, click on the filename on the file manager as you usually do to open the Excel worksheet. The worksheet is made of two spreadsheets, 'main' and 'fosc', together with three macro module sheets, 'lsf', 'stat' and 'iterate'. All the setup can be done in 'main' sheet so you have nothing to do with other sheets. Only when you want to modify the limit state function, you will have to modify the macro definitions in 'lsf' sheet. You will get graphic outputs on 'gamma' for partial coefficient $\gamma (= x^* / \mu_x)$, and on 'fos' for the first order sensitivity. The function of the sheets are summarized in Table C1.

Table C1 summary of sheet functions

sheet	function
main	global setup, user interface
fosc	Rackwitz algorithm, can be treated as 'Black Box'
stat	macro module for commonly used statistic functions
iterate	macro to carry out the iterative process automatically, can be treated as 'Black Box'
lsf	macro functions to define limit state functions, problem dependent.
gamma	graphic output of partial coefficients
fos	graphic output of first order sensitivity

3.2 'main' sheet

The 'main' sheet looks like as Figure C5.

[Column C-F (Input)]

Specify the parameters, $\alpha, R, N, Area, H, W, f, awt, M_s, M_D, M_E$ with their mean, standard deviations well as distribution type. The distribution type can be selected from 'L' (Log Normal), 'N' (Normal), 'U' (Uniform), 'T' (Triangular) and 'D' (Deterministic).

[Column G-H (Output)]

The mean values and standard deviations of the input variables are calculated in these cells.

[Column J(Calculated Results)]

The first estimate of the most probable failure point is given in these cells. The calculations are automatically carried out in 'fosc' sheet based on your input.

[Column O-S(Calculated Results)]

The partial coefficient (Column O) and first order sensitivity (Column Q-S) are calculated.

[Macro Buttons]

You will find two macro buttons on this worksheet. The 'initialize' button can be pressed to set your initial guess equal to mean values. The 'start iteration' button is used to activate the iteration process. After the iterative procedure is finished, the 'error in design point' in the cell J18 will be zero. If it is far from zero, you can press the 'start iteration' button to improve the solution.

[acceleration coeff. (Cell J17)]

When you have very complicated problem, it is recommended to put the acceleration coefficient to a smaller value than unity. Usually a value between 0.3 and 0.6 are appropriate to get a better result.

3.3 'lsf' sheet

When you modify your limit state function, you only have to change the macro functions in this 'lsf' sheet. The macro sheet looks like as the following. This sheet has more than 100 lines, however, only part of it is shown below. See the comments on this sheet for details.

[definition of smoke filling time S and its derivatives dS/da.]

'(smoke filling time and its derivative by alpha)

Function SmkNoSp(alpha, h, area)

SmkNoSp = 1.67 * (alpha ^ (-0.26)) * (h ^ 0.44) * (area ^ 0.54)

End Function

Function SmkNoSpDa(alpha, h, area)

```

SmkNoSpDa = -0.26 * 1.67 * (alpha ^ (-1.26)) * (h ^ 0.44) * (area ^ 0.54)
End Function

[definition of detection time D and its derivatives dD/da.]
'(detection time and its derivative by alpha)

Function Detect(alpha, h)
    Detect = 5.36 * (alpha ^ (-0.478)) * (h ^ 0.7)
End Function

Function DetectDa(alpha, h)
    DetectDa = -0.478 * 5.36 * (alpha ^ (-1.478)) * (h ^ 0.7)
End Function

```

(continued)

3.4 Graphic Output

You can get graphic output of partial coefficient and first order sensitivity on 'gamma' and 'fos' sheets. Examples are shown in Figures C6 and C7.

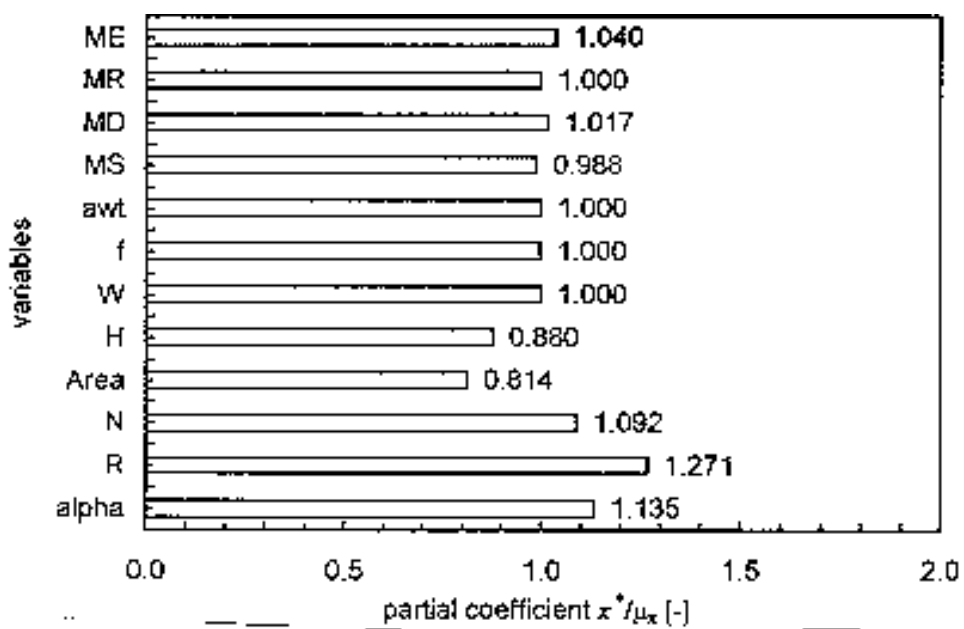


Figure C6 An example of graphic output of partial coefficient

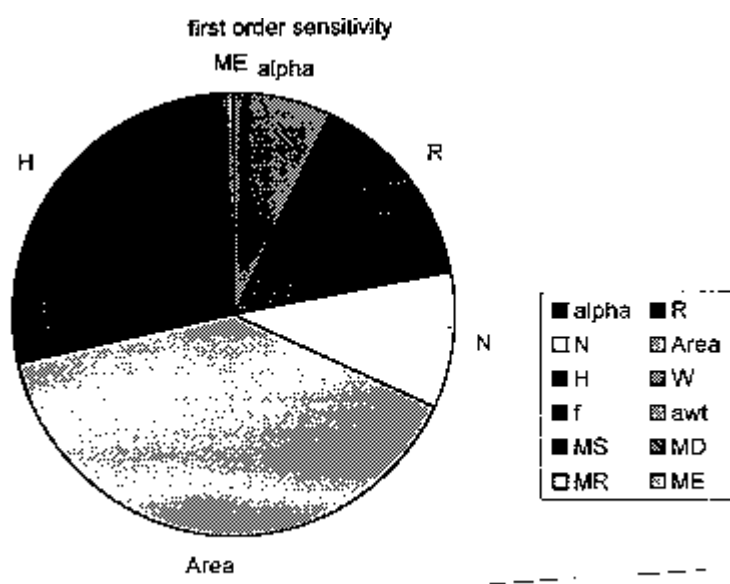


Figure C7 An example of graphic output of first order sensitivity

A	B	C	D	E	F	G	H	I	J	N	O	P	Q	R	S
1 FOSM(First Order, Second Moment) method for Scenario 6															
2															
3 distribution of stochastic parameters															
4 var. [unit] type															
5 alpha [Km^2/s^2]															
6 R [g]	U	0.001	0.100	0.0505	0.02475	0.05734	1.135	-831.6	891.0	7.09%					
7 N [cm^2]	L	130	120	130	120	105.174	1.271	-1.0	1440.0	14.76%					
8 Area [m ²]	T	0.100	0.890	1.000	0.63333	0.3976	0.09161	1.092	-123.5	975.5	10.01%				
9 H [m]	U	200.00	1200	700	250	569.942	0.814	0.2	3847.9	39.43%					
10 W [m]	U	3.00	12	7.5	2.25	6.5997	0.880	1.35	26436	27.08%					
11 f [ps.m]	D	4.80	0.001	4.8	0	4.8	1.000	1.00	0	0	0.00%				
12 avn [s]	N	1.00	0.00	1	0.001	1	1.000	1.00	0	0	0.00%				
13 Ms [-]	O	0.00	0.11	0.00001	D	0.00001	1.000	0.0	0	0	0.00%				
14 Mo [-]	N	1.35	0.11	1.35	0.11	1.33338	0.988	247.9	744	0.76%					
15 Mx [t]	D	0.20	0.20	1	0.2	1.01695	1.017	-78.8	248	0.25%					
16 Me [-]	N	1.00	1.00	1	D	1	1.000	-165.2	0	0.00%					
17		0.30	1	0.3	1	1.03976	1.040	-82.1	807	0.82%					
						acceleration coeff. =	1								
18						error in design point =	0.00 [%]	5{g} =	97585 [s ²]						
19						b =	0.870 [-]	S{g} =	312.4 [s]						
20						21 Type should be either L, N, U, T or D		22 L=Log Normal (mean, standard deviation)							
								N=Normal (mean, standard deviation)	Initialize	start iteration					
								U=Uniform (minimum, maximum)							
								T=Triangular (minimum, most likely, maximum)							
								O=Deterministic (value)							

Figure C5 ‘main’ sheet for setup of the problems

APPENDIX D Derivation of regression equations and knowledge uncertainty

In this appendix, the procedures for deriving the regression equations are described. To carry out the analytical and numerical calculation of safety level, well-established response surface equations for smoke filling time S , detection time D are necessary.

The derivation of regression equations can be divided into two stages. The first one is to obtain sufficient number of output values of prediction models to cover the whole range of variation of stochastic parameters. Then the regression analysis will be carried out to fit an appropriate equation to the output values. The errors of the prediction made by regression equation should be quantified as well. They can be included in the knowledge of uncertain parameters.

D1. Smoke filling time for non sprinklered fires (scenario 1, 2, 5 and 6)

(1) selection of regression formula

An empirical equation is suggested in NFPA92B [4] for the smoke layer height during the t^2 -fires ($Q = \alpha t^2$ [kW]). The equation is

$$\frac{z}{H} = 0.91 \left[t H^{-4/5} \left(\frac{1000}{\alpha} \right)^{-1/5} \left(\frac{Area}{H^2} \right)^{-3/5} \right]^{-1.45} \quad (1)$$

where, z is the height of smoke layer above fire [m], S is the floor area [m^2], H is the ceiling height [m], t is the time [s], α is the fire growth rate [kW/s^2].

Solving for t , we get,

$$t = 3.74 \alpha^{-0.2} H^{0.3} Area^{0.6} z^{-0.69} \quad (2)$$

The critical time for smoke filling, S , is defined as the time at which smoke layer comes down to $1.6 + 0.1H$ meters above floor. Rounding $1.6 + 0.1H$ to 2 meters, we get

$$S = 2.32 \alpha^{-0.2} H^{0.3} Area^{0.6} \quad (3)$$

This equation is valid only for atria with $0.9 \leq (S / H^2) \leq 14$. However we selected the similar equation for our problem as,

$$S = C \alpha^{n_\alpha} H^{n_H} \text{Area}^{n_{\text{Area}}} \quad (4)$$

where the coefficient C and powers n_α , n_H and n_{Area} will be calculated by the regression analysis in the next section.

(2) calculation of smoke filling time by CFAST

A zone model code CFAST [21] was used to calculate the smoke filling time. As shown in Figure D1, a single room fire scenario was considered. A t^2 -fire, e.g. $\dot{Q} = \alpha t^2$, was put at the center of the floor. The floor area, ceiling height and fire growth rate are varied to the values in Table D1. Total number of calculations was 39. From the output of CFAST, smoke filling time was determined.

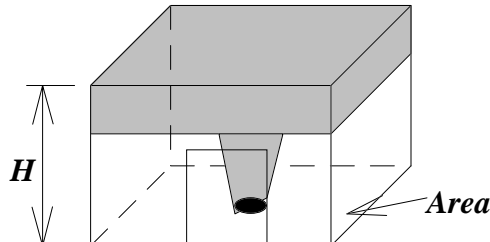


Figure D1. Calculation condition

Table D1 input values for the calculation of smoke filling time

parameters	200	500	800	1600
floor area [m^2]				
ceiling height [m]	3	5	8	
fire growth rate [kW/s^2]	0.001	0.005	0.01	0.02

(3) regression analysis of CFAST output

A regression analysis was carried out to fit the equation (4) to CFAST output values. The parameters, C , n_α , n_H , n_s are determined so as to minimize the sum of squared relative error,

$$(error)^2 = \sum_i \left(\frac{C\alpha_i^{n_\alpha} H_i^{n_H} Area_i^{n_S} - \bar{S}_i}{C\alpha_i^{n_\alpha} H_i^{n_H} Area_i^{n_S}} \right)^2 \quad (5)$$

where \bar{S}_i is the i -th CFAST output, α_i , H_i and $Area_i$ are the corresponding input values to CFAST.

The result of fitting is shown in Figure D2. The best fit equation is,

$$S = 1.67\alpha^{-0.26} H^{0.44} Area^{0.54}, \text{ [s]} \quad (6)$$

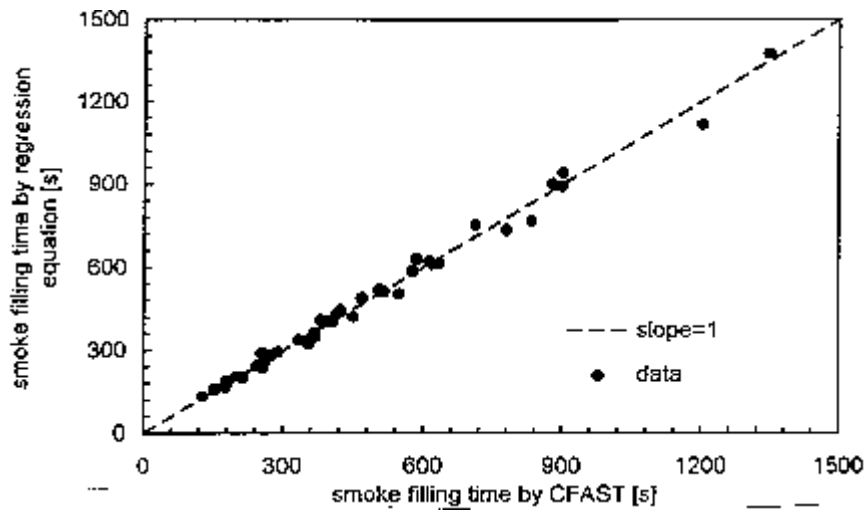


Figure D2. Result of regression analysis for non sprinklered fires

The distribution of relative error is shown in Figure D3. The mean value of relative error is zero, which shows that the regression analysis is successful. The standard error is 5.03%.

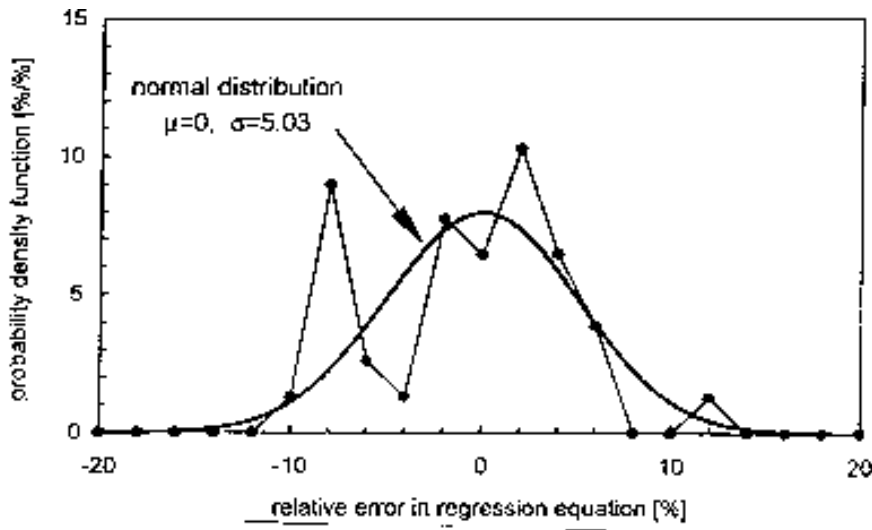


Figure D3. Distribution of relative error between regression equation and CFAST output for non sprinklered fires

(3) Correction factor for smoke filling time

The regression equation has been derived by CFAST. Therefore, the inherent error associated with CFAST must be evaluated as well. Bragason [22] compared the calculation results with full scale experiments. Some of his results on smoke filling time by CFAST and by experiments are plotted in Figure D4. It is shown that CFAST gives conservative estimate of smoke filling time.

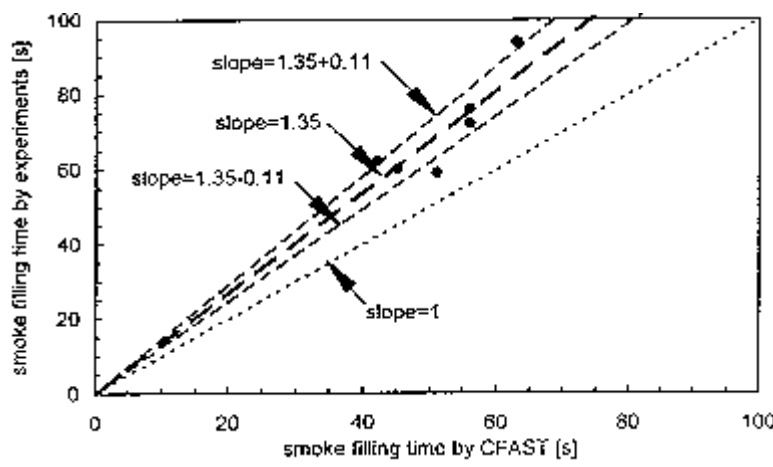


Figure D4. Comparison of smoke filling time calculated by CFAST with full scale fire experiments

The best fit value of the correction factor for smoke filling time is 1.35 as shown in Figure D4. It should be noted that the scatter of data are not negligible. The standard deviation of the correction factor is 0.11, which is also shown in the figure.

(4) Derivation of knowledge uncertain parameter M_s

The knowledge uncertain parameter M_s should include all the uncertainties described above. As was derived in (2) and (3), the error between CFAST and regression equation is $\text{Normal}(1.0, 0.05)$. The error between CFAST and experiments is $\text{Normal}(1.35, 0.11)$. These two uncertainties are merged into M_s as

$$M_s = N(1.35 \times 1.00; \sqrt{0.11^2 + 0.05^2}) = N(1.35; 0.11) \quad (7)$$

which shows that the difference between CFAST and regression equation can be neglected compared with the error between CFAST output and experiments.

D2. Smoke filling time for sprinklered fires (scenario 3, 4, 7 and 8)

The same procedure was applied to derive the regression equation for smoke filling time for sprinklered fires and its corresponding knowledge uncertain parameter.

The only difference is that the fire growth is limited by the activation of sprinkler system. Here we assumed that the RHR is reduced to 10% within 120 seconds after the sprinkler activation. Namely,

$$Q = \begin{cases} \alpha t^2 & (0 \leq t \leq t_{act}) \\ (1 - 0.9 \frac{t - t_{act}}{120}) Q_{act} & (t_{act} \leq t \leq t_{act} + 120) \\ 0.1 Q_{act} & (t_{act} + 120 \leq t) \end{cases} \quad (8)$$

where t_{act} is the activation time of sprinkler, Q_{act} is the rate of heat release at activation time. The RHR curve is shown in Figure D2. In deriving the Q_{act} and t_{act} , it was assumed that RTI of sprinkler is $50 \text{ m/s}^{1/2}$ and that the head spacing is 3.5 m. The activation temperature was 68°C .

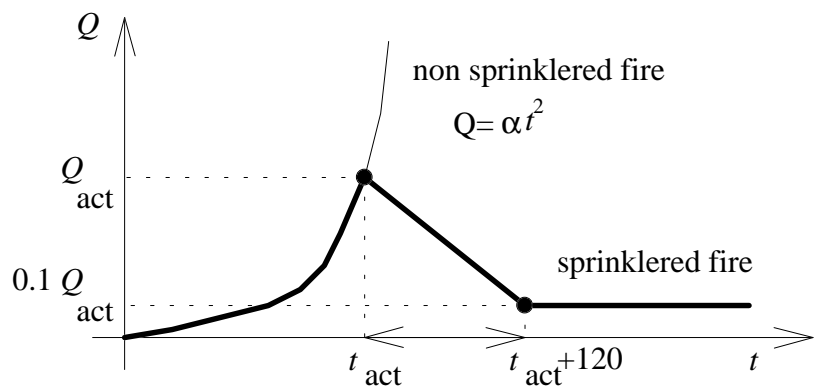


Figure D2. Rate of heat release for non-sprinklered and sprinklered fires.

Successive 34 CFAST calculations were made to cover the range of stochastic variability in α , H and $Area$. The result of regression analysis is shown in Figure D6. In this case, the regression equation does not fit the data very well, especially for the slow burning fires. The probability distribution function (PDF) of the relative error is shown in Figure D7. Comparing with the PDF in Figure D3, there is a large distribution of errors. The standard error is 21.9%.

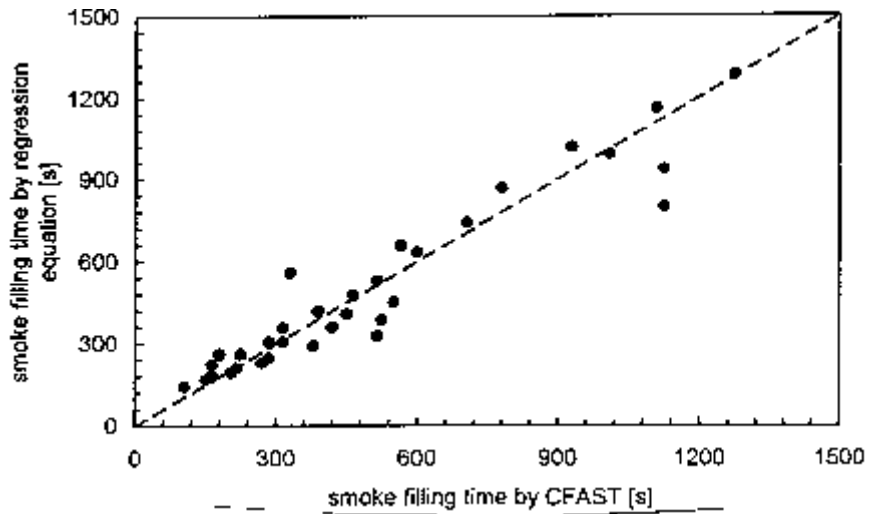


Figure D6. Result of regression analysis for sprinklered fires

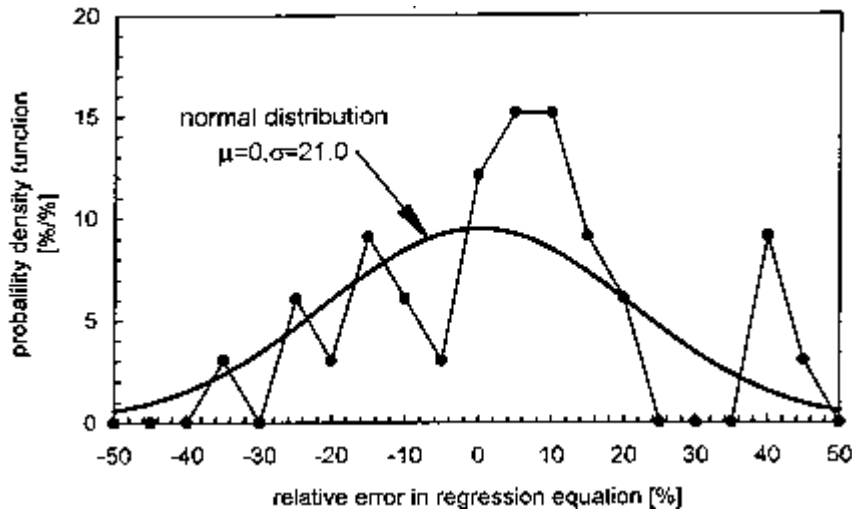


Figure D7. Distribution of relative error between regression equation and CFAST output for sprinklered fires

The knowledge uncertainty parameter M_s was also derived in the same way as in non sprinklered fires. As a result, we get

$$M_s = N(1.35 \times 1.0; \sqrt{0.11^2 + 0.22^2}) = N(1.35; 0.23) \quad (9)$$

which shows that the prediction errors are almost twice of that for the non sprinklered fires.

D3. Detection time

The DETACT-QS model was used to derive a regression equation. This model assumes that the transportation time for the hot gases from a fire to detector can be neglected. This is true for not too small fires in small rooms with short distances. To get better prediction, DETACT-T2 should be used. However this was not done for the calculations done in this paper.

In the calculation of detection time, a number of assumptions were made. The detector has the following characteristics; detection temperature is 30 °C. RTI value is 5 m/s^{1/2}. The detector spacing is 10m, which gives the maximum distance from the centerline of the fire plume is 7.07m. The ambient temperature is 20 °C.

The ceiling height was varied between 3 and 12 meters. The fire growth rate was varied between 0.0029 and 0.0467.

The regression equation

$$D = 5.36\alpha^{-0.478} H^{0.70} \quad (10)$$

was fitted to the output of DETACT-QS. The result of regression analysis is shown in Figure D8. In this case, the regression is very good. The standard error is only 1.5%.

D4. Other knowledge uncertain parameters

The remaining knowledge uncertain parameters were determined by judgment. Namely,

$$M_D = \text{Normal}(1.0, 0.2) \quad (11)$$

$$M_E = \text{Normal}(1.0, 0.3) \quad (12)$$

The distribution of these parameters are not known exactly. The above values are guessed for the state of the art of prediction models.

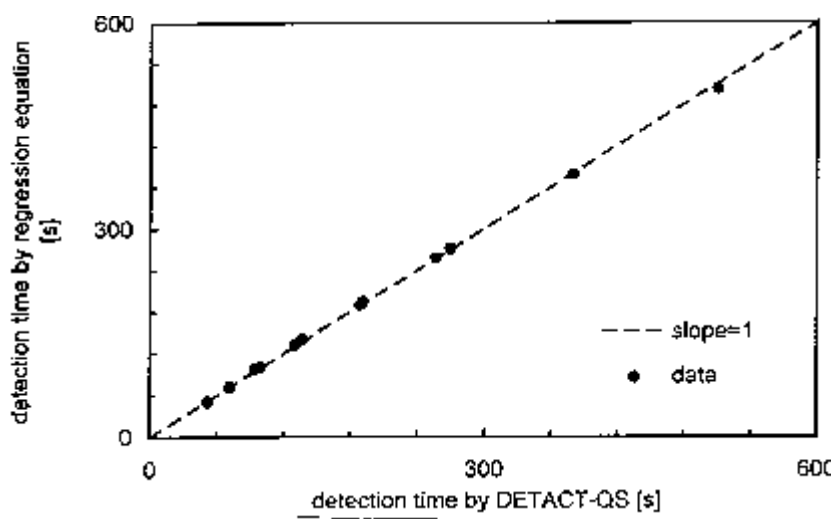


Figure D8. Result of regression analysis for detection time